UNIVERSIDADE ESTADUAL PAULISTA
"JÚLIO DE MESQUITA FILHO"
Câmpus de São José do Rio Preto

Yuri Pessoa Lemos

Microencapsulação por coacervação complexa de óleo de buriti: explorando materiais, processos e aplicação

São José do Rio Preto

2022

Yuri Pessoa Lemos

Microencapsulação por coacervação complexa de óleo de buriti: explorando materiais, processos e aplicação

Tese apresentada como parte dos requisitos para obtenção do título de Doutor em Engenharia e Ciência de Alimentos, junto ao Programa de Pós-Graduação em Alimentos, Nutrição e Engenharia de Alimentos, do Instituto de Biociências, Letras e Ciências Exatas da Universidade Estadual Paulista "Júlio de Mesquita Filho", Câmpus de São José do Rio Preto.

Financiadora: CAPES

Orientadora: Vânia Regina Nicoletti

São José do Rio Preto

2022

L557m

Lemos, Yuri Pessoa

Microencapsulação por coacervação complexa de óleo de buriti: explorando materiais, processos e aplicação / Yuri Pessoa Lemos. -- São José do Rio Preto, 2022

156 p. : il., tabs.

Tese (doutorado) - Universidade Estadual Paulista (Unesp), Instituto de Biociências Letras e Ciências Exatas, São José do Rio Preto

Orientadora: Vânia Regina Nicoletti

1. Microencapsulação. 2. Coacervação complexa. 3. Frequência de agitação. 4. Óleo de buriti. 5. Extrusão. I. Título.

Sistema de geração automática de fichas catalográficas da Unesp. Biblioteca do Instituto de Biociências Letras e Ciências Exatas, São José do Rio Preto. Dados fornecidos pelo autor(a).

Essa ficha não pode ser modificada.

Yuri Pessoa Lemos

Microencapsulação por coacervação complexa de óleo de buriti: explorando materiais, processos e aplicação

Tese apresentada como parte dos requisitos para obtenção do título de Doutor em Engenharia e Ciência de Alimentos, junto ao Programa de Pós-Graduação em Alimentos, Nutrição e Engenharia de Alimentos, do Instituto de Biociências, Letras e Ciências Exatas da Universidade Estadual Paulista "Júlio de Mesquita Filho", Câmpus de São José do Rio Preto.

Financiadora: CAPES

COMISSÃO EXAMINADORA

Profª. Drª. Vânia Regina Nicoletti
UNESP – São José do Rio Preto
Orientadora

Prof. Dr. João Cláudio Thoméo
UNESP – São José do Rio Preto

Prof. Dr. Róger Darros Barbosa
UNESP – São José do Rio Preto

Prof. Dr. Gustavo César Dacanal
USP – Pirassununga

Prof. Dr. Pedro Henrique Campelo Félix
UFAM – Manaus

São José do Rio Preto
2022

AGRADECIMENTOS

À minha orientadora, Profª. Drª. Vânia Regina Nicoletti Telis pelo incentivo, pela orientação, compreensão e pelos ensinamentos que levo para minha vida pessoal e profissional.

Aos membros da banca examinadora, pela disposição em participar da banca de defesa de tese de doutorado e correção deste trabalho.

Aos professores da pós-graduação, por todos os ensinamentos e por contribuírem com minha formação e crescimento profissional.

Aos colegas da pós-graduação e aos companheiros das jornadas no laboratório, pelos momentos de amizade, carinho, tristezas e alegrias.

A todos os professores, técnicos e funcionários do DETA que contribuíram de forma direta ou indireta para a realização deste trabalho.

A Izabela Alvim, e o ITAL, pelas análises de tamanho de partículas realizadas.

Ao técnico Alberto Camilo Alécio, do Instituto de química da Unesp de Araraquara, pelas análises de FTIR.

Aos meus irmãos Murilo e Luís, pela cumplicidade e apoio incondicional.

Aos meus pais e avós pela orientação e apoio incondicional.

A Laís, minha querida, pela paciência e compreensão

Enfim, a todas às pessoas que me apoiaram de alguma forma até hoje e contribuíram para a realização deste trabalho.

A todos vocês, minha eterna gratidão.

O presente trabalho foi realizado com apoio da Coordenação de Aperfeiçoamento de Pessoal de Nível Superior - Brasil (CAPES) - Código de Financiamento 001, à qual agradeço.

“Tudo o que temos de decidir é o que fazer com o tempo que nos é dado”

Gandalf, The Grey (Tolkien, 1991, p. 68).

RESUMO

A microencapsulação do óleo de buriti pode proteger os compostos bioativos presentes, principalmente os carotenoides, e a coacervação complexa é uma técnica de microencapsulação efetiva para proteger compostos lipofílicos. O objetivo deste trabalho foi avançar no estudo da microencapsulação de óleo de buriti pelo processo de coacervação complexa, utilizando gelatina/alginato de sódio e gelatina/goma arábica como materiais de parede, com enfoque sobre o efeito de parâmetros de processo nas características das microcápsulas, e a sua aplicação em produtos alimentícios. Para a produção das microcápsulas foi construído um vaso de agitação obedecendo às relações geométricas recomendadas e foram testados os efeitos da frequência de agitação, do tipo de impulsor e da presença de defletores sobre a coacervação. As microcápsulas sofreram influência direta dos parâmetros de processo e os resultados puderam ser correlacionados em função dos números adimensionais Reynolds e Froude. Os tamanhos médios das partículas ficaram na faixa de 36 a 186 µm e tiveram relação inversa com o número de Reynolds. A presença dos defletores se mostrou eficaz, produzindo microcápsulas com menores dispersões de tamanho. As amostras apresentaram altos valores de eficiência de encapsulação, acima de 80%, e coloração amarelo intenso. A partir desses resultados, procurou-se investigar o efeito do comportamento reológico das soluções precursoras das microcápsulas na produção das mesmas, o que foi avaliado utilizando os pares gelatina/goma arábica e gelatina/alginato de sódio. Foi possível observar que, para a formação das microcápsulas, soluções dilatantes necessitam de baixas velocidades de agitação, enquanto soluções pseudoplásticas demandam maiores velocidades de agitação. Com o intuito de explorar a possibilidade de substituir a liofilização, convencionalmente usada na secagem de microcápsulas produzidas por coacervação complexa, e assim reduzir os custos de produção, duas alternativas de secagem foram avaliadas: a secagem em leito de espuma e por formação de filme delgado. Ambas apresentaram bons resultados de eficiência de encapsulação quando comparadas às microcápsulas secas por liofilização. Por fim, a incorporação das microcápsulas em snacks extrusados de milho foi testada, visando o enriquecimento dos mesmos com carotenoides. Foram avaliadas duas estratégias de adição das microcápsulas, antes e depois da extrusão, bem como diferentes condições de processo. Os resultados foram promissores e, nas condições médias e brandas de extrusão, foi possível observar a presença de microcápsulas íntegras

nos snacks produzidos, bem como foi possível detectar a presença de carotenoides no produto, em concentrações na faixa de 0,5 a $\approx$ 5 μg/g de snack.

Palavra-chave: Microencapsulação, coacervação complexa, frequência de agitação, óleo de buriti, extrusados.

ABSTRACT

Buriti oil microencapsulation can protect the bioactive compounds present, mainly carotenoids, and complex coacervation is an effective microencapsulation technique to protect lipophilic compounds. The general objective of this work was to advance in the study of microencapsulation of buriti oil by the complex coacervation process, using gelatin/sodium alginate and gelatin/gum Arabic as wall materials, focusing on the effect of process parameters on the characteristics of the microcapsules, and its application in food products. For the production of microcapsules, an agitation vessel was built following the recommended geometric relationships and the effects of agitation frequency, type of impeller and the presence of deflectors on coacervation were tested. The microcapsules were directly influenced by the process parameters and the results could be correlated as a function of the Reynolds and Froude dimensionless numbers. The average particle sizes were in the range of 186 to 36 μm and had an inverse relationship with the Reynolds number. The presence of deflectors proved to be effective, producing microcapsules with smaller size dispersions. The samples showed high values of encapsulation efficiency, above 80%, and intense yellow color. From these results, we sought to investigate the effect of the rheological behavior of the precursor solutions of the microcapsules, which was evaluated using the pairs gelatin/gum Arabic and gelatin/sodium alginate. It was possible to observe that, for the formation of microcapsules, dilatant solutions need low stirring speeds, while pseudoplastic solutions demand higher stirring speeds. In order to explore the possibility of replacing lyophilization, conventionally used in the drying of microcapsules produced by complex coacervation, and thus reducing production costs, two drying alternatives were evaluated: foam-mat drying and thin-film formation. Both showed good encapsulation efficiency results when compared to freeze-dried microcapsules. Finally, the incorporation of microcapsules in extruded corn snacks was tested, aiming to enrich them with carotenoids. Two microcapsule addition strategies were evaluated, before and after extrusion, as well as different process conditions. The results were promising and, under medium and mild extrusion conditions, it was possible to observe the presence of intact microcapsules in the snacks produced, as well as detecting the presence of carotenoids in the product, in concentrations ranging from 0.5 to ≈ 5 μg/g of snack.

Keywords: Microencapsulation, complex coacervation, agitation frequency, buriti oil, extrudates.

LISTA DE ILUSTRAÇÕES

LISTA DE TABELAS

SUMÁRIO

Introdução geral e objetivos

INTRODUÇÃO GERAL

O bioma de cerrado brasileiro é um dos mais ricos e variados em termos de biodiversidade do mundo, sendo o segundo maior bioma da América do Sul. Muitos dos frutos encontrados no cerrado são ricos em compostos bioativos, podendo apresentar alternativas promissoras para o tratamento e prevenção de doenças. O buritizeiro (*Mauritia flexuosa* L.f.) é uma das palmeiras mais abundantes nesse bioma, e o que desperta o interesse em a sua exploração é o conteúdo de seu fruto, o óleo de buriti. O óleo é basicamente composto de carotenoides (principalmente β-caroteno), ácidos graxos com predominância do oleico e palmítico, e antioxidantes, caracterizando-se como uma das principais fontes de provitamina A encontrada na biodiversidade brasileira (BITAR; ALCÂNTARA, 2015; CRUZ et al., 2020; SOUSA et al., 2022).

O β-caroteno é um antioxidante que atua nos radicais livres que podem causar o estresse oxidativo de biomoléculas, tal estresse tem sido associado a diferentes tipos de dano celular, que acarretam em envelhecimento e ao desenvolvimento de doenças crônicas, inflamatórias e degenerativas, como câncer, doenças cardiovasculares, catarata e (CÂNDIDO, et al., 2015; RIBEIRO, 2008). Ainda, o β-caroteno é o mais potente dos compostos provitamina-A. A vitamina A é um nutriente essencial para o homem e a sua ingestão de maneira deficitária, tem relação com algumas doenças oculares (xeroftalmia e cegueira nutricional), além de ter relação com o retardo de crescimento e aumento da susceptibilidade a infecções (HUANG et al., 2022; RAMALHO et al., 2001).

As funções apresentadas pelos compostos bioativos presentes no óleo de buriti aumentam o interesse pela sua incorporação em produtos como alimentos, cosméticos ou suplementos alimentares. Há que se considerar, ainda, que além dos benefícios nutricionais, o óleo de buriti apresenta potencial para uso como corante natural nesse tipo de produtos. Por outro lado, os carotenoides são muito susceptíveis a fatores como o calor, luz, oxidação enzimática e não enzimática, levando à perda de sua atividade pró-vitamínica e até mesmo uma ligeira perda de cor (MEZZOMO, 2012). Uma alternativa para ampliar tanto a estabilidade como a gama de aplicações de óleos contendo compostos bioativos é a microencapsulação que, segundo Azeredo (2005), visa a proteção do material encapsulado contra fatores ambientais, retardando a perda de aromas, alterações de cor e/ou perda de valor nutricional. Além de proteger os compostos bioativos, a microencapsulação também pode potencializar a aplicação dos óleos vegetais, como, por exemplo, facilitar a incorporação de compostos líquidos em sistemas secos.

Segundo Thies (2007), em muitos casos, a microencapsulação visa a liberação controlada do composto encapsulado, ou seja, a liberação do composto é alcançada com a destruição da cápsula no momento desejado, seja na produção, na ingestão ou na digestão do produto. Existem, também, determinadas aplicações em que se pretende que a liberação do material encapsulado nunca ocorra. Nessas situações, a parede da cápsula deve permanecer intacta tanto no preparo do alimento quanto após a sua ingestão.

Nos últimos anos as microcápsulas estão sendo aplicadas como uma fonte de enriquecimento de vários compostos bioativos e em várias gamas industriais, desde médicas a alimentícia. Pensado na indústria alimentícia, a parede pode ser essencial para a boa preservação e consumo desses compostos, algumas das vezes esses compostos estão presentes em óleos, como o de buriti, o que pode ocasionar cheiro ou gosto desagradável e que precisa ser mascarado (JIA et al., 2021; SOLOMANDO et al., 2020; RAMÍREZ-MACEDO, VÉLEZ-RUÍZ, 2015).

A coacervação complexa é uma alternativa para microencapsular compostos lipofílicos, devido à alta eficiência de encapsulação e às condições de processamento suaves. A coacervação complexa é um fenômeno de separação de fase líquido-líquido que ocorre quando polímeros com cargas eletrostáticas opostas são submetidos a condições específicas de pH, produzindo agregados, que são chamados de complexos de biopolímeros. Esses complexos se agregam formando uma rede tridimensional devido à neutralização de carga. Para minimizar a energia livre interfacial do sistema, a fase de mistura se separa em nível macroscópico: uma fase rica nos dois biopolímeros (fase coacervada) e a outra fase rica em solvente. (THIES, 1996; 2007; GOUIN, 2004; SCHMITT; TURGEON, 2011; BORDÓN et al., 2021; BÖGER et al., 2021; COSTA et al., 2022).

As características das partículas dependem das condições de processo durante a encapsulação, como a natureza e a concentração dos polímeros e do agente ativo, agente reticulante e/ou agente surfactante, além do pH. No entanto, um dos parâmetros de processo mais importantes é a velocidade de agitação durante a dispersão do agente ativo na solução aquosa polimérica, visto que tal agitação influencia no tamanho das gotículas do agente ativo e consequentemente no tamanho das microcápsulas resultantes (JÉGAT; TAVERDET, 2000). Poucos estudos têm como objetivo descrever o efeito de parâmetros de processo (parâmetros de agitação, temperatura, tempo de residência, etc.) nas características do produto final. Em decorrência, a ampliação de escala do processo é

quase sempre feita de forma empírica, por tentativa e erro, à custa de recursos financeiros e materiais (LEMETTER et al., 2009).

Outro fator limitante da técnica, segundo Mehnert e Mader (2001), é a elevada quantidade de água necessária no meio de coacervação, que pode chegar a uma dispersão com 90% de água. Isso acarreta em uma baixa quantidade de cápsulas obtidas e compromete a produtividade do processo. A coacervação só ocorre dentro de uma faixa limitada de concentração de seus materiais de parede, sendo assim, o aumento da concentração pode interferir negativamente (THIES, 2007). Após a formação das microcápsulas, elas precisam ser secas para permitir serem armazenadas por mais tempo, ou para que possam ser aplicadas em sistemas secos. A liofilização é o método de secagem mais utilizado para microcápsulas produzidas por coacervação complexa, mas apesar de resultar em um produto de alta qualidade, é um método demorado e de alto custo. A secagem por atomização também tem sido aplicada, com a vantagem de produzir partículas individuais, mas o cisalhamento envolvido na atomização pode provocar danos às paredes das microcápsulas.

Existe, portanto, demanda de estudos para a determinação mais sistemática do efeito dos vários parâmetros de processo, obtenção de métodos de ampliação de escala, métodos alternativos de secagem das microcápsulas, bem como estudos do comportamento das mesmas quando aplicadas em diferentes produtos.

OBJETIVO GERAL

O objetivo geral deste trabalho foi estudar do processo de microencapsulação de óleo de buriti pelo processo de coacervação complexa, utilizando os pares gelatina/alginato de sódio e gelatina/goma arábica como materiais de parede, com enfoque sobre o efeito de parâmetros de processo nas características do produto final, e a sua aplicação em produtos alimentícios.

Objetivos específicos

- Avaliar os efeitos da frequência de agitação e das características geométricas do sistema de agitação sobre o rendimento de microcápsulas, morfologia e distribuição de tamanhos.

- A partir dos resultados alcançados anteriormente, obter correlações em função dos números de Reynolds, de Froude aplicáveis à descrição do processo de coacervação complexa em tanque agitado.

- Avaliar a influência das características reológicas das soluções formadoras das microcápsulas no tamanho e morfologia das mesmas.

- Avaliar a possibilidade de substituir a liofilização, convencionalmente usada na secagem nas microcápsulas produzidas por coacervação complexa, pela secagem por espuma e por filme delgado.

- Aplicar as microcápsulas de óleo de buriti produzidas na fabricação de alimentos extrusados enriquecidos com β-caroteno e avaliar a retenção desse composto.

ORGANIZAÇÃO DO TRABALHO EM CAPÍTULOS

O presente trabalho encontra-se estruturado da seguinte forma:

Introdução e objetivos

Capítulo 1: Revisão bibliográfica: os principais fundamentos teóricos dos tópicos abordados neste estudo são apresentados, incluindo informações referentes ao óleo de buriti, aos biopolímeros utilizados como material de parede, à metodologia de coacervação complexa para microencapsulação, agitadores e técnicas de secagem.

Capítulo 2: *Design and operational parameters of the stirred vessel affect formation of oil microcapsules by complex coacervation*: neste capítulo foram investigados os efeitos das características geométricas do vaso agitador e da frequência de agitação na produção das microcápsulas por coacervavção complexa e sobre o tamanho e forma final das microcápsulas obtidas.

Capítulo 3: *The role of suspension rheology on the size and morphology of complex coacervated microcapsules*: neste capítulo foi estudada a influência do comportamento reológico das soluções formadoras das microcápsulas no tamanho e forma das mesmas, utilizando dois diferentes pares de materiais de parede para a sua produção, que foram gelatina/goma arábica e gelatina/alginato de sódio.

Capítulo 4: *Foam-mat and thin-film drying as alternatives to freeze drying of complex coacervated microcapsules containing buriti oil (Mauritia flexuosa L.)*: neste capítulo foram abordadas técnicas de secagem alternativas à liofilizção para a secagem de microcápsulas produzidas por coacervação complexa; foram avaliados os métodos de secagem por formação de espuma e a secagem em filme delgado.

Capítulo 5: *Nutritional enrichment of corn extrudates with carotenoid microcapsules: physicochemical properties and carotene retention*: neste capitulo foi abordada a aplicação das microcápsulas de óleo de buriti como possível fonte de carotenoides para o enriquecimento de snacks extrusados de milho.

Conclusões gerais: neste item são apresentadas as conclusões gerais do trabalho.

REFERÊNCIAS

AZEREDO, H. M. C. Encapsulação: aplicação à tecnologia de Alimentos. **Alimentos e Nutrição**, v. 16, n. 1, p. 89-97, 2005.

BITAR, M. J. R.; ALCÂNTARA, M. M. Extração do óleo vegetal da palmeira de buriti, *Mauritia flexuosa L. f.*, em Itumbiara. **Anais da III semana interdisciplinar, X seminário de iniciação científica e IV semana da família**, v. 1, n.1, 2015.

BÖGER, B. R.; ACRE, L. B.; VIEGAS, M. C.; KUROZAWA, L. E.; BENASSI, M. T. Roasted coffee oil microencapsulation by spray drying and complex coacervation techniques: Characteristics of the particles and sensory effect**. Innovative Food Science & Emerging Technologies**, v. 72, p. 102739, 2021.

BORDÓN, M. G.; PAREDES, A. J.; CAMACHO, N. M.; PENCI, M. C.; GONZÁLEZ, A.; PALMA, S. D.; RIBOTTA, P. D.; MARTINEZ, M. L. Formulation, spray-drying and physicochemical characterization of functional powders loaded with chia seed oil and prepared by complex coacervation. **Powder Technology**, v. 391, p. 479-493, 2021.

CÂNDIDO, T. L. N.; SILVA, M. R.; AGOSTINI-COSTA, T. S. Bioactive compounds and antioxidant capacity of buriti (*Mauritia flexuosa* L.f.) from the Cerrado and Amazon biomes. **Food Chemistry**, v. 177, p. 313-319, 2015.

CARVALHO, C. O. **Comparação entre métodos de extração do óleo de *Mauritia flexuosa l.f.* (ARECACEAE - buriti) para o uso sustentável na reserva de desenvolvimento tupé: rendimento e atividade antimicrobiana.** 2011, 100 f. Dissertação (Mestrado em Biotecnologia e Recursos Naturais) – Universidade do Estado do Amazonas, Manaus, 2011.

CRUZ, M. B.; OLIVEIRA, W. S.; ARAÚJO, R. L.; FRANÇA, A. C. H.; PERTUZATTI, P. B. Buriti (*Mauritia Flexuosa* L.) pulp oil as an immunomodulator against enteropathogenic *Escherichia coli*. **Industrial Crops and Products**, v. 149, p. 112330, 2020.

COSTA, A. M. M.; GASPAR, B. R. A.; CALADO, V.; TONONONCEPTUALIZATION, R. V.; TORRES, A. G. Microencapsulation of pomegranate (*Punica granatum* L.) seed oil by complex coacervation: Stability and application in an instant caffè latte beverage. **Food Chemistry**, v. 381, p. 132199, 2022.

GOUIN, S. Microencapsulation: industrial appraisal of existing technologies and trends. **Food Science and Technology**, v. 15, p. 330–347, 2004.

HUANG, Q.; WANG, X.; BU, X.; SONG, Y.; YOU, J.; ZHANG, C.; QIN, C.; QIN, J.; CHEN, L. Dietary vitamin A affects growth performance, immunity, antioxidant capacity, and lipid metabolism of juvenile Chinese mitten crab *Eriocheir sinensis*. **Aquaculture**, v. 548, p. 737556, 2022.

JÉGAT, C.; TAVERDET, L. J. Stirring speed influence study on the microencapsulation process an on the drug release from microcapsules. **Polymer Bulletin**, v. 44, p. 345-351, 2000.

JIA, C.; HUANG, S.; LIU, R.; YOU, J.; XIONG, S.; ZHANG, B.; RONG, J. Storage stability and in-vitro release behavior of microcapsules incorporating fish oil by spray drying. **Colloids and Surfaces A: Physicochemical and Engineering Aspects**, v. 628, p. 127234, 2021.

LEMETTER, C.Y.G.; MEEUSE, F. M.; ZUIDAM, N. J. Control of the morphology and the size of complex coacervate microcapsules during scale-up. **AIChE Journal**, v. 56, p. 1487-1496, 2009.

MEHNERT, W. E MADER, K. Solid lipid nanoparticles: production, characterization and applications. **Advanced Drug Delivery Reviews**, v. 47, n. 2, p. 165-196, 2001.

MEZZOMO, N. **Extração e encapsulamento de compostos com importância tecnológica e biológica proveniente do resíduo de processamento de camarão.** 2012, 261 f. Tese – (Doutorado em Engenharia de Alimentos), Universidade de Santa Catarina, Florianópolis, 2012.

RAMALHO, R. A.; ANJOS, L. A.; FLORES, H. Valores séricos de vitamina a e teste terapêutico em pré-escolares atendidos em uma unidade de saúde do rio de janeiro, brasil. **Revista Nutrição**, v. 14, n. 1, p. 5-12, 2001

RAMÍREZ-MACEDO, R. C.; VÉLEZ-RUÍZ, J. F. Physicochemical and Flow Properties of a Seated Yogurt Enriched with Microcapsules containing Omega 3 Fatty Acids. **Información Tecnológica**, v. 26, p. 87-96, 2015.

RIBEIRO, B. D. **Aplicação de Tecnologia Enzimática na Obtenção de β-Caroteno a partir de Óleo de Buriti (*Mauritia vinifera*)**. 2008, 103 f. Dissertação – (Mestrado em Tecnologia de Processos Químicos e Bioquímicos), Universidade do Rio de Janeiro, Rio de Janeiro, 2008.

SCHMITT, C.; TURGEON, S. L. Protein/polysaccharide complexes and coacervates in food systems. **Advances in Colloid and Interface Science**, v. 167, p. 63-70, 2011.

SOLOMANDO, J. C.; ANTEQUERA, T.; PEREZ-PALACIOS, T. Lipid digestion products in meat derivatives enriched with fish oil microcapsules. **Journal of Functional Foods**, v. 68, p. 103916, 2020.

SOUSA, S. V.; DIOGENES, L. V.; OLIVEIRA, R. L.; SOUZA, M. N. S.; MAZZA, P. H. S.; SILVA JÚNIOR, J. M.; PEREIRA, E. S.; PARENTE, M. O. M.; ARAÚJO, M. J.; OLIVEIRA, J. P. F.; BEZERRA, L. R. Effect of dietary buriti oil on the quality, fatty acid profile and sensorial attributes of lamb meat. **Meat Science**, v. 186, p. 108734, 2022.

THIES, C. Microencapsulation of flavors by complex coacervation. In: LAKKIS, J. M. **Encapsulation and controlled release Technologies in food systems.** Iowa: Blackwell Publishing Ltd., 2007, Chap. 7, p. 149 – 170.

THIES, C. A survey of microencapsulation processes. In: BENITA, S. **Microencapsulation: Methods and industrial applications.** New York: Marcel Dekker, Inc., 1996 Chap. 1, p. 1 - 19.

Tolkien, J. R. R. **The Lord of the Rings**, Londres: Harper Collins Publishers, 1991, p. 68.

CAPÍTULO 1

Revisão bibliográfica

1. REVISÃO BIBLIOGRÁFICA

1.1. Microencapsulação

A microencapsulação pode ser descrita como um processo de empacotamento de matérias sólidos, líquidos e gasosos, utilizando como revestimento materiais poliméricos, que individualmente formam as chamadas microcápsulas. O polímero forma um filme em torno do material encapsulado e irá funcionar como barreira a exposições não desejadas (SILVA et al., 2014). A ideia da microencapsulação teve como base o conceito da célula, em que um núcleo é revestido por uma parede celular que o protege do exterior, promovendo trocas controladas e a entrada e saída de substâncias celulares, o que pode ser simulado com o filme polimérico e o material encapsulado nas microcápsulas, em que, dado um gatilho específico, inicia-se a liberação do material embalado (SERVAT et al., 2010).

Os primeiros estudos sobre microencapsulação foram iniciados na década de 1930, no entanto o primeiro produto teve registro em 1954, sendo um papel de cópia sem carbono desenvolvido por uma empresa americana. O carbono foi substituído por microcápsulas contendo tinta que eram rompidas por pressão, liberando o conteúdo interno (SUAVE et al., 2006). Nos dias atuais as microcápsulas apresentam uma grande gama de aplicações nas áreas farmacêutica, alimentícia, cosmética, tendo cada uma sua aplicação específica.

A princípio a encapsulação visa garantir a proteção do seu núcleo, que geralmente é composto por substâncias sensíveis às condições do meio em que são armazenadas, podendo sofrer degradação em presença de luz, variações de temperatura e pH (SILVA et al., 2013). Além da proteção, a encapsulação apresenta a vantagem de promover uma possível liberação controlada, como abordado por De Vos et al. (2010), que reportaram que as microcápsulas podem resistir às condições de digestão no estômago, tendo o início de sua liberação somente no intestino.

Várias técnicas podem ser utilizadas para a produção de microcápsulas, as quais podem ser classificadas em físicas, químicas e fisico-químicas. A escolha da técnica utilizada depende do material a ser encapsulado, dos materiais de parede, além das características das microcápsulas desejadas, como a funcionalidade, tamanho e liberação (VANISKI et al., 2017). Os métodos de microencapsulação mais conhecidos são:

a) físico-químicos: coacervação simples ou complexa (separação em fase aquosa), emulsificação seguida de evaporação do solvente, pulverização em agente formador de reticulação e envolvimento lipossômico;

b) métodos físicos: spray drying, spray coating, spray chilling, gelificação iônica, leito fluidizado, extrusão, centrifugação com múltiplos orifícios, co-cristalização, liofilização;

c) métodos químicos: polimerização interfacial, inclusão molecular.

1.1.1. Coacervação complexa

O processo de microencapsulação por coacervação ocorre com a deposição do polímero sobre o núcleo a ser encapsulado; o gatilho para o início da deposição pode ser realizado de diferentes maneiras, sempre atuando no meio em que os polímeros estão solubilizados. Entre elas pode-se citar modificações de pH, força iônica, temperatura e polaridade (SILVA et al., 2014).

Segundo Azeredo (2005), o processo de microencapsulação por coacervação segue as seguintes etapas, as quais se encontram representadas na Figura 1.1.

• Dispersão do agente ativo a ser encapsulado em uma solução do polímero;

• Indução da coacervação, formando partículas de coacervado;

• Deposição das partículas de coacervado em torno dos núcleos contendo o princípio ativo;

• Coalescência das partículas de coacervado para formar uma camada polimérica;

• Endurecimento da camada polimérica por meio da difusão do solvente, adição de um agente reticulante ou mudança de temperatura.

Finalmente, as microcápsulas obtidas são separadas do sistema por centrifugação ou filtração.

Figura 1.1 Representação esquemática das etapas do processo de microencapsulação por coacervação.

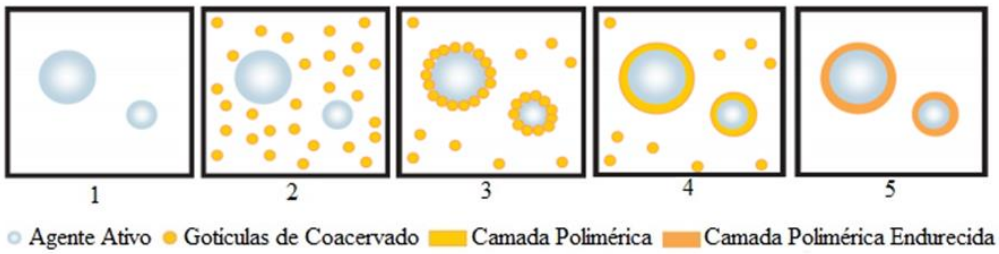

Fonte: Adaptado de MÜLLER, 2011.

O processo de coacervação complexa ocorre quando dois ou mais biopolímeros com uma carga líquida oposta são misturados em um solvente, de modo que, em suspensão, podem interagir. A interação entre os biopolímeros tem natureza eletrostática, tornando o processo de coacervação fortemente dependente da densidade de carga molecular, pH e força iônica. A coacervação também é dependente da proporção dos dois polímeros, visto que o poder eletrostático de interação depende do número de moléculas e dos sítios ativos disponíveis nas cadeias dos biopolímeros (PATHAK et al., 2017). Segundo Lemos et al. (2017), a agitação do sistema em que os polímeros se encontram dispersos tem efeito direto na forma e tamanho das microcápsulas obtidas, sendo que maiores valores de frequência de agitação geram menores tamanhos de microcápsulas.

A obtenção de microcápsulas por coacervação complexa é um processo relativamente simples, com baixos custos e utilizando temperaturas brandas. O processo é usualmente aplicado para encapsular materiais hidrofóbicos, como óleos vegetais. Uma das maiores desvantagens da coacervação é que ocorre apenas dentro de faixas limitadas de pH, concentrações de polímeros e força iônica, e envolvendo grandes volumes de água (COMUNIAN et al., 2013).

Atualmente alguns autores tiveram uma abordagem diferente para a produção de microcápsulas por coacervação complexa, como a tentativa de um processo contínuo ou semicontínuo (FERREIRA; e NICOLETTI, 2020; 2021a, b), além de um possível escalonamento para o aumento de escala, e para que isso ocorra, as condições operacionais utilizadas durante a complexação dos polímeros é de suma importância, e tais condições tem relação direta com a capacidade de produção e a morfologia apresentada pelas microcápsulas obtidas. Algumas condições de processo podem ser citadas, como a frequência de agitação empregada durante a coacervação, a concentração dos polímeros utilizados para a formação das microcápsulas, a temperatura utilizada,

além da viscosidade dos polímeros, todos esses fatores têm influência direta para a interação dos polímeros, de maneira mais simples, podem favorecer ou interferir no encontro desses polímeros favorecendo a sua complexação (PATHAK, et al., 2017).

1.1.2. Materiais de parede

1.1.2.1. Gelatina

A gelatina é muito utilizada na produção de microcápsulas por coacervação complexa devido às suas propriedades funcionais, como gelificação, estabilização, texturização, emulsificação, adesividade, sedimentação, e capacidade de encapsulamento (DURAK et al., 2016). Tais características fornecem à gelatina a capacidade de estabilizar a superfície das microcápsulas, fornecendo consistência e favorecendo a formação da parede das microcápsulas.

Além dessas características tecnológicas, a gelatina é amplamente difundida no mercado, obtida de peles, ossos e tendões de animais, sendo composta de glicina, prolina/hidroxiprolina em maior abundância e outros 17 aminoácidos. A prolina e a hidroxiprolina desempenham papel de reestruturação da gelatina durante a gelificação, o que favorece a formação de filmes (CHENA et al., 2015). Como é um subproduto de frigoríficos, apresenta um baixo custo em países como o Brasil - grande produtor de carne e derivados - favorecendo a sua utilização (DUCONSEILLE et al., 2015).

Como todas as proteínas, a gelatina apresenta caráter anfótero, ou seja, é capaz de variar a carga de sua cadeia dependendo da faixa de pH em que se encontra, o que a torna apropriada para o processo de coacervação complexa, favorecendo a interação polimérica pelas forças eletrostáticas (BADKE, 2017; MARFIL; 2014).

1.1.2.2. Goma arábica

A goma arábica é originária das regiões tropicais e sub tropicas do planeta, sendo altamente produzida em alguns países da África, como Nigéria e Sudão, a partir do exsudado das árvores de acácia (BEMILLER; HUBER, 2010).

Como a gelatina, a goma arábica é amplamente utilizada na produção de microcápsulas por coacervação complexa, sendo os dois polímeros o par mais usualmente aplicado para esse fim. A goma arábica é um polissacarídeo complexo, com a cadeia

altamente ramificada. A sua composição pode ser dividida em três partes: arabinogalactana, arabinogalactana-proteína e glicoproteína (BADKE, 2017). A parte arabinogalactana-proteína é a responsável pela característica de maior interesse da goma arábica, isto é, a função emulsificante. A fração proteica da arabinogalactana-proteína, atua na interface óleo-água da dispersão, favorecendo uma maior estabilidade da emulsão (BADKE, 2017). Outra característica importante é que, em baixos pHs, a goma arábica apresenta carga negativa, favorecendo a coacervação complexa, interagindo por forças de natureza eletrostática com a gelatina (SOUZA, 2016).

1.1.2.3. Alginato de sódio

Como a goma arábica, o alginato de sódio também é um polissacarídeo, no entanto menos estudado para a produção de microcápsulas. O alginato de sódio é proveniente de algas marinhas pardas, apresentando-se com função biológica estrutural e não nutricional, possuindo apenas ligações glicosídeas de cadeia linear (LIMA, 2018).

É muito utilizado na indústria alimentícia e farmacêutica devido a sua capacidade de formar géis quando em contato com água. Os géis formados são uniformes e insolúveis em água e termo-irreversíveis à temperatura ambiente, o que provê ao alginato vantagens para a utilização como material de parede para a produção de microcápsulas (COMAPOSADA et al., 2015; NOGUEIRA, 2017).

O alginato é um polímero natural, barato, biodegradável, de fácil acesso, além de atóxico, o que o torna amplamente utilizado como material encapsulante e formador de filmes, não necessitando de solventes ou elevadas temperaturas para a sua utilização (FUJIWARA et al., 2010).

1.2. Métodos de secagem

A técnica de microencapsulação por coacervação complexa consiste em formação da emulsão base, formação das microcápsulas através de um gatilho, separação das microcápsulas do solvente e pôr fim a secagem das microcápsulas. Neste trabalho três técnicas de secagem serão avaliadas na produção das microcápsulas: a liofilização, a secagem por espuma e a secagem por filme delgado. A liofilização é a técnica de secagem mais utilizada para a secagem de microcápsulas, apresentando produtos de alta qualidade, mas é um processo longo e demanda muita energia, por isso técnicas alternativas para a

secagem vêm sendo empregadas para a desidratação das microcápsulas. Algumas técnicas permitem a produção de partículas individuais, utilizando baixas temperaturas, podendo ser mais econômicas que a liofilização e não agressivas ao material encapsulado, sendo elas a secagem por espuma e a secagem por filme delgado (QUADRI; SRIVASTAVA; YOUSUF, 2020; HARDY; JIDEANI, 2017).

1.2.1. Liofilização

A desidratação por liofilização é um processo usado para preservar alimentos com componentes sensíveis a variações de temperatura. Uma vez que não se utiliza temperatura alta para a remoção da água, esse método de desidratação produz alimentos secos com uma elevada qualidade em suas características sensoriais, mantendo cor, brilho, luz, odor, textura, sabor e valor nutricional. O processo pode ser descrito como "secagem por sublimação", removendo toda a água do alimento por transferência do líquido diretamente para a fase gasosa (HAMMAMI et al., 1999).

O processo de desidratação por liofilização pode ser separado em três etapas: a primeira fase, em que o produto é congelado; a secagem primária, em que a água e retirada por sublimação; e por fim, a secagem secundária, quando ocorre a dessorção, que seria a remoção da água ligada à estrutura base do material. As duas etapas de secagem são realizadas sob vácuo (TATTINI JUNIOR et al., 2006).

A etapa de congelamento imobiliza a água contida no produto e cessa as reações biológicas e químicas, além de ter influência direta nas etapas subsequentes, visto que o tamanho dos cristais pode influenciar na secagem. Congelamentos lentos causam a formação de maiores cristais de gelo, que darão origem aos poros criados na matéria seca (ORDÓÑEZ, 2005).

Na etapa de secagem primária, cerca de 80 - 90% do solvente congelado é retirado por sublimação com auxílio do vácuo presente na câmara de secagem. O interior da câmara fornece baixas pressões que geram o calor latente necessário para a remoção do solvente (SOARES, 2018).

Na última etapa do processo ocorre a retirada do solvente adsorvido ao material. A secagem secundária é essencial para a conservação do produto seco, já que ao eliminar quase toda água residual da secagem primária, garante um produto com baixa atividade de água, inibindo o desenvolvimento microbiológico (ARAÚJO et al., 2017).

1.2.2. Secagem por espuma

A secagem por é uma tecnologia muito empregada para a secagem de alimentos líquidos. Sua grande vantagem é reduzir o tempo de secagem e possibilitar a utilização de uma temperatura menor de secagem, o que pode evitar a degradação de alguns compostos sensíveis ao calor presentes nos alimentos. Esse menor tempo empregado durante a secagem também pode garantir menores alterações físicas nas propriedades dos alimentos, gerando pós que são facilmente reconstituídos e economicamente mais viáveis quando comparados com a secagem por liofilização ou por *spray drying* (KANDASAMY et al., 2014).

Esse método apresenta alta taxa de secagem em baixas temperaturas quando comparada com outras técnicas, como a secagem convectiva por exemplo, sendo a sua utilização adequada para todos os tipos de sucos e polpas, até mesmo os mais viscosos e pegajosos, obtendo um pó final com uma grande gama de aplicação em diversos seguimentos, como em padarias, sorvetes e pastas (HARDY; JIDEANI, 2017).

O princípio dessa técnica de secagem é criar uma espuma com auxílio de agentes formadores de espuma, utilizando algum instrumento, geralmente agitadores, para a incorporação do ar, que gera um aumento da superfície de contato para uma secagem mais eficaz. O agente espumante deve garantir a estabilidade dessa espuma durante todo o processo. Durante a secagem, o vapor de água contido no produto escapa pelos canais e pelos vacúolos criados pela espuma aumentando a taxa de secagem (SHAFIQ, et al., 2020).

Além disso, os agentes espumantes podem regular significativamente as propriedades físico-químicas do pó final obtido, como a porosidade, estabilidade, cor e solubilidade em água. Sendo sempre importante considerar que a estrutura, expansão e estabilidade das espumas desempenham grande função durante a difusão da umidade durante a secagem (GAO, et al., 2022; FALADE; OLUWASANMI, 2021). Os principais agentes espumantes utilizados são a albumina, metilcelulose e a goma arábica, apresentando características boas e ruins para a produção e estabilidade das espumas. A albumina apresenta a característica anfifílica, atuando como emulsificante entre a fase continua e dispersa estabilizando a espuma, no entanto necessita de faixa de pH e força iônica adequada para um desempenho adequado. A metilcelulose é derivada da celulose e é um aditivo muito utilizado para ajudar na estabilidade da espuma das massas de bolos, sendo um bom emulsificante, porém o fator limitante do seu uso é que em maiores

concentrações gera uma sensação ruim na boca. A goma arábica é facilmente dissolvida em água e em baixas concentrações apresenta atividade de superfície, o que favorece a estabilidade de emulsões, porém a sua melhor performance acontece em soluções ácidas (HARDY; JIDEANI, 2017; IQBAL, et al., 2018).

1.2.3. Secagem por filme delgado

A teoria por trás da secagem de filmes é baseada no gradiente diferencial entre a pressão de vapor de água da superfície do produto e a pressão parcial de vapor de água no ar de secagem. A umidade presente no material sólido exerce uma pressão de vapor que é dependente de como a água está ligada ao sólido, de como é a estrutura do sólido e da sua temperatura. Já o ambiente, apresenta a sua pressão parcial de vapor que é relacionada à umidade relativa e à temperatura do ar em questão. Desse modo, a água presente no interior do material migra para a superfície para a sua evaporação, se iniciando a secagem. A secagem ocorre pelos processos de transferência de massa e calor que podem ser conduzidos pelas diferentes formas de propagação de calor, como condução e convecção e irradiação (CHIRIFE, 1983; GEANKOPLIS, 1993).

Muitos estudos utilizaram a secagem por ar quente em estufa de circulação forçada, esse é um método direto de secagem, onde o ar aquecido empregado “rouba” o solvente volátil do material que está sendo seco. O sistema é fechado e o ar é sugado por uma tubulação, até a câmara de aquecimento, onde o mesmo é aquecido até a temperatura desejada e levado para a câmara de secagem. O ar aquecido entra em contato e arrasta a temperatura presente no produto, o que pode reduzir o tempo de secagem quando comparada a secagem com ar sem circulação (FOUST et al., 1982; RATTI, 2001).

Inicialmente os filmes se encontram em forma de suspensão; se são secos em altas temperaturas podem resultar em altas taxas de evaporação do solvente, podendo formar materiais mais secos e amorfos, e essas altas taxas podem criar bolhas que afetam a estrutura final dos filmes, já que, a aparição das bolhas pode formar cavidades tornando a espessura não uniforme (BANKER, 1966; DEVAVI et al., 2009).

No entanto a secagem é o fator limitante na produção de filmes, sendo a temperatura o maior fator de influência nas caraterísticas finais. Além da formação de bolhas, altas temperaturas podem afetar as características físico-química os materiais formadores dos filmes, afetando diretamente a sua estrutura. Por isso, é recomendado a

secagem em baixas temperaturas, mesmo que, o fator econômico seja prejudicado (BAGHERI, et al., 2019; DEVAVI et al., 2009).

1.3. Agitação e mistura

A agitação é uma operação unitária que visa a movimentação de um material induzido por um equipamento, com o objetivo de movimentar um fluido em uma direção específica, geralmente dentro de um tanque, utilizando-se de impulsores giratórios que produzem um perfil circulante. Tal operação promove a dispersão de líquidos miscíveis, troca de calor, aceleração de reações químicas e físicas, redução da aglomeração de partículas entre outros (MENEGALLI et al., 2016).

Essa operação unitária é amplamente empregada na indústria química e de alimentos, por isso, o seu estudo buscando a maior eficiência e otimização do processo é amplamente realizado, visando um menor custo de produção e operacional e uma maior eficiência e qualidade do projeto. Nagata (1975), dividiu as aplicações de mistura em grupos, que são apresentados na Tabela 1.1.

Tabela 1.1 Processos de mistura

Processo físico	**Classe de aplicação**	**Processo químico**
Suspensão	Líquido-sólido	Dissolução
Dispersão	Líquido-gás	Absorção
Emulsão	Líquidos imiscíveis	Extração
Mistura	Líquidos miscíveis	Reação
Bombeamento	Movimentação de fluido	Transferência de calor

Fonte: Nagata et al., 1975.

A mistura entre o conteúdo dentro do tanque ocorre pelos impelidores, que são impulsores giratórios. O que determina a velocidade de movimentação do fluido contido dentro do tanque, segundo Perry (1986), são três componentes de movimentação, a axial, a radial e a tangencial. A radial tem a direção de descarga coincidente com a normal do eixo de agitação, a axial tem direção paralela ao eixo de agitação e a tangencial tem a característica de criar o movimento circular ao redor do eixo de agitação.

A taxa de agitação do fluido impulsionada pelo impelidor é classificada pela velocidade empregada, podendo ser classificada em fraca, moderada ou vigorosa. A velocidade empregada e o impelidor utilizado devem ser suficientemente fortes para atingir todos os lugares do tanque carregando a energia dissipada de atrito, devido à força cisalhante. Esse cisalhamento é gerado devido à diferença de velocidade entre dois pontos do líquido contido no recipiente, sendo de suma importância quando se deseja dissipar aglomerados e promover a mistura de materiais com viscosidades discrepantes (SILVA e SABIONI, 2013; BORGES, 2021).

1.3.1. Relações geométricas

Devido à complexidade existente nos processos de agitação e mistura, e os diferentes componentes presentes em um tanque de agitação, o projeto desses sistemas são realizados basicamente utilizando o método de semelhança de sistemas, que é baseada na análise dimensional, seguindo as etapas de escolha do impulsor, cálculo das dimensões geométricas, cálculo da frequência rotacional do impulsor e o cálculo da potência requerida. A utilização dessas relações tem o intuito de facilitar a fabricação desses tanques, a Figura 1.2 apresenta as dimensões utilizadas no projeto dos tanques e a Tabela 1.2, apresenta os as correlações entre as mesmas (MENEGALLI, et al., 2016; RIBEIRO, 2012).

Figura 1.2 Dimensões de um tanque agitado.

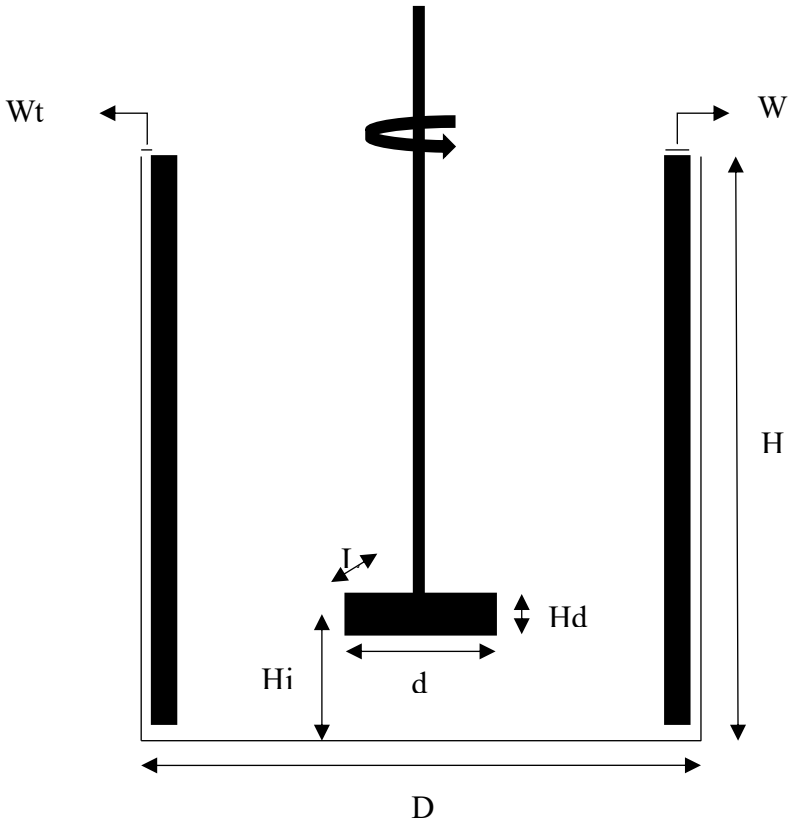

Fonte: elaborado pelo próprio ator.

Tabela 1.2 Correlações para o desenvolvimento de um tanque de agitação

Codificação	Componente	Correlação	Valor da Correlação
H	Altura do tanque	H/d	3
Hi	Altura do impelidor	Hi/H	1/3
d	Diâmetro do impelidor	d/Dt	1/3
Dt	Diâmetro do tanque	Hi/d	1
w	Tamanho da pá	w/Dt	1/12
L	Largura do impelidor	d/4	-
Hd	Altura da hélice do impelidor	d/5	-

Fonte: Adaptado de MENEGALLI, et al., 2016; RIBEIRO, 2012.

Ciofalo et al. (1996), descreve que a montagem de um tanque com defletores busca dois objetivos: diminuir a formação de um vórtex ao redor da haste de agitação e favorecer o transporte do conteúdo dentro do recipiente. Os defletores minimizam o

movimento circular do fluido, resultando em uma superfície quase sempre lisa e plana, além de favorecer o movimento axial o que gera o aumento da taxa de mistura dentro do vaso de agitação.

No entanto, a presença de defletores pode criar zonas mortas em mistura de fluidos com maiores viscosidades, resultando em possíveis aglomerações ou incrustações, como demonstrado na Figura 1.3. Os defletores devem ser evitados em misturas onde os componentes possam ser susceptíveis ao cisalhamento criado pelas pontas dos defletores, como soluções que contenham cristais ou microrganismos (RIBEIRO, 2012).

Figura 1.3 Formação de vórtices em vasos agitadores com defletores.

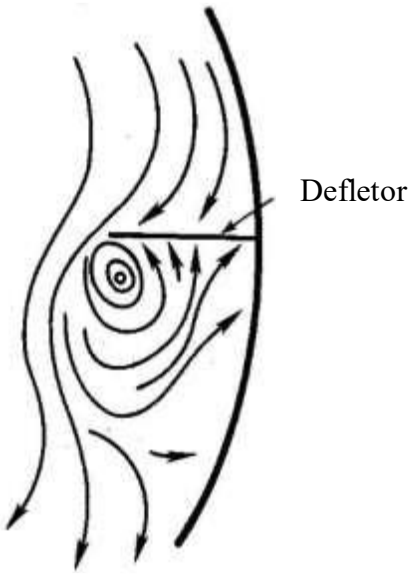

Fonte: adaptado de JAKOBSEN, 2008.

A Figura 1.4 apresenta o efeito que é possível observar macroscopicamente da presença de defletores em um tanque de agitação. Na imagem da esquerda da Figura 1.4, a superfície se mantém plana durante a agitação, enquanto na da direita a formação de um vórtice central durante a agitação é observada. De acordo com a frequência de agitação empregada, é natural que um vórtice seja formado mesmo com a presença dos defletores, esse vórtice é formado pela relação entre a força centrífuga, gerada pelo eixo de agitação que lança o fluido nas paredes do tanque gerando essa depressão no centro do tanque, com a força da gravidade que tem a tendência de manter a superfície do fluido plana, o equilíbrio entre essas forças pode ser expresso pelo número de Froude, representado pela Equação 1.1 (BUSCIGLIO et al., 2011).

$$\mathrm{Fr} = \frac{N^2 D_a}{g} \qquad \text{Equação 1.1.}$$

onde N é a velocidade de rotação (rps), D_a é o diâmetro do impulsor (m) e g a constante gravitacional ($m.s^{-1}$).

Figura 1.4 Efeito da presença de defletores durante a agitação em um vaso (adaptado de CIAFOLO et al., 1996).

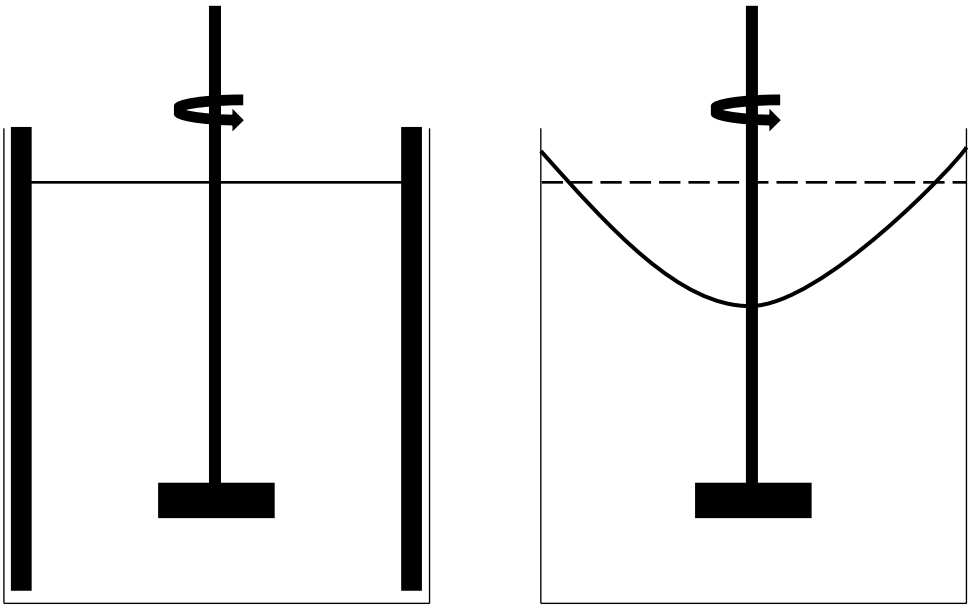

Fonte: Adaptado de Ciafolo et al., 1996.

1.3.2. Impulsores

A escolha do impulsor utilizado no processo de mistura não é tão trivial como parece. A sua escolha depende de estudos experimentais com os materiais que serão utilizados durante a agitação, para que o seu uso seja empregado de forma correta e eficiente. Perry (1986) dividiu os impulsores em duas classes diferentes de acordo com o escoamento produzido pelos mesmos, os impulsores axiais e os impulsores radiais. A Figura 1.5 apresenta os padrões de escoamento

Os impulsores axiais são muito aplicados em suspensões de sólidos, agitação de fluidos miscíveis e aumento da taxa de transferência de calor. Esse tipo de impulsor não causa tensão de cisalhamento, sendo utilizando em uma grande faixa de frequências rotacionais. Já os impulsores radiais atuam em regimes turbulentos ou de transição, sendo

bastante utilizados para a mistura de gases em líquidos; geralmente operam em altas frequências de agitação favorecendo essa turbulência, no entanto, quando as pás presentes em seu eixo são retas, apresentam bons resultados para produzir emulsões líquido-líquido (MENEGALLI, et al., 2016).

A frequência de agitação utilizada para a produção de microcápsulas por coacervação complexa é determinante na morfologia das microcápsulas, maiores frequências de agitação criam menores microcápsulas, no entanto, essa diminuição tem um limite, onde o tamanho médio das microcápsulas se aproximam de um valor constante. A frequência de agitação empregada também pode acarretar de maneira negativa, como a aparição de aglomerados, de espumas e bolhas (WU; e MCCLEMENTS, 2015; LEMOS et al., 2017; MA et al., 2019).

Figura 1.5 Padrões de escoamento em função do tipo do impulsor.

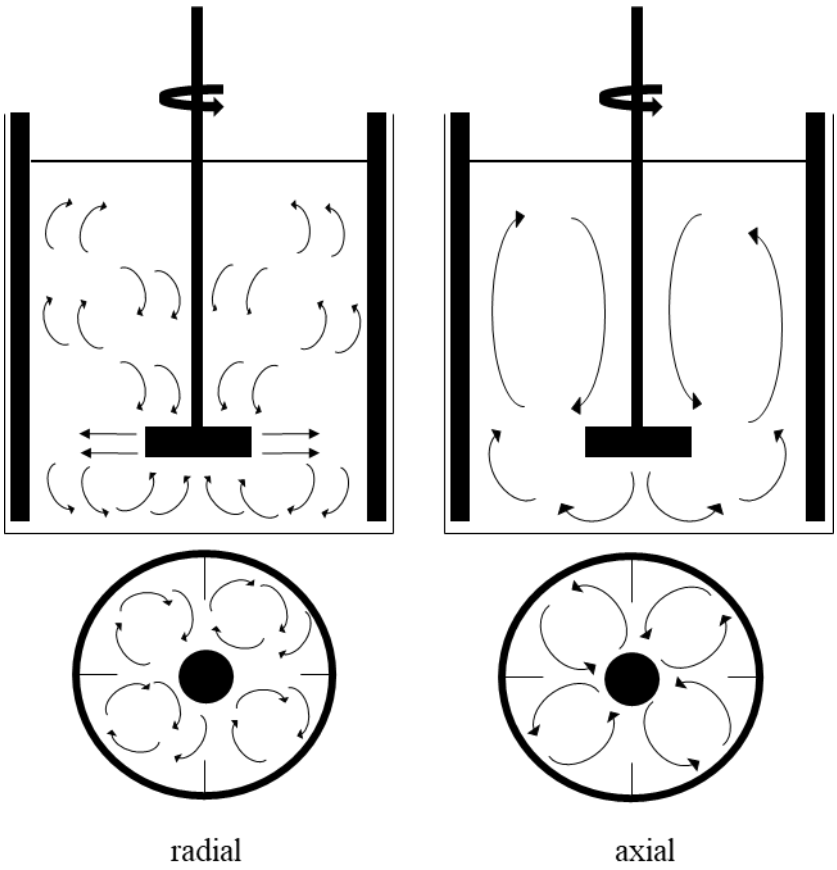

Fonte: adaptado de MENEGALLI et al., 2016

1.4. Aplicação de microcápsulas em alimentos

O enriquecimento ou fortificação de alimentos, é a adição de nutrientes ou suplementos nos produtos finais. Historicamente, a adição de fortificantes em alimentos se iniciou com caráter de saúde pública, onde micronutrientes eram adicionados em alimentos para combater doenças em pessoas com carências nutricionais, como por exemplo o raquitismo. Atualmente, esses fortificantes passaram a ser usados pelas indústrias com o foco em outros consumidores, que buscam nutrientes para uma dieta mais saudável (MARTIN et al., 2019).

A busca por esses alimentos se torna maior a cada dia, e os consumidores estão mais exigentes procurando alimentos capazes de influenciar beneficamente na saúde e na função corporal, além de atender às necessidades nutricionais básicas. Na ciência da nutrição, a atenção tem sido dada a elaboração e produção de alimentos funcionais utilizando compostos biotivos e nutracêuticos (JAMSHIDI et al. ,2020; RIVERO-PINO et al., 2020).

Os compostos mais comumente utilizados para enriquecer os alimentos são vitaminais e minerais ou produtos naturais que contenham esses componentes. No entanto, a estabilidade e a solubilidade desses compostos biológicos podem afetar significativamente as propriedades e a biodisponibilidade desses compostos, visto que, são facilmente influenciadas pelos parâmetros ambientais de armazenamento, como luz, temperatura, pH, oxigênio e umidade. Além disso, esses compostos podem sofrer interações moleculares com o próprio alimento em que é adicionado, perdendo as suas características ou promovendo propriedades organolépticas indesejáveis. Outro fator que pode afetar a sua aplicação é que esses compostos são consumidos oralmente e o trato gastrointestinal pode afetar a sua estrutura química e modificar a sua bioatividade (BERENDSEN et al., 2016; DELFANIAN; SHARI, 2020).

Por esses motivos a microencapsulação se configura como um método adequado para a incorporação de compostos bioativos em alimentos. Geralmente as técnicas de microencapsulação são aplicadas na indústria alimentícia em algumas circunstâncias, como na busca pela proteção dos compostos em relação ao meio ambiente, melhorar a entrega e a liberação, mascarar o sabor dos materiais presentes no núcleo, além de evitar a reação entre os compostos e a matriz alimentar em que será aplicado (DELFANIAN; SHARI, 2020).

Muitos estudos abordam o enriquecimento de alimentos com a utilização de microcápsulas pelos motivos citados acima. As microcápsulas são aplicadas em vários produtos da indústria alimentícia, como em bolos, em pães e alguns estudos já abordam sua aplicação como agente antimicrobiano. Mais recentemente a sua aplicação vem se expandindo, sendo encontradas em derivados lácteos e em snacks (KOUAMÉ et al., 2021; FIGUEIREDO et al., 2021; JAMSHIDI et al., 2020; WANG et al., 2015).

Outro produto que vem sendo estudado para a incorporação de microcápsulas são os extrusados. Nos últimos tempos a tecnologia de extrusão foi muito desenvolvida, com uma atenção especial para produtos extrusados enriquecidos com proteínas vegetais e animais, fibras alimentares, frutas e compostos bioativos como antocianinas e carotenoides. No entanto, os parâmetros operacionais utilizados durante a extrusão são deletérios para compostos sensíveis, visto que muitos deles são degradados a elevadas temperaturas e podem sofrer com o cisalhamento empregado durante o processo. Assim, a produção de produtos funcionais é dificultada por essa instabilidade da maioria dos compostos bioativos. Com isso a microencapsulação se torna alternativa para minimizar essa limitação, promovendo uma barreira protetora as condições geradas durante o processo de extrusão (DEHGHAN-SHOAR et al., 2010; FAVARO-TRINDADE et al., 2020).

1.5. Óleo de Buriti e seus principais compostos bioativos

O buriti é um fruto silvestre nativo de alguns estados das regiões Norte e Nordeste do Brasil e, atualmente, apresenta diversas aplicações, que vão de empregos nutricionais até medicinais. Apesar dos poucos estudos sobre a sua atividade funcional, existem alguns estudos demonstrando certo potencial fotoprotetivo devido ao alto teor de carotenoides, além de atividade antibacteriana e cicatrizante. Seus compostos bioativos vêm sendo recomendados para a prevenção de doenças degenerativas, apresentando grande ação antioxidante (ROCHA et al., 2017; SARAIVA; SILVA, 2017).

Segundo Gomes (2018), o buritizeiro é uma das espécies brasileiras com grande potencial socioeconômico, com produtos que são oriundos de todas as partes da palmeira. O tronco pode ser usado como estrutura para construções, as fibras utilizadas para a produção de redes de pesca e de dormir, construção de produtos artesanais, a polpa é utilizada com caráter alimentício, produzindo doces, bebidas e néctares e, com maior relevância, o óleo extraído da polpa apresenta várias aplicabilidades industriais.

O buriti (*Mauritia flexuosa L.*) é uma palmeira da família Arecaceae, ocorrendo em terrenos alagáveis e úmidos, e o óleo extraído da polpa dos seus frutos é composto principalmente por tocoferóis, clorofila, carotenoides e ácidos graxos (FERREIRA et al., 2017). O óleo de buriti é amplamente rico em β-caroteno, com valores de 30 mg para cada 100 g de polpa, números bem maiores que os apresentados pela cenoura, que são perto de 6,6 mg para cada 100 g de polpa (MANHÃES, 2007).

Porém, o β-caroteno é suscetível a degradações pela temperatura, umidade, oxidação durante o armazenamento, por isso o estudo da microencapsulação desse composto se torna viável para a proteção e aumento da vida de prateleira, além de vantagens no aspecto nutricional, medicinal e econômico. Muitos estudo vêm sendo realizados para a produção de microcápsulas de óleo de buriti e alguns com o enfoque nos parâmetros de produção das microcápsulas, como Lemos et al, (2017), que estudou a produção de microcápsulas de óleo de buriti por coacervação complexa utilizando o par gelatina/ alginato de sódio e explorou os efeitos da frequência de agitação durante a sua produção; Moser et al. (2019), estudou os parâmetros de produção por spray drying de microcápsulas de óleo de buriti utilizando proteínas de grão de bico.

REFERÊNCIAS

ARAÚJO, A.; PEREIRA, D.; AMARAL, F.; SOARES, J.; ALVES, J.; FERRARI, M.; RIBEIRO, M.; CORREIA, M.; PINHEIRO, P.; FÉLIX, R.; COVA, S.; SOUSA, V.; RIBEIRO, L. F. Dimensionamento de uma câmara de liofilização e de uma câmara de secagem por ar seco frio para alimentos *in* III Congresso Ibero-Americano de Empreendedorismo, Energia, Ambiente e Tecnologia. **Anais do III Congresso Ibero-Americano de Empreendedorismo, Energia, Ambiente e Tecnologia**. Bragança: Instituto Politécnico de Bragança, 2017. p. 355- 361.

AZEREDO, H. M. C. Encapsulação: aplicação à tecnologia de Alimentos. **Alimentos e Nutrição**, v. 16, n. 1, p. 89-97, 2005.

BADKE, L. B. **Síntese e caracterização de microcápsulas de gelatina/goma arábica contendo óleos essenciais ou ácidos graxos de microalgas empregados na cosmetologia pelo método de coacervação complexa**. 2017. 97 f. Dissertação de mestrado (em Engenharia e Ciência dos Materiais), Universidade Federal do Paraná, Curitiba, 2017.

BAGHERIA, F.; RADIA, M.; AMIRI, S. Drying conditions highly influence the characteristics of glycerol-plasticized alginate films. **Food Hydrocolloids**, v. 90, p. 162-171, 2019.

BANKER, G. S. Film coating theory and practice. **Journal Pharmacology Science**, v. 55, p. 81-891, 966.

BEMILLER, J. N.; HUBER, K. C. Carboidratos. In: DAMODARAN, S.; PRAKIN, K. L.; FENNEMA, O. R. **Química dos alimentos**. 4 Ed. Porto Alegre: Artmed, p. 75 – 130, 2010.

BERENDSEN, A. A. M.; LIESHOUT, L. E. L. M.; ELLEN G.H.M.VAN DEN HEUVEL, E. G. H. M. MATTHYS, C.; PÉTER, S.; GROOT, L. C. P. G. M.

Conventional foods, followed by dietary supplements and fortified foods, are the key sources of vitamin D, vitamin B6, and selenium intake in Dutch participants of the NU-AGE study. **Nutrition Research**, v. 36, p. 1171-1181, 2016.

BORGES, A. A. **Análise da interação ar-gliceirna na formação de vórtices em tanques de msitura de alto cisalhamento**. 2021. 36 f. Trabalho de conclusão de curso (Graduação em Engenharia Química), Faculdade de Engenharia de Várzea Grande, Universiade do Mato Grosso, Mato Grosso, 2021.

BUSCIGLIO, A.; GRISAFI, F.; SCARGIALI, F.; DAVÌ, M. L.; BRUCATO, A. Vortex Shape in Unbaffled Stirred Vessels: Experimental Study via Digital Image Analysis. **Chemical Engineering Transactions**, v. 24, p. 1387-1392, 2011.

CHIRIFE, J. **Fundamentals of the Drying Mechanism during Air Dehydration of Foods. In Advances in Drying**; Mujumdar, A.S.; Ed.; Hemisphere Publishing Corp.: Washington, DC, 1983; p. 73–102.

CHENA, S.; TANGA, L.; SUA, W.; WENGA, W.; OSAKOC, K.; TANAKAD, M. Separation and characterization of alpha-chain subunits from tilapia (Tilapia zillii) skin gelatin using ultrafiltration. **Food Chemistry**, v. 188, p. 350-356, 2015.

CIOFALO, M.; BRUCATO, A.; GRISAFI, F.; TORRACA, N. Turbulent flow in closed and free-surface unbaffled tanks stirred by radial impellers. **Chemical Engineering Science**, v. 51, p. 3557-3573, 1996.

COMAPOSADA, J.; GOU, P.; MARCOS, B.; ARNAU, J. Physical properties of sodium alginate solutions and edible wet calcium alginate coatings. **LWT - Food Science and Technology, v.** 64, n. 1, p. 212–219, 2015.

COMUNIAN, T. A.; THOMAZINI, M.; ALVES, A. J. G.; JUNIOR, F. E. M.; BALIEIRO, J. C. C.; FAVARO-TRINDADE, C. S. Microencapsulation of ascorbic acid by complex coacervation: Protection and controlled release. **Food Research International**, v.52, n.1, p.373-379, 2013.

DE VOS, P.; FAAS, M. M.; SPASOJEVIC, M.; SIKKEMA, J. Encapsulation for preservation of functionality and targeted delivery of bioactive food components. **International Dairy Journal**, v. 20, n. 4, p. 292-302, 2010.

DELFANIAN, M.; SAHARI, M. A. Improving functionality, bioavailability, nutraceutical and sensory attributes of fortified foods using phenolics-loaded nanocarriers as natural ingredients. **Food Research International**, v. 137, p. 109555, 2020.

DEHGHAN-SHOAR, Z.; HARDACRE, A. K.; BRENNAN, C. S. The physico-chemical characteristics of extruded snacks enriched with tomato lycopene. **Food Chemistry**, v. 123, p. 1117-1122, 2010.

DEVAKI, C. S.; SARASWATHI, G.; MATHURA, C. V.; SWAMY, V. S. S.; VASUDHEESH, C. P.; PREMAVALLI, S. Impact of supplementation of flaxseed based as mid morning snacks on school children. **The Indian Journal of Nutrition and Dietetics**, v. 46, p. 192-197, 2009.

DUCONSEILLE, A.; ASTRUC, T.; QUINTANA, N. et al. Gelatin structure and composition linked to hard capsule dissolution: A review. **Food Hydrocolloids**, v.43, p. 360-376, 2015.

DURAK, N. C. M. Z.; TOKER, O. S.; SAGDIC, O.; ARICI, M. An evaluation of Fourier transforms infrared spectroscopy method for the classification and discrimination of bovine, porcine and fish gelatins. **Food Chemistry**, v. 190, p. 1109-1115, 2016.

FALADE, K. O.; G. A. OLUWASANMI. Instant soups from cowpea varieties using foam-mat drying. **LWT**, v. 151, p. 112191, 2021.

FAVARO-TRINDADE, C. S.; PATEL, B.; SILVA, M. P.; COMUNIAN, T. A.; FEDERICI, E.; JONES, O. G.; CAMPANELLA, O. H. Microencapsulation as a tool to producing an extruded functional food. **LTW**, v. 128, p. 109433, 2020.

FERREIRA, L. S.; SANTOS, M. R. P.; FIGUEIRA, L. C.; NAGATA, K. M. R.; REMÉDIOS, C. M. R.; SOUSA, F. F. Caracterização de óleos e resinas vegetais da Amazônia por espectroscopia de absorção. **Scientia Plena,** v. 13, n. 1, 2017.

FERREIRA, S.; NICOLETTI, V. R. Microencapsulation of ginger oil by complex coacervation using atomization: Effects of polymer ratio and wall material concentration. **Journal of Food Engineering**, v. 291, p. 110214, 2021a.

FERREIRA, S.; NICOLETTI, V. R. Use of a tubular heat exchanger to achieve complex coacervation in a semi-continuous process: Effects of capsules curing temperature and shear rate. **Journal of Food Engineering**, v. 310, p. 110698, 2021b.

FIGUEIREDO, J. A..; SILVA, C. R. P.; OLIVEIRA, M. F. S.; NORCINO, L. B.; CAMPELO, P. H.; BOTREL, D. A.; BORGES, S. V. Microencapsulation by spray chilling in the food industry: Opportunities, challenges, and innovations. **Trends in Food Science & Technology**, v. 120, p. 274-287, 2021.

FOUST, A. S.; WENZEL, L. A.; CLUMP, C. W.; MAUS, L.; ANDERSEN, L. B. **Princípios das Operações Unitárias**, 2 Ed. LTC – Livros Técnicos e Científicos. Editora AS, Rio de Janeiro, 1982.

FUJIWARA, G. M.; KAMINSKI, G. T. A.; FIN, M. T.; SASSO, D. G. B.; TIBERIO, C. C.; MIGUEL, M. D.; ZANIN, S. M. W. Comparação entre os perfis de liberação de azul de metileno a partir de micropartículas de alginato-quitosana em pH ácido. **Visão Acadêmica**, v. 11, n. 2, p. 51-58, 2010.

GAO, R.; XUE, L.; ZHANG, Y.; LIU, Y.; SHEN, L.; ZHENG, X. Production of blueberry pulp powder by microwave-assisted foam-mat drying: Effects of formulations of foaming agents on drying characteristics and physicochemical properties. **LWT**, v. 154, p. 112811, 2022.

GEANKOPLIS, C. J. **Transport Processes and Unit Operations**, 3rd Ed. New Jersey: Inc Prentice Hall, 1993.

GOMES, R. M. S. **Óleo de buriti e babaçu na composição da dieta de ovinos**. 2018. 50 f. Dissertação (Mestrado em Ciência Animal). Universidade Federal do Maranhão, Chapadinha, 2018.

HAMMAMI, C.; RENÉ, F.; MARIN, M. Process–quality optimization of the vacuum freezedrying of apple slices by the response surface method. **International Journal of Food Science and Technology**, v. 34, p. 145–160, 1999.

HARDY, Z.; JIDEANI, V. A. Foam-mat drying technology: A review**. Critical Reviews in Food Science and Nutrition**, v. 57, p. 2560-2572, 2017.

IQBAL, M. J.; ABBAS, A.; RAFIQUE, H.; NAWAZ, M. F.; RASOOL, A. A review paper on foam-mat drying of fruits and vegetables to develop powders. **MOJ Food Process Technology**, v. 6, p. 465–467, 2018.

JAKOBSEN, H. A. **Packed Bed Reactors. Chemical Reactor Modeling**; Springer: Berlin, Heidelberg, Germany, 2009.

JAMSHIDI, A.; CAO, H.; XIAO, J.; SIMAL-GANDARAF, J. Advantages of techniques to fortify food products with the benefits of fish oil. **Food Research International**, v. 137, p. 109353, 2020.

KANDASAMY, P.; VARADHARAJU, N.; KALEMULLAH, S.; MALADHI, D. Optimization of process parameters for foam-mat drying of papaya pulp. **Journal of Food Science and Technology**, v. 51, p. 2526–2534, 2014.

KOUAMÉA, K. J. E. P.; BORA, A. F. M.; LI, X.; SUN, Y.; LIU, L. Novel trends and opportunities for microencapsulation of flaxseed oil in foods: A review. **Journal of Functional Foods**, v. 87, p. 104812, 2021.

LEMOS, Y. P.; MARFIL, P. H. M.; NICOLETTI, V. R. Particle size characteristics of buriti oil microcapsules produced by gelatin-sodium alginate complex coacervation: Effect of stirring speed. **International Journal of Food Properties**, v. 20, n. 2, p. 1438–1447, 2017.

LIMA, T. A. **Aplicação de nanopartículas de prata e titânio na melhoria das propriedades de filmes de alginato de sódio para uso em curativos**. 2018. 76 f. Dissertação (Mestrado em Ciência dos Materiais), Universidade Estadual Paulista, Ilha Solteira, 2018.

HARDY, Z.; JIDEANI, V. A. Foam-mat drying technology: A review. **Critical Reviews in Food Science and Nutrition**, v. 57, n. 12, p. 2560-2572, 2017.

MA, T.; ZHAO, H.; WANG, J.; SUN, B. Effect of processing conditions on the morphology and oxidative stability of lipid microcapsules during complex coacervation. **Food Hydrocolloids**, v. 87, p. 637-643, 2019.

MARFIL, P. H. M. **Microencapsulação de óleo de palma por coacervação complexa em matrizes de gelatina/goma arábica e gelatina/alginato.** 2014. 135 f. Tese (Doutorado em Engenharia e Ciência de Alimentos), Universidade Estadual Paulista, São José do Rio Preto, 2014.

MANHÃES, L. R. T. **Caracterização da polpa de buriti (*Mauritia flexuosa*): um potente alimento funcional**. 2007, 78 f. Dissertação (Mestrado em Ciência e Tecnologia de Alimentos). Universidade Federal Rural do Rio de Janeiro, Rio de Janeiro, 2007.

MARTIN, C. L.; CLEMENS, J.; MOSHFEGH, A. J. Items designated as fortified: Food and Nutrient Database for Dietary Studies (FNDDS), 2015–2016. **Journal of Food Composition and Analysis**, v. 84, p. 103255, 2019.

MENGALLI, F. C. TELIS, V. R. N., TELIS ROMERO, J. Bombeamento, agitação e mistura de fluidos alimentícios. In: TADINI, C. C., TELIS, V. R. N., MEIRELLES, A. J. A., FILHO, P. A. P. **Operações unitárias na indústria de alimentos**. São Paulo: LTC, 2015. Cap. 5, p 169-209.

MOSER, P.; FERREIRA, S.; NICOLETTI, V. R. Buriti oil microencapsulation in chickpea protein-pectin matrix as affected by spray drying parameters, **Food and Bioproducts Processing**, v. 117, p. 183-193, 2019.

MÜLLER, S. P. **Microencapsulação de óleo essencial de laranja**. 2011. 98 f. Dissertação (Mestrado em Tecnologia de Alimentos), Universidade Federal do Paraná, Curitiba, 2011.

NAGATA, S., N. YOSHIOKA, T. YOKOY AMA, **Mixing, Principles and Applications**, Universidade de Kyoto, 1975.

NOGUEIRA, M. T. **Extração e caracterização de alginato de sódio da macroalga *Sargassum cymosum C. Agardh*.** 2017. 58 f. Dissertação (Mestrado em Biociências), Universidade Estadual Paulista, Assis, 2017.

ORDÓÑEZ, J. A. **Tecnologia de alimentos: Componentes dos alimentos e processos.** Porto Alegre: Artmed, v.1, p.294, 2005.

PATHAK, J.; PRIYADARSHINI, E.; RAWAT, K.; BOHIDAR, H. B. Complex coacervation in charge complementary biopolymers: Electrostatic versus surface patch binding. **Advances in Colloid and Interface Science**, v. 250, p. 40–53, 2017.

PERRY, R. H.; CHILTON, C. H. **Chemical Engineers' Handbook**, 5th. edt., New York, McGraw-Hill Book Co, 1973.

QADRI, O. S.; SRIVASTAVA, A. K.; YOUSUF, B. Trends in foam mat drying of foods: Special emphasis on hybrid foam mat drying technology. **Critical Reviews in Food Science and Nutrition**, v. 60, n.10, p. 1667-1676, 2020.

RATTI, C. Hot air and freeze-drying-value foods: a review. **Journal of Food Engineering**, v. 49, p. 311-319, 2001.

RIBEIRO, D. C. **Modelagem e simulação do escoamento de sistemas multifásicos em reatores agitados mecanicamente**. 2012. 206 f. Tese (Doutorado em Engenharia Química), Universidade Federal de Santa Catarina, Florianópolis, 2012.

RIVERO-PINO, F.; ESPEJO-CARPIO, F. J.; GUADIX, E. M. Evaluation of the bioactive potential of foods fortified with fish protein hydrolysates. **Food Research International**, v. 137, p. 109572, 2020.

ROCHA, S. M.; RODRIGUES, M. T. O. S.; SILVA, D. S.; COSTA, F. M.; FILHO, O. F.; NUNE, Y. R. F.; ARRUDAS, S. R.; FIDÊNCIO, P. H. Efeito do armazenamento nas propriedades físico-químicas do óleo de *Mauritia flexuosa L. f.* (Arecaceae). **Caderno de Ciências Agrárias**, v. 9, n. 1, p. 31-37, 2017.

SARAIVA, L. C. F.; SILVA, R. B. Desenvolvimento de um creme à base de óleo de buriti (*Mauritia flexuosa*). **Revista FAESF**, v. 1, n. 1, p. 8-19, 2017.

SHAFIQ, Q. O.; SRIVASTAVA, A. K.; YOUSUF, B. Trends in foam mat drying of foods: Special emphasis on hybrid foam mat drying technology. **Critical Reviews in Food Science and Nutrition**, v. 60, p. 1667-1676, 2020.

SILVA, Ezequias, SABIONI, Lucas. Sistemas de agitação e mistura. 2013. 19p. Artigo cientifico – Faculdade de Tecnologia de Garça – FATEC. Garça, 2013.

SILVA, P. T.; FRIES, L. L. M.; MENEZES, C. R.; HOLKEM, A. T.; SCHWAN, C. L.; WIGMANN, E. F.; BASTOS, J. O.; SILVA, C. O. Microencapsulation: concepts, mechanisms, methods and some applications in food technology. **Ciência Rural**, v. 44, n.7, p.1304-1311, 2014.

SILVA, F. C.; FONSECA, C. R.; ALENCAR, S. M.; THOMAZINI, M.; BALIEIRO, J. C. C.; PITTIA, P.; FAVARO-TRINDADE, C. S. Assessment of production efficiency, physicochemical properties and storage stability of spray-dried propolis, a natural food additive, using gum Arabic and OSA starch-based carrier systems. **Food and Bioproducts Processing**, v. 91, n. 1, p. 28-36, 2013.

SOARES, C. T. **Secagem da polpa de pequi por liofilização**. 2018. 96 f. Dissertação (Mestrado em Engenharia Agrícola), Universidade de Campinas, Campinas, 2018.

SUAVE, J.; DALL'AGNOL, E. C.; PEZZIN, A. P. T.; SILVA, D. A. K.; MEIER, M. M.; SOLDI, V. Microencapsulação: Inovação em diferentes áreas. **Revista Saúde e Ambiente**, v. 7, n. 2, p. 12-20, 2006.

SERVAT, L.; SPINDOLA, H. M.; RODRIGUES, R. A. F.; FOGLIO, M. A. Microencapsulação: uma Alternativa Promissora para Preservação de Produtos Naturais. **Revista Fitos**, v. 5, n. 2, p. 52-57, 2010.

SOUZA, V. B. **Extração e encapsulação por coacervação complexa das proantocianidinasda canela (*Cinnamomum zeylanicum* Blume)**. 2016. 184 f. Tese (doutorado em Ciências da engenharia de alimentos), Universidade de São Paulo, Pirassununga, 2016.

TATTINI JUNIOR, V.; PARRA, D. F.; PITOMBO, R. N. M. Influência da taxa de congelamento no comportamento físico-químico e estrutural durante a liofilização da albumina bovina. **Revista Brasileira de Ciências Farmacêuticas**, v. 42, n. 1, p. 127-136, 2006.

VANISKI, R.; CORTI, D.; DRUNKLER, D. A. Técnicas e materiais empregados na microencapsulação de probióticos. **Brazilian Journal of Food Research**, v. 8, n. 1, p. 156-184, 2017.

WANG, B.; VONGSVIVUT, J.; ADHIKARI, B.; BARROW, C. J. Microencapsulation of tuna oil fortified with the multiple lipophilic ingredients vitamins A, D_3, E, K_2, curcumin and coenzyme Q_{10}. **Journal of Functional Foods**, v. 19, p. 893-901, 2015.

WU, B.-C.; MCCLEMENTS, D. J. Functional hydrogel microspheres: Parameters affecting electrostatic assembly of biopolymer particles fabricated from gelatin and pectin. **Food Research International**, v. 72, p. 231-240, 2015.

CAPÍTULO 2

DESIGN AND OPERATIONAL PARAMETERS OF THE STIRRED VESSEL AFFECT FORMATION OF OIL MICROCAPSULES BY COMPLEX COACERVATION

2. DESIGN AND OPERATIONAL PARAMETERS OF THE STIRRED VESSEL AFFECT FORMATION OF OIL MICROCAPSULES BY COMPLEX COACERVATION

Abstract

Microencapsulation by complex coacervation using a stirred vessel proved to be effective for the production of buriti oil microcapsules using gum Arabic and gelatin as wall materials. The produced microcapsules resulted in high values of encapsulation efficiency and their physical properties were affected by the process parameters, mainly those associated to the fluid dynamics in the stirred vessel. The processing parameters were expressed by the dimensionless numbers Reynolds and Froude of agitation. Higher Reynolds values resulted in lower particle size values, and higher Froude values resulted in smaller particle size distributions.

2.1. Introduction

Complex coacervation is a well-known and valuable microencapsulation technique, highly indicated for the enveloping of oils - when starting with a single oil-in-water emulsion - or even for encapsulating hydrophilic compounds - when starting with a double water-in-oil-in-water emulsion (COSTA et al., 2020; FRAJ et al., 2021). The process is based on the associative interaction between oppositely charged polymers, usually a protein and a polysaccharide, which must be highly dispersed in an aqueous suspension. The molecular interactions involved in complex coacervation have an electrostatic nature, making the process strongly dependent on the molecular weight density, pH, and ionic strength. Coacervation is also dependent on the proportion between the two polymers, since the electrostatic interaction depends on the amount of blending, as well as on the active sites available in the polymer chains (PATHAK et al., 2017; MARFIL et al., 2018).

Microcapsules containing bioactive compounds have a wide range of applications in the pharmaceutical, food and cosmetic areas, each of them having a specific application. The primary goal of encapsulation is to guarantee protection for the core material, which usually consists of a compound that is sensitive to the conditions of the medium - light, temperature, pH - in which the microcapsules are stored (SILVA et al., 2013). In addition to protection, encapsulation has the advantage of a possible controlled

release; the microcapsules can withstand digestion in the stomach, initiating release of their content only under intestinal conditions (DE VOS et al., 2010). The functionality of the microcapsules, however, is linked to their morphological characteristics, which in turn are affected by the process conditions (ACH et al., 2015).

Despite alternative approaches have been presented to allow scaling up (CHAPEAU et al., 2017) or the implementation of complex coacervation as a continuous or semicontinuous process (FERREIRA; NICOLETTI, 2020; 2021a, b), the operational conditions during the biopolymer complexation are known to be a critical step to produce the required microcapsule morphology. In particular, in the traditional process configuration that uses an agitated vessel to perform the complexation, the stirring speed has proven to be crucial to define the shape and size of the microcapsules obtained. In general, the particle sizes and formation of polynucleated microcapsules decreased as the stirring rate increased up to certain limit, above which the sizes approached a constant value (WU; MCCLEMENTS, 2015; LEMOS et al., 2017) or secondary effects appeared, such as agglomeration (MA et al., 2019) and foam formation (LEMETTER et al., 2009). Nevertheless, the direct comparison of these results is limited due to the different types of agitation systems used, which varied from 2 L- or 50 L-standardized vessels stirred with a Rushton turbine (LEMETTER et al., 2009) to a magnetic stirring hotplate (WU; MCCLEMENTS, 2015).

Buriti (*Mauritia flexuosa* L.) is a wild fruit native from the Amazon region, where it usually grows in permanent or periodically flooded areas along rivers, forests and savannas in northern-central Brazil. In these areas, buriti palm tree plays a major role in ecology, economics, and culture. The oil obtained from the pulp of buriti fruits is considered as a source of high-added-value phytochemicals (SANTOS et al., 2015; FREITAS et al., 2017). Studies have demonstrated that buriti oil functionalities include photo protection potential due to its high carotenoid content, antibacterial and healing activities, and prevention of degenerative diseases due to the presence of antioxidant compounds (ROCHA et al., 2017; SARAIVA; SILVA, 2017). The high content of carotenoids - which are highly sensitive compounds - in the buriti pulp oil justifies its microencapsulation for increased preservation.

The aim of this work was to investigate the effects of different types of impellers, the presence of baffles, and stirring speed, expressed as dimensionless numbers – Reynolds and Froude - on the size and morphology of buriti oil microcapsules produced by complex coacervation between gelatin and gum Arabic.

2.2. Materials and Methods

2.2.1. Materials

Buriti oil (Amazon Oil, Brazil) was microencapsulated by complex coacervation using gelatin extracted from bovine skin, type B, with gel strength of 240 bloom (Gelita, Brazil) and gum Arabic (Dinâmica, Brazil). The pH adjustment of coacervation (3.5 ± 0.1) was performed with 99.7% acetic acid (Dinâmica, Brazil). The solutions were prepared using distilled water.

2.2.2. Methods

2.2.2.1. Design of the agitated vessel

The design of the jacketed vessel for the production of microcapsules by complex coacervation followed some relationships described by MENEGALLI et al. (2015) (Table 2.1). The relationships used describe the size of the vessel and its components, which are the agitator impellers and the deflectors. Figure 2.1 is the schematic representation of the stirring tank, radial and axial propellers.

Figure 2.1 Schematic of the stirring tank and its propellers.

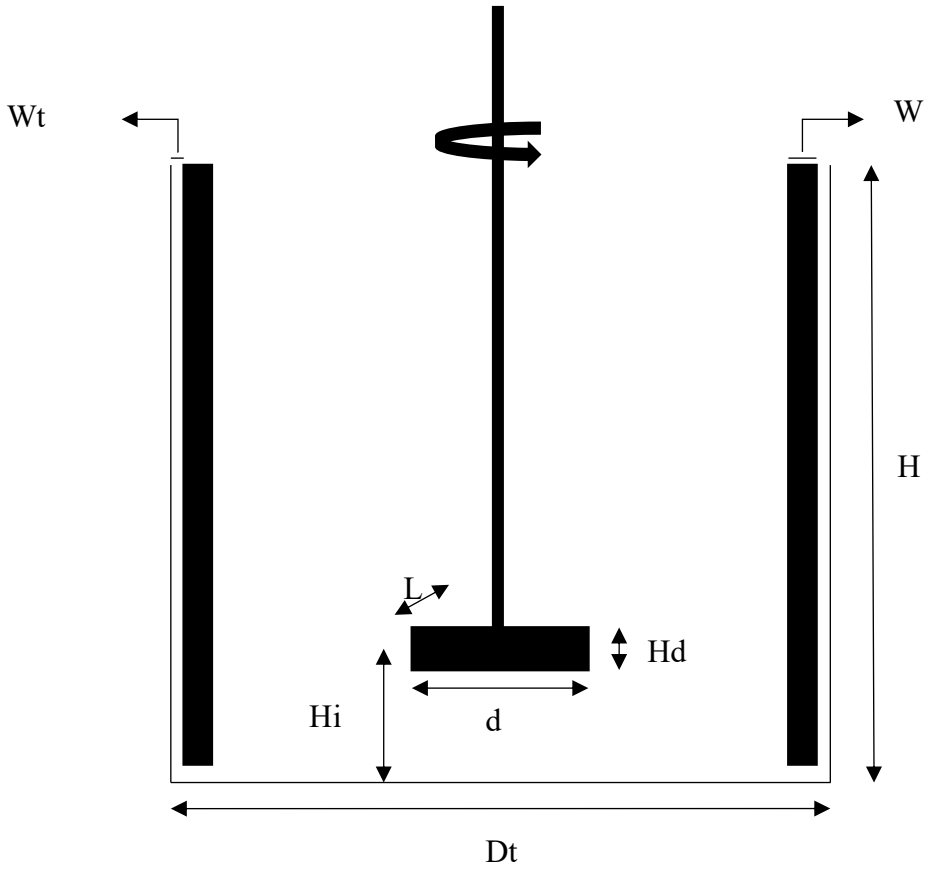

Source: prepared by the author himself.

Table 2.1 Correlations for the design of the stirring tank

Code	Component	Correlation	Correlation value
H	tank height	H/d	3
Hi	impeller height	Hi/H	1/3
d	impeller diameter	d/Dt	1/3
Dt	tank diameter	Hi/d	1
w	baffle size	w/Dt	1/12
L	impeller width	d/4	-
Hd	impeller propeller height	d/5	-

Source: prepared by the author himself.

2.2.2.2. Complex coacervation

The production of the microcapsules was carried out according to conditions shown in Table 2.2, based on the methodology described by Lemos et al. (2017) and Marfil et al. (2016). Initially solutions of gum Arabic (1% w / w) and gelatin (1% w / w) were stirred and heated 50 ± 3 °C until complete dispersion of the polymers. Buriti oil was incorporated (1% w/w) into the gelatin solution and homogenized using Ultraturrax (IKA, model T25, Germany) at 15,000 rpm for 5 min. Both solutions (in equal volumes of 500mL) were transferred to the jacketed stirred vessel for inducing the coacervation, which was triggered by adjusting the pH to 3.5 ± 0.01 using acetic acid and maintaining temperature at 50 ± 3 °C. In this step, different stirring frequencies were used, allowing to evaluate their influence on the microcapsules' production. The stirring was performed using a mechanical stirrer (Marconi, model MA 261, Brazil) and the frequencies tested were 400, 600, 800, 1000, 1200, 1600 and 2000 rpm. The agitation system consisted of two alternative stirring impellers - an axial flow impeller and a radial flow impeller - in addition to removable coupled baffles; the effects of these components were studied during the production of the microcapsules.

After coacervation, stirring was interrupted and the dispersion inside the jacketed vessel was cooled to 10 ± 2 °C with the aid of cooling water flowing from a thermostatic bath. Then, the dispersion was transferred to a beaker, covered with aluminum foil for protection from light, and stored for 24 hours in a refrigerator (Consul, model 280, Brazil) at 5 °C for complete sedimentation of the microcapsules. Finally, the dispersion was filtered and the coacervates were placed in aluminum trays and frozen in an ultra-freezer (Liobrás, model FV 500, Brazil) at -40 °C for 24 hours, followed by freeze drying (Liobrás, model L101, Brazil) for approximately 72 h. The dried microcapsules were comminuted in a mortar, protected from light and stored in a desiccator to be characterized.

2.2.2.3. Determination of the hydrodynamic conditions during coacervation

The hydrodynamic conditions during coacervation were characterized by the Reynolds (Re, Equation 2.1) and Froude (Fr, Equation 2.2) numbers:

$$Re = \frac{\rho N D_a^2}{\eta_{ap}} \tag{2.1}$$

$$\mathrm{Fr} = \frac{N^2 D_a}{g} \quad (2.2)$$

in which ρ is the emulsion density (kg·m^{-3}), *N* is the rotational velocity (rps), D_a is the impeller diameter (m), η_{ap} is the apparent viscosity (Pa·s) of the coacervate suspension at the shear rate ($\dot{\gamma}$, s^{-1}) corresponding to *N*, and g the gravitational constant (m·s^{-1}).

The shear rate at the rotational speed *N* was estimated according to Equation 3.1 (STEFFE, 1996):

$$\dot{\gamma} = \frac{d\Omega}{D-d} \quad (3.1)$$

in which *d* is the impeller size (m), *Ω*the stirring speed (s^{-1}), *D* is the vessel diameter (m). The rheological behavior of the emulsion was evaluated in shear rates varying from 1 to 1000 s^{-1}, at 50 ºC, using a rotational rheometer (AR2000ex, TA Instruments, New Castle, USA) with concentric cylinders geometry.

The Power Law model (Equation 2.4) was fitted to the experimental flow curves.

$$\tau = k\dot{\gamma}^n \quad (2.4)$$

in which τ is the shear stress (Pa), *k* is the consistency index (Pa·s), and *n* is the flow behavior index (dimensionless).

2.2.2.4. Characterization of the microcapsules

The particle size distribution was determined from images obtained by optical microscopy (Olympus, model CX31RTSF, Japan). The excess water was removed and the particles were assessed using the CellSens 1.11 image analysis software (Olympus, Japan). Figure 2.2 shows a typical image used for particle size measurement with the applied software. Three slides were prepared for each treatment, with 100 particles from each slide being analyzed individually. The data collected were treated statistically.

Figure 2.2 Particle size analysis by CellSens software 1.11.

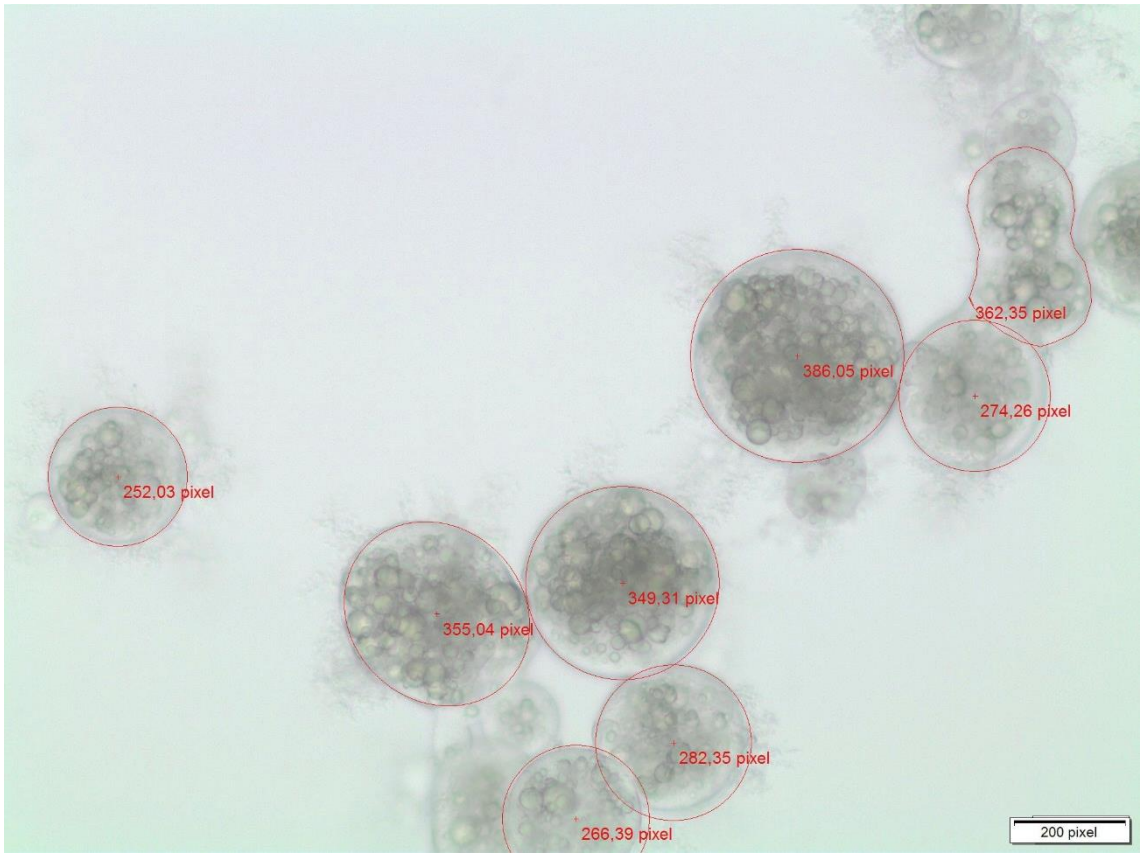

Source: prepared by the author himself.

The morphology of the microcapsules was evaluated in three steps of the production process: After coacervation, after freeze-drying and after rehydration. The samples were placed on slides and assessed using an optical microscopy (Olympus, CX31) coupled to an 8.1-megapixel digital camera (Sony Cyber-Shot, DSC-W150).

Color analysis was performed using a Konica Minolta colorimeter (CR-S, Konica Minolta, Japan). The color coordinates lightness (L^*), chroma (C^*) and hue angle (h), were measured with D65 illuminant and 10º observation angle.

The encapsulation efficiency (%*EE*) was calculated by quantifying the initial carotenoid content in the buriti oil (*EC*), the carotenoid content on the surface of the microcapsules and the total content of carotenoids in the microcapsules (*TC*), in triplicate, as described by Aranha (2015) with some modifications. The content of carotenoids

expressed in β-carotene was determined by Equation 2.5. The encapsulation efficiency was calculated by the Equation 2.6.

$$C = \frac{Abs \times V \times 10^4}{2396 \times g} \quad (2.5)$$

$$\%EE = \frac{EC}{TC} \times 100 \quad (2.6)$$

2.2.2.5. Statistical analysis

The assays were repeated three times in sequence and the analyses were performed in triplicate. The values of the analytical determinations were subjected to analysis of variance (ANOVA) and mean comparisons by Tukey's test ($p < 0.05$) using the software Minitab 16.1.1.

2.3. Results and Discussion

The morphology of the microcapsules was greatly affected by the hydrodynamic conditions in the stirred vessel during coacervation. These conditions changed as a consequence of the stirring frequency - which varied from 400 to 2000 rpm -, different types of impellers that promoted radial or axial flow, in addition to the presence or absence of deflectors in the vessel. Figures 2.3 to 2.6 demonstrate the microcapsules shortly after coacervation, in which it is possible to observe that all the process parameters tested were successful for the production of microcapsules using the gelatin/gum Arabic pair. The microcapsules were polynucleated with rounded shape. The increase in the agitation frequency caused two effects when comparing the groups: the first is the clear reduction of the average particle size; the second is that, at high frequencies, bubbles began to appear with the buriti oil trapped only in the wall of the microcapsules and not inside, as shown in Figure 2.7.

Figure 2.3 Optical microscopy of microcapsules produced in the vessel equipped with radial impeller and deflectors, at different stirring frequencies: a) 400 rpm, b) 600 rpm, c) 800 rpm, d) 1000 rpm, e) 1200 rpm, f) 1600 rpm, g) 2000 rpm (bar is equal to 50 μm).

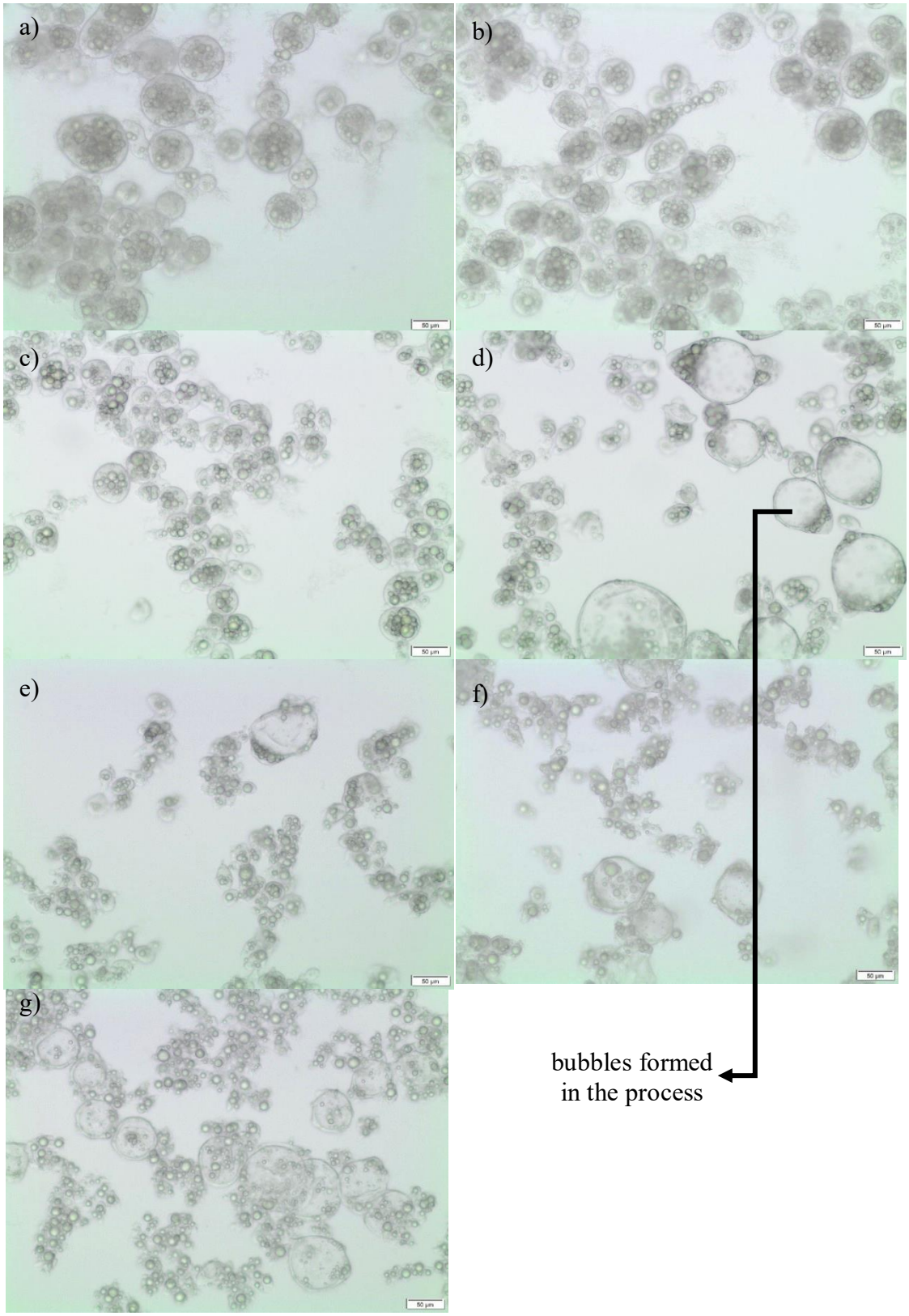

Source: prepared by the author himself.

Figure 2.4 Optical microscopy of microcapsules produced in the vessel equipped with radial impeller without deflectors, at different stirring frequencies: a) 400 rpm, b) 600 rpm, c) 800 rpm, d) 1000 rpm, e) 1200 rpm, f) 1600 rpm, g) 2000 rpm (bar is equal to 50 μm).

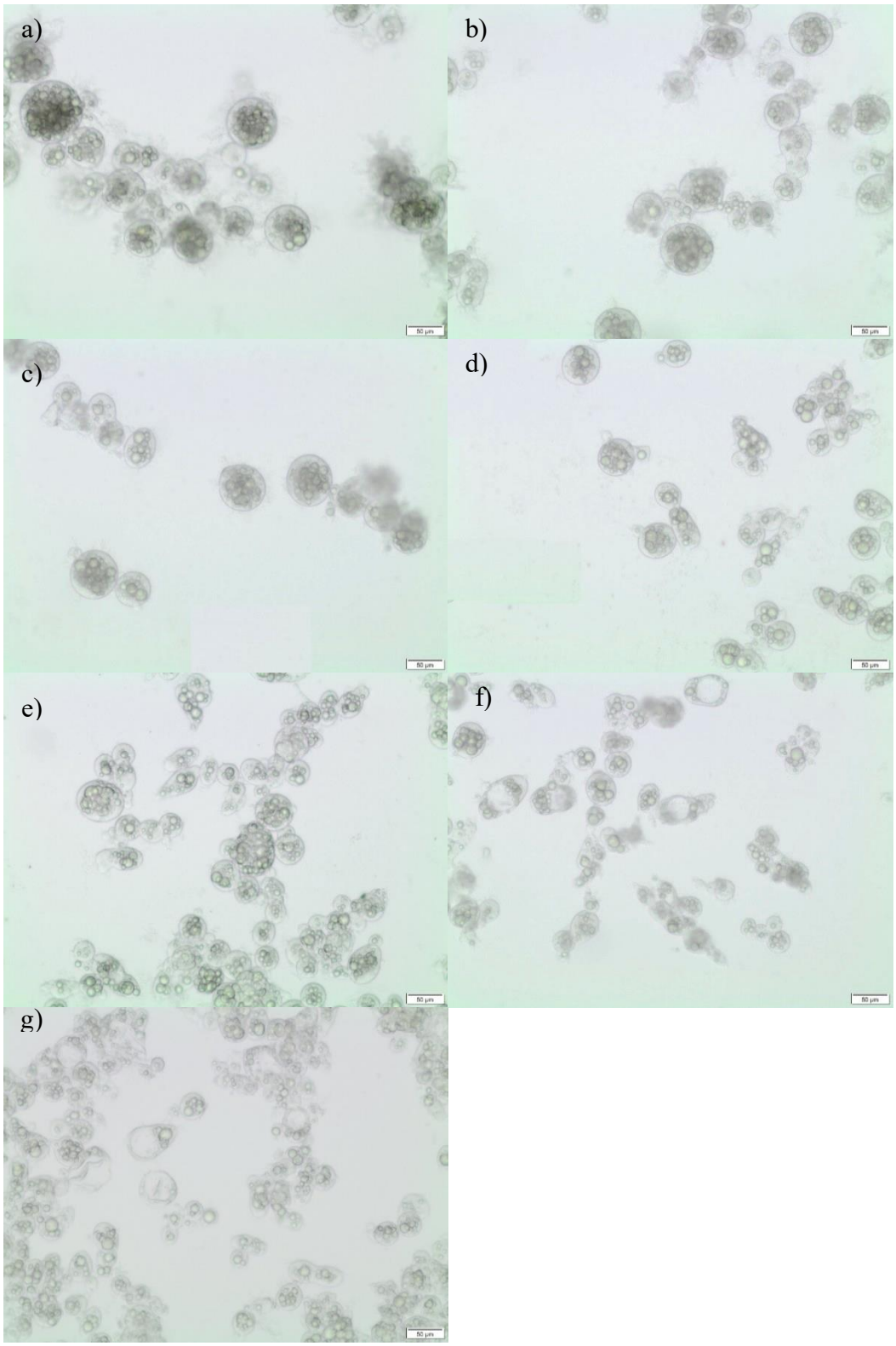

Source: prepared by the author himself.

Figure 2.5 Optical microscopy of microcapsules produced in the vessel equipped with axial impeller and deflectors, at different stirring frequencies: a) 400 rpm, b) 600 rpm, c) 800 rpm, d) 1000 rpm, e) 1200 rpm, f) 1600 rpm, g) 2000 rpm (bar is equal to 50 μm).

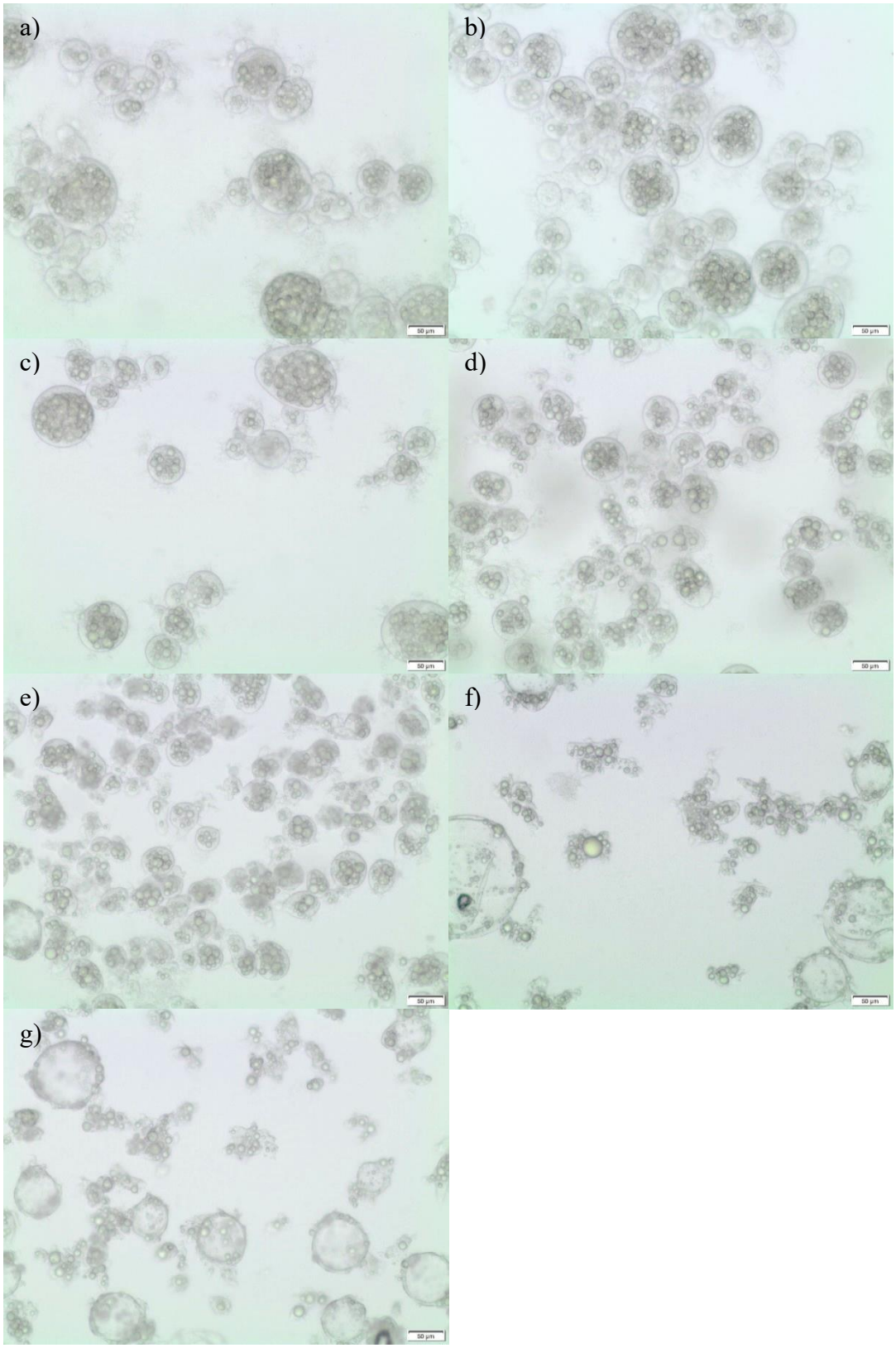

Source: prepared by the author himself.

Figure 2.6 Optical microscopy of microcapsules produced in the vessel equipped with axial impeller without deflectors, at different stirring frequencies: a) 400 rpm, b) 600 rpm, c) 800 rpm, d) 1000 rpm, e) 1200 rpm, f) 1600 rpm, g) 2000 rpm (bar is equal to 50 μm).

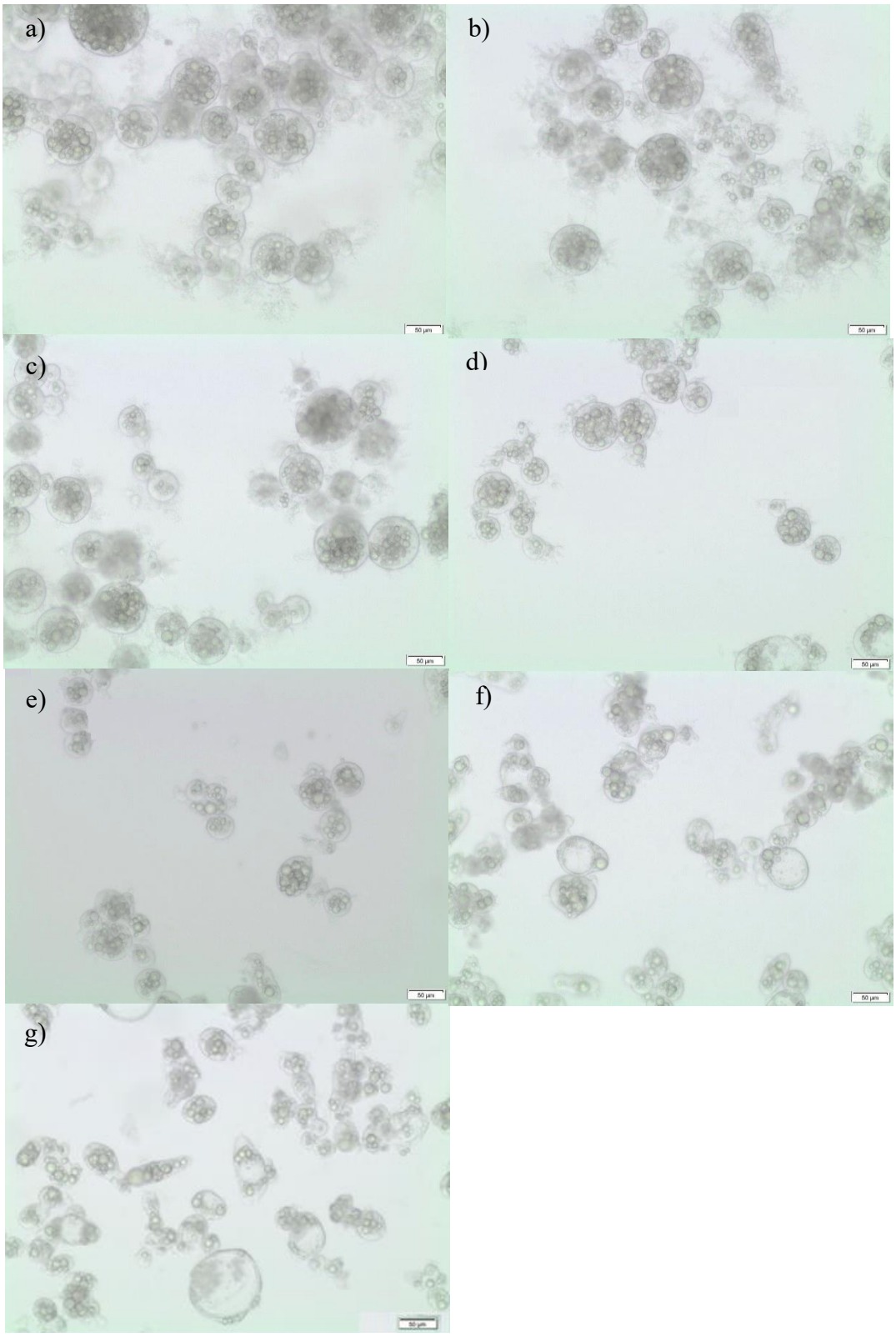

Source: prepared by the author himself.

Figure 2.7 Representation of the bubbles formed during coacervation (bar is equal to 200 μm).

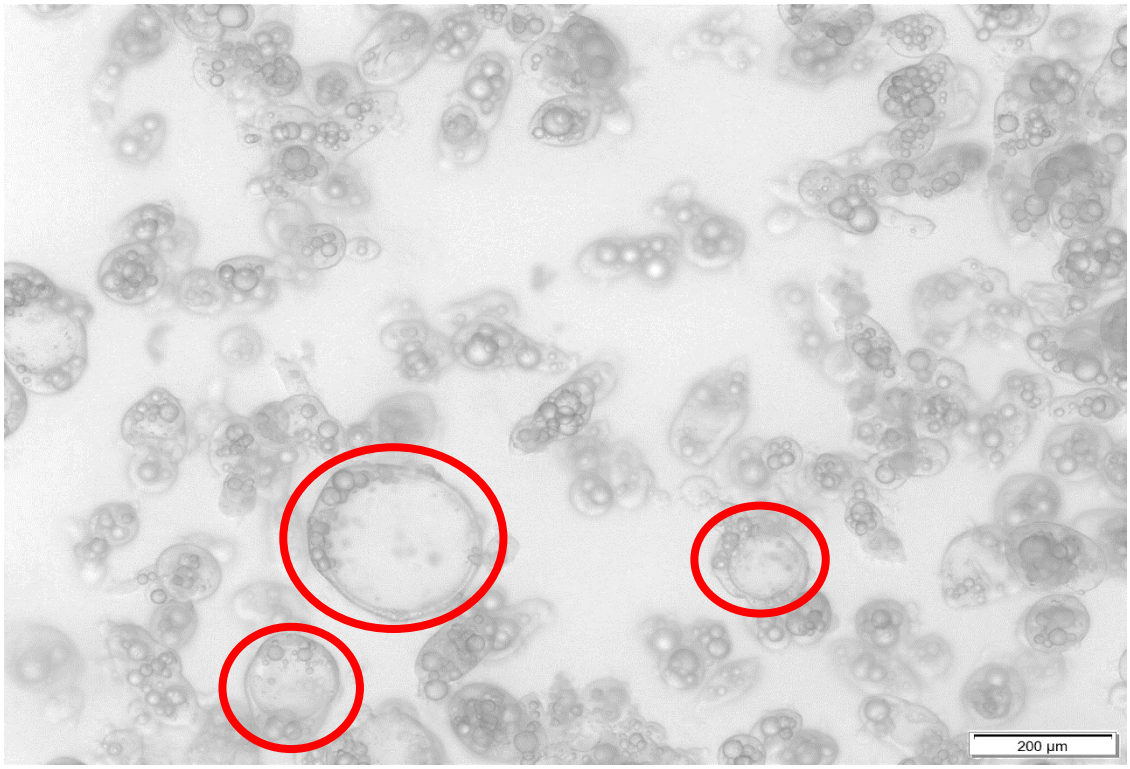

Source: prepared by the author himself.

2.3.1. Influence of hydrodynamic conditions during coacervation on particle size

The mean diameter of the produced microcapsules, including all the process conditions assayed, varied from 29.1 to 111.5 μm (Table 2.2), being important to note that these average values were calculated excluding the bubbles, as they did not result in solid particles after drying and thus, were not observed after rehydration.

Taking into account the values in Table 2.2, the influence of the stirring frequency is easily observed, as the increase in rotational frequency caused a decrease in the average particle diameter, independently of the vessel configuration. This same trend was found by Lemos et al. (2017) and Jégat and Taverdet (2000). On the other hand, when comparing the different vessel configurations at the same stirring frequency, it is possible to observe that the samples produced with radial impellers were smaller than those produced with the axial impellers. In addition, the presence of deflectors in the vessel also resulted in smaller average diameter for the microcapsules, except for frequencies of 400 and 600 rpm with the radial impeller. This can be explained by the energy input in the

system, combined with the turbulence degree of the suspension flow inside the vessel. Higher stirring frequencies input higher energy amount in the fluid and, consequently, result in smaller diameter values for the microcapsules. The presence of deflectors creates a larger disturbance in the flow profile. In addition, the radial impeller generates a higher turbulence in the fluid due to the agitation vessel configurations, as the vessel height is greater than its radius, and the radial impeller moves the fluid against the vessel wall, which being close to the impeller increases the turbulence that results from stirring.

In order to generalize the description of the effects of processing parameters and configurations on the size of the coacervated microcapsules, the hydrodynamic conditions in the stirred vessel were expressed by the dimensionless numbers Reynolds and Froude, calculated by Equations 2.1 and 2.2, respectively. To allow calculation of the Reynolds number (Equation 2.1), it was necessary to determine the apparent viscosity of the emulsion inside the vessel. This was obtained by fitting the Power Law model (Equation 2.4) to the rheological data, which resulted in a regression coefficient of 0.999, with the consistency index $k = 1.042^{-4}$ Pa·s and the flow behavior index $n = 1.495$.

The obtained values for Reynolds and Froude are shown in Table 2.3, which includes the values of the *span*, i.e., the distribution width of the particle size histogram, expressed as:

$$span = \frac{D_{90} - D_{10}}{D_{50}} \tag{2.7}$$

in which D_{90}, D_{50}, and D_{10}, are the particle diameters at which 90%, 50%, and 10% of the population lies below these values, respectively.

Table 2.3 indicates that most of the microcapsules were produced at laminar flow conditions, with Reynolds values < 10,000, except those produced with stirring frequencies greater than 1200 rpm (GABELLE et al., 2013), and the clear influence of the Reynolds number on the size of microcapsules is demonstrated in Figure 2.8, which shows a similar behavior to the observed by Lemos et al. (2017) and Lemetter et al. (2009). Such a decrease in particle size with increasing Reynolds number can be explained by the process of coacervation. The occurrence of complex coacervation depends on the polymer molecules to have a chance of “meeting” each other, thus interacting and forming the electrostatic complex. However, more intense stirring causes

great energy input in the system, and Reynolds values close to the transition region to the turbulent regime may have caused the breakage of the microcapsules. This increasing flow disturbance results in the formation of bubbles at Reynolds levels above 8700, as presented in Figures 2.3 to 2.7 (optical microscopy), the same was observed by Ach, (2014), who produced microcapsules by complex coceration using the pair gelatin and acacia gum.

In general, the presence of the baffles caused smaller values of *span* when comparing the data obtained with the same impellers (Table 2.3). It is important to note that for the vessel configurations with the presence of deflectors the Froude number is 0, as the Froude number evaluates the relation between the gravitational and inertial forces, and the presence of deflectors decreases this interaction by hindering formation of the vortex during agitation (ALVES, 2008). At the higher frequency values (1200 rpm), the Froude number is above the laminar range ($Fr < 1$), and it is exactly the range where the bubbles begin to form in the system (BEZERRA; CANTALICE, 2006). Figure 2.8 shows the correlation between the Froude number and the *span* values, and it is possible to observe a tendency of decreasing the *span* with the increase of the Froude number in the laminar range.

Table 2.2 Average diameter of microcapsules as a function of stirring frequency and stirring vessel configurations.

Rotational frequency (rpm)	400	600	800	1000	1200	1600	2000
Vessel configuration	Average diameter (μm)						
Radial	78.1 ± 17.3^{Ac}	75.3 ± 15.9^{Ab}	69.1 ± 13.2^{Bc}	59.4 ± 11.0^{Cc}	59.4 ± 10.8^{Cb}	49.8 ± 9.5^{Da}	48.5 ± 8.8^{Da}
Radial – Deflector	89.2 ± 17.1^{Ad}	76.4 ± 15.9^{Bb}	57.9 ± 9.6^{Cd}	45.5 ± 7.9^{Dd}	41.9 ± 6.7^{Dd}	32.2 ± 7.6^{Ec}	29.1 ± 6.8^{Ec}
Axial	111.9 ± 25.7^{Aa}	88.7 ± 17.6^{Ba}	84.9 ± 15.5^{Ba}	75.2 ± 10.1^{Ca}	63.7 ± 10.8^{Da}	52.5 ± 8.8^{Ea}	47.2 ± 8.0^{Ea}
Axial Deflector	101.5 ± 22.3^{Ab}	93.6 ± 28.0^{Ba}	77.0 ± 13.8^{Cb}	67.6 ± 12.0^{Db}	54.0 ± 8.1^{Ec}	38.1 ± 9.0^{Fb}	36.5 ± 6.9^{Fb}

Statistical analysis was performed in two steps, first between the rotational frequencies represented by the capital letters, and then between the stirring vessel configurations, represented by the lower-case letters.

Source: prepared by the author himself.

Table 2.3 Distribution width (span) of the particle size histogram, Froude and Reynolds numbers in function of the processing conditions.

Stirring frequency (rpm)	Deflectors	Impeller	Span	Froude	Reynolds
400	Present	Radial	0.82	-	5005
		Axial	0.97		
	Absent	Radial	1.19	0.15	
		Axial	0.86		
600	Present	Radial	0.77	-	6142
		Axial	0.91		
	Absent	Radial	0.91	0.35	
		Axial	1.03		
800	Present	Radial	0.65	-	7103
		Axial	0.78		
	Absent	Radial	0.82	0.62	
		Axial	0.71		
1000	Present	Radial	0.78	-	7950
		Axial	0.86		
	Absent	Radial	0.91	0.96	
		Axial	0.56		
1200	Present	Radial	0.74	-	8717
		Axial	0.70		
	Absent	Radial	0.78	1.39	
		Axial	0.70		
1600	Present	Radial	1.57	-	10080
		Axial	0.97		
	Absent	Radial	0.91	2.46	
		Axial	0.91		
2000	Present	Radial	0.97	-	11282
		Axial	0.91		
	Absent	Radial	1.20	3.85	
		Axial	0.79		

Source: prepared by the author himself.

Figure 2.8 Correlation between Reynolds number and mean particle size of microcapsules

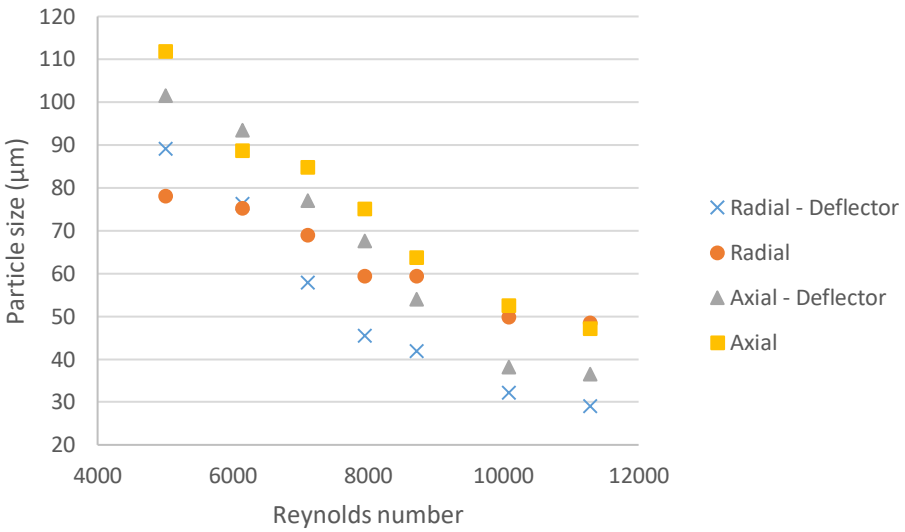

Source: prepared by the author himself.

Figure 2.9 Correlation between Froude number and span

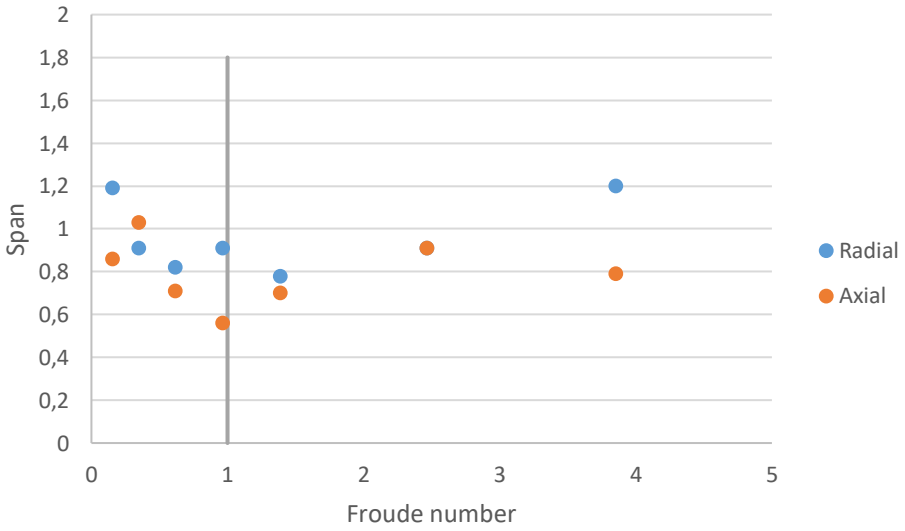

Source: prepared by the author himself.

2.3.2. Encapsulation efficiency and color parameters of the microcapsules

The encapsulation efficiency (*%EE*), calculated with basis on the β-carotene contents obtained by absorbance, were not affected by the process parameters (Table 2.4), confirming the trend that had been previously seen by Lemos et al. (2017). However, the encapsulation efficiency values were high and close to the values presented by Timilsena

et al. (2019) in his review, in which microcapsules formed by complex coacervation between gelatin and Arabic gum, containing lemon oil and lutein, presented *%EE* values of 80-90 and 85-86, respectively.

The color parameters of the microcapsules -lightness, chroma and hue angle - are also included in Table 2.4. The results demonstrate that the process conditions applied influence the final colorimetric characteristics of the microcapsules produced. However, in spite of the occurrence of significant differences between the samples, when analyzing the hue angle, all the samples presented values near 80, which is located in the region of intense yellow coloration. This is originated from the buriti oil that displays an orange-red color. The same can be described when analyzing only the chroma, since, for all the samples the values are greater than 53, demonstrating that all the samples presented high saturation of color. However, by analyzing the lightness, a tendency of decreasing clarity can be observed with the increased stirring frequency, which can be a result of differences in the powder compaction caused by the particle size differences, results similar to those observed by Lemos et al. (2017).

Table 2.4 Encapsulation efficiency (%EE), lightness (L*), hue angle (h), and chroma (C*) of buriti oil microcapsules.

Code	*%EE*	*L**	*C**	*H*
1G1GA400DR	85.64±1.20^{A}	83.00±0.00^{A}	54.19±0.03^{P}	81.12±0.00^{B}
1G1GA600DR	85.79±0.76^{A}	82.17±0.01^{E}	55.69±0.02^{N}	81.31±0.03^{A}
1G1GA800DR	85.64±0.57^{A}	82.35±0.02^{D}	56.54±0.02^{M}	80.95±0.02^{C}
1G1GA1000DR	84.52±0.94^{A}	82.51±0.03^{C}	56.72±0.10^{L}	81.08±0.00^{B}
1G1GA1200DR	84.59±1.21^{A}	81.85±0.00^{J}	57.39±0.04^{IJ}	80.66±0.01^{FGHI}
1G1GA1600DR	85.17±2.16^{A}	82.08±0.02^{FG}	57.33±0.02^{JK}	80.80±0.01^{DE}
1G1GA2000DR	85.25±0.91^{A}	82.21±0.05^{E}	55.79±0.08^{N}	81.02±0.02^{BC}
1G1GA400R	85.19±1.24^{A}	82.14±0.01^{EF}	56.59±0.01^{LM}	80.69±0.01^{FGH}
1G1GA600R	84.66±0.86^{A}	81.92±0.02^{IJ}	58.98±0.05^{D}	80.32±0.03^{N}
1G1GA800R	85.25±0.83^{A}	82.63±0.01^{B}	54.86±0.11^{O}	80.73±0.01^{EF}
1G1GA1000R	85.31±0.72^{A}	82.15±0.01^{EF}	58.12±0.05^{G}	80.62±0.02^{GHI}
1G1GA1200R	85.96±0.62^{A}	81.94±0.02^{HI}	59.02±0.03^{D}	80.43±0.03^{LM}
1G1GA1600R	84.10±0.52^{A}	81.63±0.04^{LM}	58.97±0.07^{D}	80.80±0.05^{DE}
1G1GA2000R	84.14±0.96^{A}	82.50±0.00^{C}	59.74±0.01^{B}	80.50±0.01^{KL}
1G1GA400DA	84.58±1.69^{A}	81.71±0.01^{KL}	56.64±0.06^{LM}	80.57±0.07^{IJK}
1G1GA600DA	85.76±0.64^{A}	81.44±0.01^{N}	58.66±0.02^{E}	80.18±0.01^{O}

1G1GA800DA	85.14±0.99^{A}	81.93±0.03^{IJ}	57.35±0.02^{JK}	80.84±0.02^{D}
1G1GA1000DA	84.57±1.49^{A}	81.91±0.02^{IJ}	58.44±0.02^{F}	80.60±0.02^{HIJK}
1G1GA1200DA	84.30±1.33^{A}	81.24±0.02^{O}	59.71±0.03^{B}	80.39±0.01^{MN}
1G1GA1600DA	84.71±1.39^{A}	81.21±0.02^{O}	59.83±0.04^{B}	80.62±0.03^{GHI}
1G1GA2000DA	83.52±0.58^{A}	82.03±0.00^{GH}	58.32±0.01^{F}	80.51±0.01^{JKL}
1G1GA400A	85.35±0.91^{A}	81.37±0.09^{N}	57.22±0.09^{K}	80.71±0.10^{EFG}
1G1GA600A	84.93±1.38^{A}	81.85±0.02^{IJ}	57.54±0.03^{I}	80.50±0.01^{JKL}
1G1GA800A	84.31±2.11^{A}	81.71±0.03^{KLM}	60.20±0.00^{A}	80.03±0.00^{P}
1G1GA1000A	85.03±1.73^{A}	81.73±0.04^{K}	59.49±0.06^{C}	80.36±0.00^{MN}
1G1GA1200A	85.26±1.27^{A}	81.62±0.010^{M}	57.91±0.09^{H}	80.12±0.02^{OP}
1G1GA1600A	83.06±0.43^{A}	82.06±0.03^{FG}	57.94±0.10^{GH}	80.60±0.02^{HIJ}
1G1GA2000A	85.70±1.27^{A}	82.57±0.01^{BC}	58.33±0.08^{F}	80.65±0.04^{FGHI}

Source: prepared by the author himself.

2.4. Conclusions

This work demonstrated the possibility of producing microcapsules of buriti oil by complex coacervation, resulting in microcapsules with high encapsulation efficiency and intense yellow coloration. The process configurations that showed the best results were those carried out at stirring frequency of 1000 rpm with deflectors and and radial impeller, which presented microcapsules with smaller size and size distribution, this being the best configuration for the production of buriti oil microcapsules by complex coacervation.

REFERENCES

ACH, D.; BRIANÇON, D.; BROZE, G.; PUEL, F.; RIVOIRE, A.; GALVAN, J.-M.; CHEVALIER, Y. Formation of microcapsules by complex coacervation. **The Canadian Journal of Chemical Engineering**, v. 93, n. 2, p. 183 – 191, 2015.

ALVES, A. G. M. **Caracterização das solicitações hidrodinâmicas em bacias de dissipação por ressalto hidráulico com baixo número de Froude.** 2008. 157 f. Dissertação (Mestrado em Recursos Hídricos e Saneamento Ambiental), Universidade Federal do Rio Grande do Sul, Porto Alegre, 2008.

ARANHA, C. P. M. **Microencapsulação por gelificação iônica e interação eletrostática do corante de buriti (*Mauritia flexuosa* L. f.).**, 2015. 117 p. Tese (Doutorado em Engenharia e Ciência de Alimentos), Universidade Estadual Paulista, São José do Rio Preto, 2015.

BEZERRA, S. A.; CANTALICE, J. R. B. Erosão entre sulcos em diferentes condições de cobertura do solo, sob cultivo da cana-de-açúcar. **Revista Brasileira Ciência do Solo**, v. 30, p. 565-573, 2006.

CHAPEAU, A.-L.; HAMON, P.; ROUSSEAU, F. CROGUENNEC, T.; PONCELET, D.; BOUHALLAB, S. Scale-up production of vitamin loaded heteroprotein coacervates and their protective property. **Journal of Food Engineering**, v. 206, p. 67 – 76, 2017.

COSTA, A. M. M.; MORETTI, L. K.; SIMÕES, G.; SILVA, K. A.; CALADO, V.; TONON, R. V.; TORRES, A. G., 2020. Microencapsulation of pomegranate (Punica granatum L.) seed oil by complex coacervation: development of a potential functional ingredient for food application. **LWT – Food Science and Technology**, v. 131, p. 109519, 2020.

DE VOS, P.; FAAS, M. M.; SPASOJEVIC, M.; SIKKEMA, J. Encapsulation for preservation of functionality and targeted delivery of bioactive food components. **International Dairy Journal**, v. 20, n. 4, p. 292-302, 2010.

FERREIRA, S.; NICOLETTI, V. R. Complex coacervation assisted by a two-fluid nozzle for microencapsulation of ginger oil: Effect of atomization parameters. **Food Research International**, v. 138, Part B., p. 109828, 2020.

FERREIRA, S.; NICOLETTI, V. R. Microencapsulation of ginger oil by complex coacervation using atomization: Effects of polymer ratio and wall material concentration. **Journal of Food Engineering**, v. 291, p. 110214, 2021a.

FERREIRA, S.; NICOLETTI, V. R. Use of a tubular heat exchanger to achieve complex coacervation in a semi-continuous process: Effects of capsules curing temperature and shear rate. **Journal of Food Engineering**, v. 310, p. 110698, 2021b.

FRAJ, J.; PETROVIC, L.; ĐEKIC, L.; BUDINCIC, J. M.; BUCKO, S., KATONA, J. Encapsulation and release of vitamin C in double W/O/W emulsions followed by complex coacervation in gelatin-sodium caseinate system. **Journal of Food Engineering**, v. 292, p. 110353, 2021.

FREITAS, M. L. F.; CHISTÉ, R. C.; POLACHINI, T. C.; SARDELLA, L. A. C. Z.; ARANHA, C. P. M.; RIBEIRO, A. P. B.; NICOLETTI, V. R. Quality characteristics and thermal behavior of buriti (Mauritia flexuosa L.) oil. **Grasas y Aceites**, v. 68, n. 4, p. e220, 2017.

GABELLE, J. C.; MORCHAIN, J.; ANNE-ARCHARD, D.; AUGIER, F.; LINÉ, A. Experimental determination of the shear rate in a stirred tank with a non-Newtonian fluid: carbopol, **AIChE Journal**, v. 59, p. 2251-2266, 2013.

LEMETTER, C. Y. G.; MEEUSE, F. M.; ZUIDAM, N. J. Control of the morphology and the size of complex coacervate microcapsules during scale-up. **AIChE Journal**, v. 56, p. 1487-1496, 2009.

JÉGAT, C.; TAVERDET, L. J. Stirring speed influence study on the microencapsulation process an on the drug release from microcapsules. **Polymer Bulletin**, v. 44, p. 345-351, 2000.

LEMOS, Y. P.; MARFIL, P. H. M.; NICOLETTI, V. R. Particle size characteristics of buriti oil microcapsules produced by gelatin-sodium alginate complex coacervation: Effect of stirring speed**. International journal of food properties**, v. 20, n. S2, p. S1438–S1447, 2017.

MA, T.; ZHAO, H.; WANG, J.; SUN, B. Effect of processing conditions on the morphology and oxidative stability of lipid microcapsules during complex coacervation. Food Hydrocolloids, v. 87, p. 637-643, 2019.

MARFIL, P. H. M.; PAULO, B. B.; ALVIM, I. D.; NICOLETTI, V. R. Production and characterization of palm oil microcapsules obtained by complex coacervation in gelatin/gum Arabic. **Journal of Food Process Engineering**, v. 41, n. 4, p. e12673, 2018.

MARFIL, P. H. M.; VASCONCELOS, F. H. T.; PONTIERI, M. H.; TELIS, V. R. N. Development and validation of analytical method for palm oil determination in microcapsules produced by complex coacervation. **Química Nova,** v. 39, n. 1, p. 94-99, 2016.

MENEGALLI, F. C.; TELIS, V. R. N.; TELIS ROMERO, J. Bombeamento, agitação e mistura de fluidos alimentícios. In: TADINI, C. C.; TELIS, V. R. N.; MEIRELLES, A. J. A.; FILHO, P. A. P. **Operações Unitárias na Indústria de Alimentos**. São Paulo: LTC, 2015. Cap. 5, p 169-209.

PATHAK, J.; PRIYADARSHINI, E.; RAWAT, K.; BOHIDAR, H. B. Complex coacervation in charge complementary biopolymers: Electrostatic versus surface patch binding. **Advances in Colloid and Interface Science**, v. 250, p. 40–53, 2017.

ROCHA, S. M.; RODRIGUES, M. T. O. S.; SILVA, D. S.; COSTA, F. M.; FILHO, O. F.; NUNE, Y. R. F.; ARRUDAS, S. R.; FIDÊNCIO, P. H. Efeito do armazenamento nas propriedades físico-químicas do óleo de *Mauritia flexuosa* L. f. (Arecaceae). **Caderno de Ciências Agrárias**, v. 9, n. 1, p. 31-37, 2017.

SANTOS, M. F. G.; ALVES, R. E.; ROCA M. Carotenoid composition in oils obtained from palm fruits from the Brazilian Amazon. **Grasas y Aceites**, v. 66, p. 1–8, 2015.

SARAIVA, L. C. F.; SILVA, R. B. Desenvolvimento de um creme à base de óleo de buriti (*Mauritia flexuosa*). **Revista FAESF**, v. 1, n. 1, p. 11-19, 2017.

SILVA, F. C.; FONSECA, C. R.; ALENCAR, S. M.; THOMAZINI, M.; BALIEIRO, J. C. C.; PITTIA, P.; FAVARO-TRINDADE, C. S. Assessment of production efficiency, physicochemical properties and storage stability of spray-dried propolis, a natural food additive, using gum Arabic and OSA starch-based carrier systems. **Food and Bioproducts Processing**, v. 91, n. 1, p. 28-36, 2013.

STEFFE, J. F. **Rheological methods in food process engineering**. Freeman Press, East Lansing, USA, 1996.

TIMILSENA, Y. P.; AKANBI, T. O.; KHALID, N.; ADHIKARI, B.; BARROW, C. J. Complex coacervation: Principles, mechanisms and applications in microencapsulation. **International Journal of Biological Macromolecules**, v.121, p. 1276–1286, 2019.

WU, B.-C.; MCCLEMENTS, D. J. Functional hydrogel microspheres: Parameters affecting electrostatic assembly of biopolymer particles fabricated from gelatin and pectin. **Food Research International**, v. 72, p. 231-240, 2015.

CAPÍTULO 3

THE ROLE OF SUSPENSION RHEOLOGY ON THE SIZE AND MORPHOLOGY OF COMPLEX COACERVATED MICROCAPSULES

3. THE ROLE OF SUSPENSION RHEOLOGY ON THE SIZE AND MORPHOLOGY OF COMPLEX COACERVATED MICROCAPSULES

Abstract

The rheological behavior of the suspensions from which complex coacervated microcapsules are formed are of paramount importance for defining their final size and morphology. Gelatin/gum Arabic and gelatin/sodium alginate were used as wall materials for the microencapsulation of buriti oil as they generated suspensions with different rheological behavior: shear-thickening and shear-thinning, respectively. Both biopolymer combinations proved to be efficient for complex coacervation, resulting in microcapsules with size values ranging from 37 µm to 112 µm in the case of gelatin/gum Arabic, and 29 µm to 55 µm for gelatin/sodium alginate. However, the production and the size of the microcapsules were influenced by the processing conditions: the shear-thickening suspension led to better results at low agitation speeds, whereas the shear-thinning suspension showed better results at high agitation speeds.

3.1 Introduction

Over the years, microencapsulation has become a widely explored technique at the research and industrial levels, as good results have been obtained in various applications in which there is a need to protecting sensitive lipophilic compounds from oxidation, to control the release of flavors, or to favor the release of nutrients at specific points along the gastrointestinal tract. Microencapsulation consists in protecting the material of interest, forming a physical barrier composed by the wall material, which contributes to isolate the encapsulated core material from the potentially harmful contact with the environment and their associated moisture and oxygen contents. The lower or higher permeability of the microcapsule wall must be modulated in accordance with the desired functionality, i.e., for a more efficient storage of the encapsulated material or for a controlled release, respectively. Substances encapsulated in their nuclei may have longer storage or release compared to their natural state (ZANG, et al., 2022; CASTEJÓN, et al., 2021; KOUAMÉ, et al., 2021).

One of the techniques used for microencapsulation is complex coacervation, which is based in the electrostatic interaction between polymers with opposite charges. Generally, two polymers are used, a protein with a negative charge and a polysaccharide with a positive charge, favoring the interaction. This combination can be used to develop some specific attributes in protection, stabilization and release, which can enhance the application of microcapsules in pharmaceutical, food and agricultural industries (MUHOZA, et al., 2022; LI, et al., 2021; LUO, et al., 2021).

Microencapsulation by complex coacervation has been widely used to encapsulate oils, as they are very susceptible to conditions in the environment where they are stored, being affected, for example, by temperature and oxygen. Carotenoids are lipophilic compounds that are prone to oxidation and there is interest in their encapsulation in order to promote oxygen exclusion. Buriti (*Mauritia flexuosa*) are among the most useful vegetable resources in the Amazon region. Buriti oil has a high concentration of monounsaturated fatty acids and contains β-carotene at higher concentrations than foods traditionally known as carotenoid-rich sources, such as carrots and papaya. In addition, buriti oil presents high levels of tocopherols, turning to be a reliable source of antioxidant compounds (FREITAS et al., 2017). Buriti oil has become a very promising ingredient in the pharmaceutical, cosmetics, and food industry, and its encapsulation has proven to be very interesting (CRUZ et al., 2020; MANSUR et al., 2020; MOSER et al., 2020).

Complex coacervation has some advantages, such as thermal stability, controlled release and large loading capacity. However, the microcapsule formation and the resulting characteristics can be affected by pH variations, the ionic strength of the materials, the length and density of the polymer chains used, the concentration and charge density of the polymers, in addition to the suspension viscosity, since lower viscosities facilitate the interaction between the polymers to form the complexes that generate the microcapsules (LIU, et al., 2017; PATHAK et al., 2017). The initial processing step for complex coacervation is the emulsification of the oil in the polymer dispersion that will give origin to the microcapsule wall; the rheological properties of these polymeric aqueous dispersions, associated to the process operational conditions, may affect the size and morphology of the produced microcapsules (LEMOS; MARFIL; NICOLETTI, 2017; MOSER; FERRREIRA; NICOLETTI, 2019).

Based on these considerations, this work aimed to study the influence of the rheological behavior of the wall material dispersion for the production of buriti oil microcapsules by complex coacervation. Different flow curves (shear stress versus shear

rate) were obtained by using two combinations of protein/polysaccharide - gelatin/gum Arabic and gelatin/sodium alginate, which generated suspensions with shear-thickening and shear-thinning behavior, respectively - thus presenting different responses to increasing stirring frequency during coacervation.

3.2 Materials and Methods

3.2.1 Materials

Buriti oil (Amazon Oil, Brazil) was encapsulated by complex coacervation using two combinations of protein/polysaccharide: the first was formed by gelatin (extracted from bovine skin, type B, with gel strength of 240 bloom - Gelita, Brazil) and gum Arabic (Dinâmica, Brazil); and the second was composed by gelatin and sodium alginate GRINDSTED® FD 175 (Danisco, Brazil). The pH adjustment for coacervation (3.5 ± 0.1) was performed with 99.7% acetic acid (Dynamica, Brazil).

3.2.2 Methods

3.2.2.1 Complex Coacervation

The preparation of the microcapsules was based on the work of Lemos et al. (2017), and was carried out according to Table 3.1. The buriti oil was added to the pre-heated gelatin solution at 50 °C and homogenized in ultraturrax at 1500 rpm for 5 min. In sequence, the solution was added in a stirred vessel with a volume of 1 L and added with the alginate or gum Arabic solutions at 50 °C, and the pH was corrected to 3.5 under constant stirring, for the beginning of coacervation. This step was performed under continuous agitation, using a mechanical stirrer (Marconi, model MA 261, Brazil) maintaining temperature at 50 ± 3 °C throughout the process. The configuration of the coacervation vessel was based on the system used by Lemos et al. (2017), and the influence of different stirring speeds in the range of 400 to 2000 rpm (Table 3.1) was evaluated. After formation of the microcapsules, they were cooled to 10 °C under constant agitation and the suspension was then stored in a refrigerator for 24 h (at about 5 °C). Finally, the microcapsules were filtered, frozen in an ultra-freezer (model FV 500, Liobrás, Brazil), and freeze-dried (Liobrás, model L101, Brazil) for approximately 72 h.

The dried material was ground in a mortar, protected from light and stored in a desiccator to further analysis.

Table 3.1 Formulation and processing conditions applied for microencapsulation of buriti oil, and the respective treatment codification.

Sample Code	Gelatin (g/100g)	Arabic Gum (g/100g)	Sodium Alginate (g/100g)	Buriti Oil (g/100g)	Stirring Speed (rpm)
GG400	1	1	-	1	400
GG600	1	1	-	1	600
GG800	1	1	-	1	800
GG1000	1	1	-	1	1000
GG1200	1	1	-	1	1200
GG1600	1	1	-	1	1600
GG2000	1	1	-	1	2000
GA400	1	-	3	1	400
GA600	1	-	3	1	600
GA800	1	-	3	1	800
GA1000	1	-	3	1	1000
GA1200	1	-	3	1	1200
GA1600	1	-	3	1	1600
GA2000	1	-	3	1	2000

Source: prepared by the author himself.

3.2.2.2 Rheological analysis of solutions used for complex coacervation

The final solutions for the production of buriti oil microcapsules were analyzed in a rheometer (TA Instruments, model AR 2000ex), using the geometry of concentric cylinders. The rheological measurements were done following a strain rate ramp from 1 to 1000 s^{-1}. This strain rate range was selected based on the results of Equation 3.1 (STEFFE, 1996), by which it is possible to estimate the strain rate applied during coacervation by the mechanical stirrer, through a correlation between the diameters of the stirring propeller and the size of the coacervation vessel. To model the flow curves

(rheograms) obtained, the models of Newton (Eq. 3.2), Power Law (Eq. 3.3), Bingham (Eq. 3.4), and Herschel-Bulkley (Eq. 3.5) were tested.

$$\dot{\gamma} = \frac{d\Omega}{D-d} \tag{3.1}$$

$$\tau = \mu\dot{\gamma} \tag{3.2}$$

$$\tau = k\dot{\gamma}^n \tag{3.3}$$

$$\tau = \tau_0 + \mu_B\dot{\gamma} \tag{3.4}$$

$$\tau = \tau_0 + k_{HB}\dot{\gamma}^n \tag{3.5}$$

in which τ is the shear stress in Pa, $\dot{\gamma}$ the strain rate in s^{-1}, d is the impeller diameter (m), (Ω) is the stirring speed, D is the vessel diameter (m), μ the viscosity in Pa·s, k the consistency index in $Pa \cdot s^n$, n is the fluid behavior index, τ_0 the yield stress in Pa, μ_B the Bingham viscosity in Pa·s, and $k_{H\text{-}B}$ the Herschel-Bulkley consistency index in $Pa \cdot s^n$.

3.2.2.3 Characterization of buriti oil microcapsules

3.2.2.3.1 Particle size

Particle size was determined using a laser diffraction particle size distribution analyzer LA-950V2 (HORIBA, Japan) using distilled water as the dispersing medium. The wet particles were previously dispersed in distilled water in a mechanical stirrer for one minute and treated in an ultrasonic bath (model USC-1400A, Unique, Brazil) for 30 seconds to break agglomerates. The results were expressed in terms of mean particle diameter.

3.2.2.3.2 Optical microscopy

The morphology of the capsules was evaluated in two steps of the production process: after freeze-drying and after rehydration. The samples were placed on slides and analyzed using an optical microscopy (Olympus, CX31) coupled to an 8.1-megapixel digital camera (Sony Cyber-Shot, DSC-W150).

3.2.2.3.3 Color analyses

Color analysis was performed using a Konica Minolta colorimeter (CR-S, Konica Minolta, Japan). The color coordinates (CIE L^*, a^* and b^*) were measured with D65 illuminant and 10º observation angle. Chroma (C^*) and hue angle (h) were calculated according to Equations 3.6 and 3.7.

$$C^* = \sqrt{\left(a^*\right)^2 + \left(b^*\right)^2} \tag{3.6}$$

$$h = arctg\left(\frac{b^*}{a^*}\right) \tag{3.7}$$

3.2.2.3.4 Fourier-transform infrared spectroscopy (FTIR)

The FTIR spectra of the materials forming the microcapsules and the microcapsules themselves were read in (Bruker Vertex 70). The wavelength used in the analyzes were from 400 to 4000 cm^{-1}.

3.2.2.3.5 Encapsulation efficiency

The encapsulation efficiency (%EE) was determined by quantifying the initial carotenoid content in the buriti oil (TC), the carotenoid content on the surface of the microcapsules and the total content of carotenoids in the microcapsules (EC), in triplicate, as described by Aranha (2015) with some modifications. The content of carotenoids (C) expressed in β-carotene was determined by Equation 3.8. The encapsulation efficiency (%EE) was calculated by the Equation 3.9.

$$C = \frac{Abs \times V \times 10^4}{2396 \times g} \quad (3.8)$$

$$\%EE = \frac{EC}{TC} \times 100 \quad (3.9)$$

where Abs is the absorbance, V is the sample volume, and g is the sample mass.

3.2.2.4 Statistical analysis

The assays were repeated three times in sequence and the analyses were performed in triplicate. The values of the analytical determinations were subjected to analysis of variance (ANOVA) and mean comparisons by Tukey's test ($p < 0.05$) using the software Minitab 16.1.1.

3.3 Results and Discussion

All the treatments applied to carry out complex coacervation (Table 3.1) were effective to the formation of coacervates. However, the presence of individual microcapsules, which were mostly multinucleated but with a visible protective wall, was observed only at specific stirring speeds used during complex coacervation. The samples produced with gum Arabic had a circular and more homogeneous shape, whereas those produced with alginate had more ellipsoid characteristics and less homogeneous characteristics, corroborating the studies by Shaddel et al. (2018) and Lemos et al. (2017), respectively. The morphology of microcapsules is shown in Figures 3.1 e 3.2.

Figure 3.1 Optical microscopy images of the microcapsules produced with gelatin/gum Arabic at different stirring speeds (bar = 200 µm).

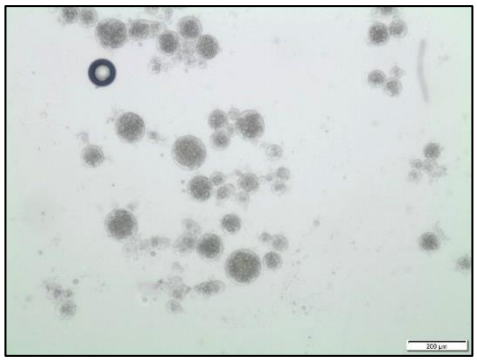

400 GG

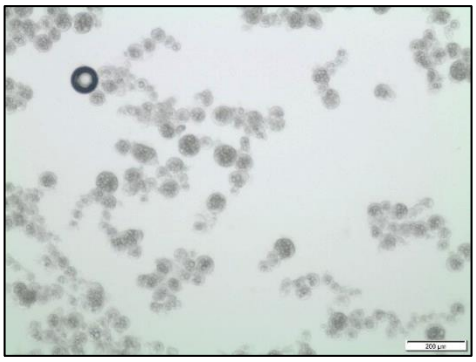

600 GG

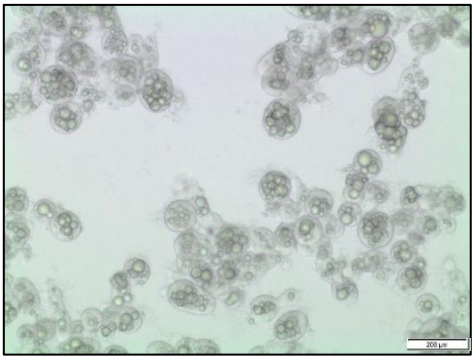

800 GG

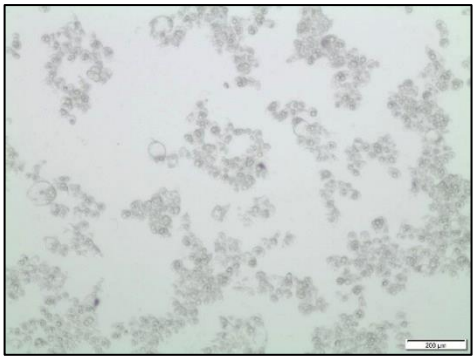

1000 GG

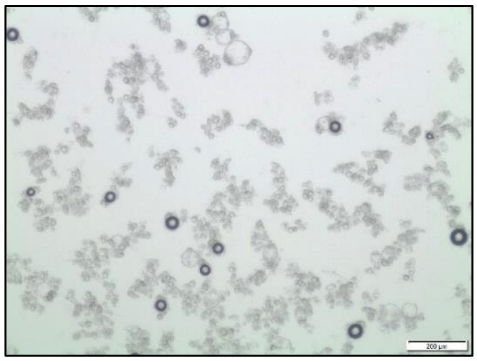

1200 GG

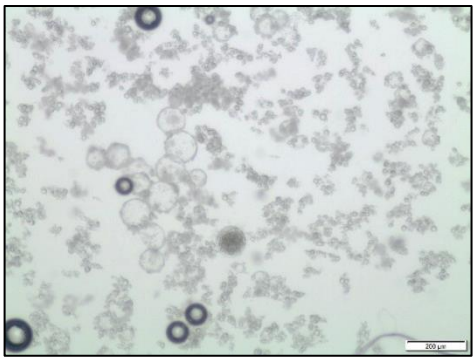

1600 GG

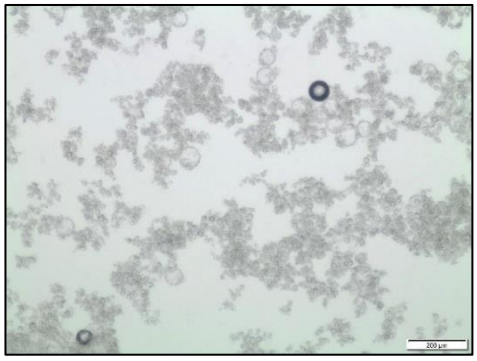

2000 GG

Source: prepared by the author himself.

Figure 3.2 Optical microscopy images of the microcapsules produced with gelatin/ sodium alginate at different stirring speeds (bar = 200 µm).

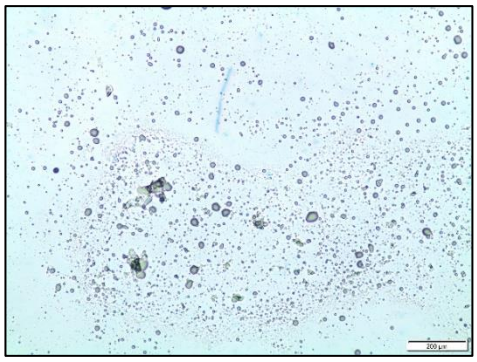

400 AG

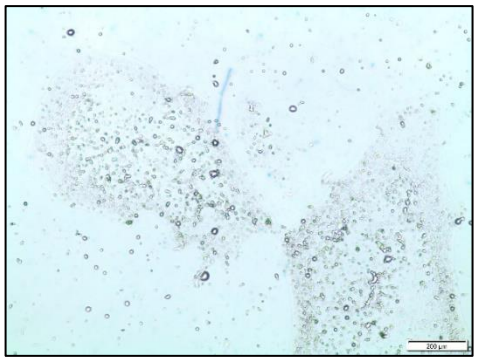

600 AG

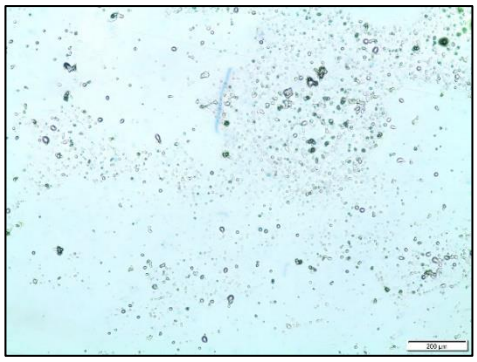

800 AG

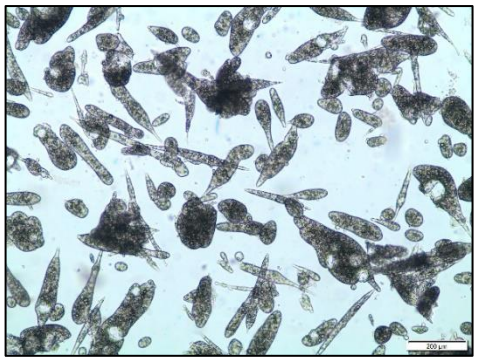

1000 AG

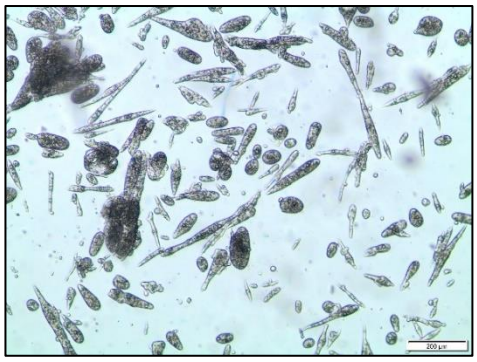

1200 AG

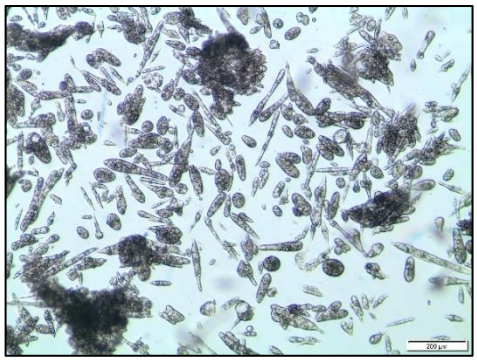

1600 AG

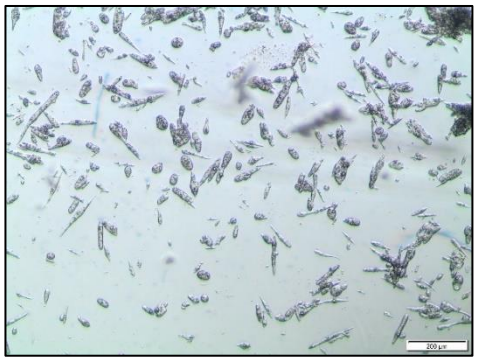

2000 AG

Source: prepared by the author himself.

3.3.1 Influence of hydrodynamic conditions during coacervation on particle formation.

The rheograms of the solutions are shown in Figures 3.3 and 3.4, for the gelatin/gum Arabic and gelatin/sodium alginate solutions. The rheological models described in Equations (3.2) to (3.5) were tested and the one that presented the best fitting results was the power law (Eq. 3.3). The fitting parameters for both solutions are presented in Table 3.2.

Table 3.2 Rheological characteristics of microcapsule forming solutions.

Sample	**n**	**k (Pa·s^n)**	**r^2**
Gelatin/Gum Arabic	1.51	1.22×10^{-4}	0.999
Gelatin/Sodium Alginate	0.88	0.075	0.999

Source: prepared by the author himself.

According to Liu et al. (2017) and Pathak et al. (2017), viscosity can directly interfere with the molecular interaction between the polymers used in coacervation, and lower viscosities facilitate the movement of these polymers and their complexation, which corroborates the results obtained. The solution composed of gelatin and gum Arabic presented values of n > 1, representing characteristics of a dilatant (shear thickening) fluid, in which the increase in tension causes an increase in viscosity, which is shown in Figure 3.3. This increase in viscosity makes it difficult the formation of microcapsules which is demonstrated by Figure 3.1; at the highest agitation rates used, there was a large formation of bubbles and agglomerates. On the other hand, analyzing Figure 3.4, the solution of the pair gelatin and sodium alginate presented the characteristic of a pseudoplastic (shear thinning) fluid, with n < 1, in which the increase in applied tension generates a decrease in viscosity favoring the formation of microcapsules. This is shown in Figure 3.2, in which microcapsules only started to form at the highest shear rates applied.

Figure 3.3 Rheological behavior of the gelatin/gum Arabic solution used for the production of microcapsules.

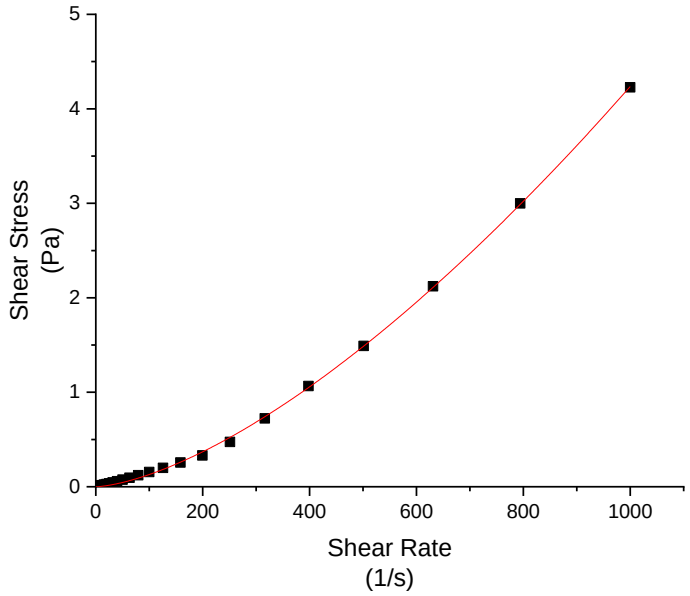

Source: prepared by the author himself.

Figure 3.4 Rheological behavior of gelatin/sodium alginate solution used for the production of microcapsules.

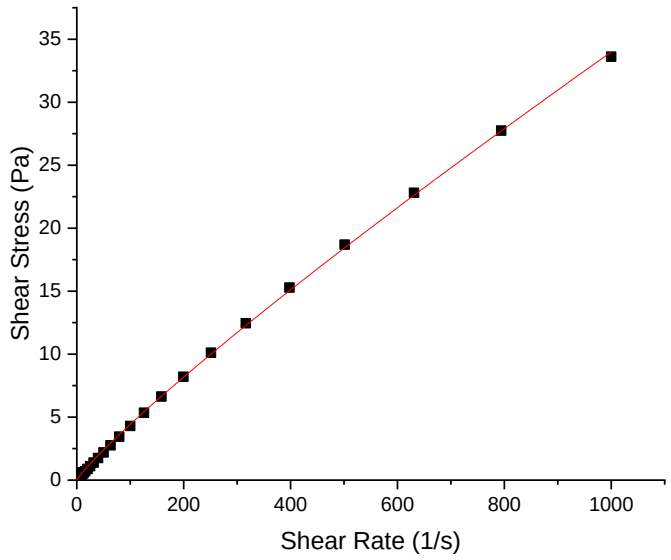

Source: prepared by the author himself.

3.3.2 Particle size

Particle size is of paramount importance when incorporating materials into food products, as it can change organoleptic characteristics, such as the sensation of sandiness in the mouth. The microcapsules produced with different wall materials had different characteristics. Those produced with alginate had their average particle sizes ranging from 55 µm to 29 µm, similar to the values found by Savana and Rao (2010), that encapsulated drugs with gelatin and sodium alginate by complex coacervation. Observing Figure 3.2, the formation of microcapsules started with agitation speed values above 1000 rpm. The microcapsules produced with gum Arabic presented values from 112 µm to 37 µm values close to those found by Shadel et al. (2018), that used the pair gelatin and gum Arabic for encapsulation of black raspberry anthocyanins by complex coacervation.

Figure 3.5 shows the relationship between the size of the microcapsules and the frequency of agitation used during their formation, being possible to observe that, starting from the frequency of agitation at which the formation of the microcapsules occurs (pair gelatin/gum arabic from 400 to 1000 rpm; pair gelatin/sodium alginate from 1200 to 2000 rpm), increase agitation frequency causes the decrease of the average size of microcapsules. Similar results were found by Lemos et al. (2017), who produced microcapsules by complex coacervation of buriti oil using gelatin/sodium alginate as wall materials.

Figure 3.5 Effect of agitation speed on the size of microcapsules produced with gelatin/gum Arabic (GG) and gelatin/sodium alginate (AG).

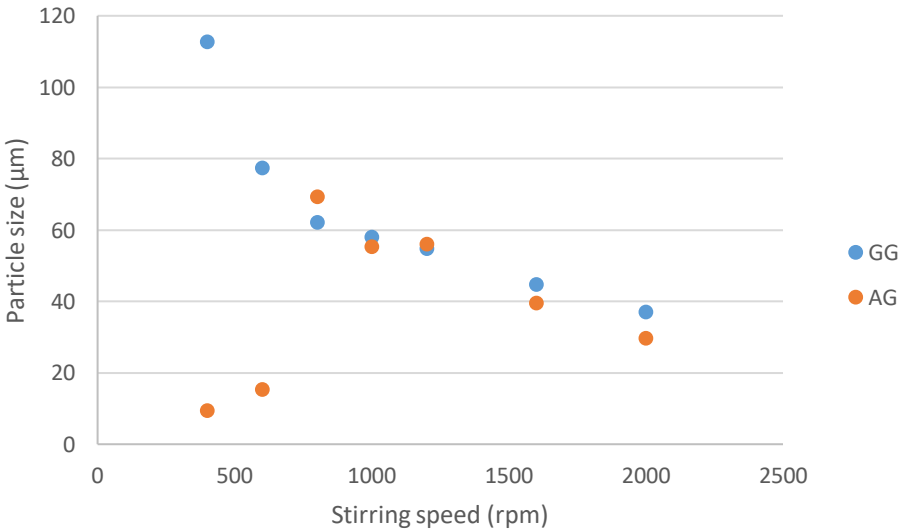

Source: prepared by the author himself.

Figure 3.6 shows the particle size distributions of the microcapsules produced with gelatin and gum Arabic as wall materials. It is possible to observe that in all agitation speeds the histograms presented monomodal characteristics with a decrease in the average particle size for increasing stirring speeds, but with an increase in span, which was possibly caused by the high rate of deformation applied during the formation of microcapsules, thus leading to the appearance of bubbles in the formed complexes.

Figure 3.7 represents the histograms of the microcapsules formed by the gelatin and sodium alginate coacervation, where it is possible to observe that up to the stirring speed 1000 rpm the histograms are bimodal and with high span values, which can be explained by the non-formation of the microcapsules at lower speeds and the formation of very uniform complexes at medium agitation speeds, which may indicate that higher speeds and higher deformation rates are more effective for the production of these microcapsules, which was also seen in the studies by Lemos et al. (2017) and Jegát and Taverdet (2000).

Figure 3.6 Particle size distributions of the microcapsules produced with gelatin/Arabic gum at different stirring speeds.

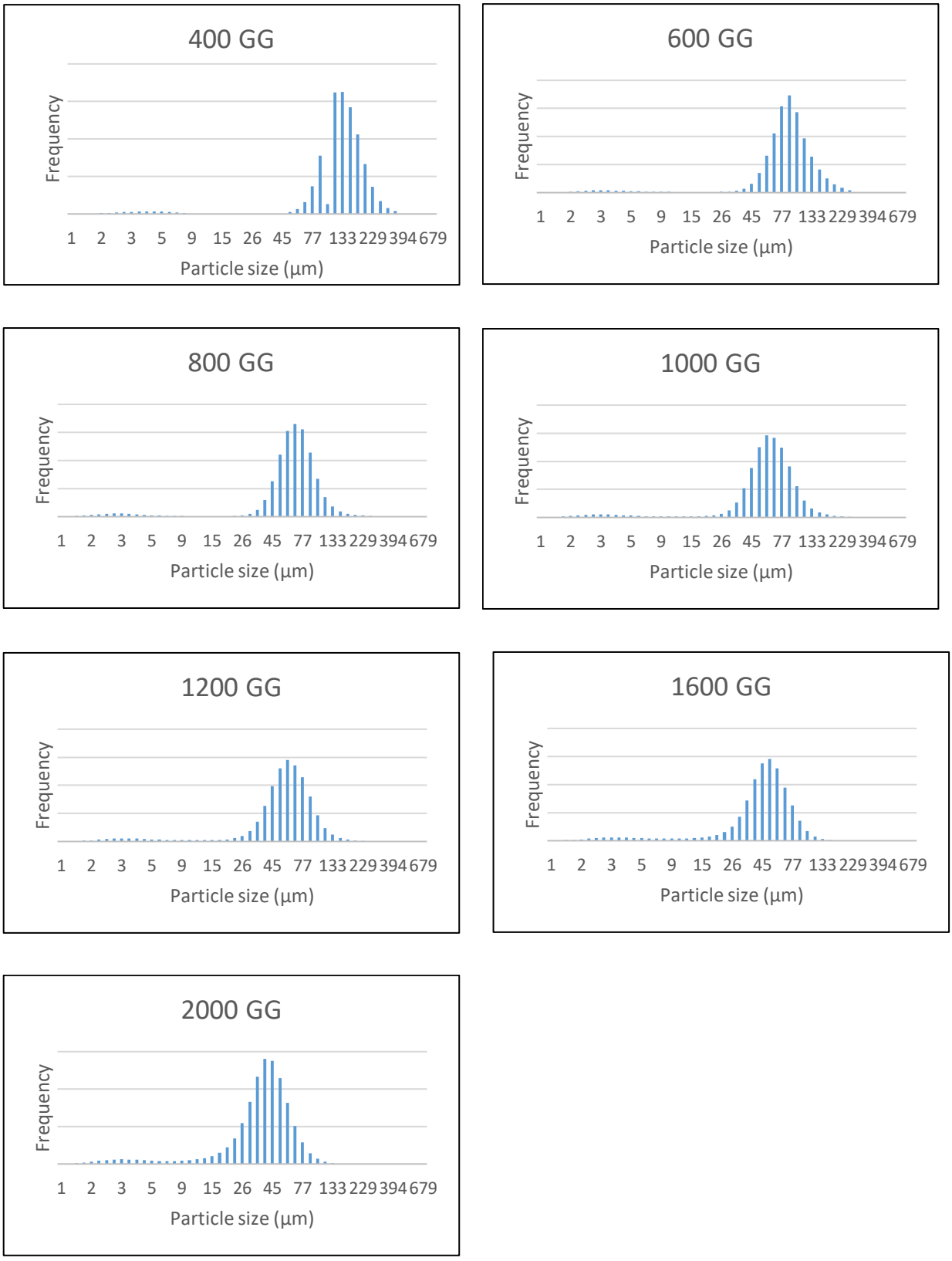

Source: prepared by the author himself.

Figure 3.7 Particle size distributions of the microcapsules produced with gelatin/sodium alginate at different stirring speeds.

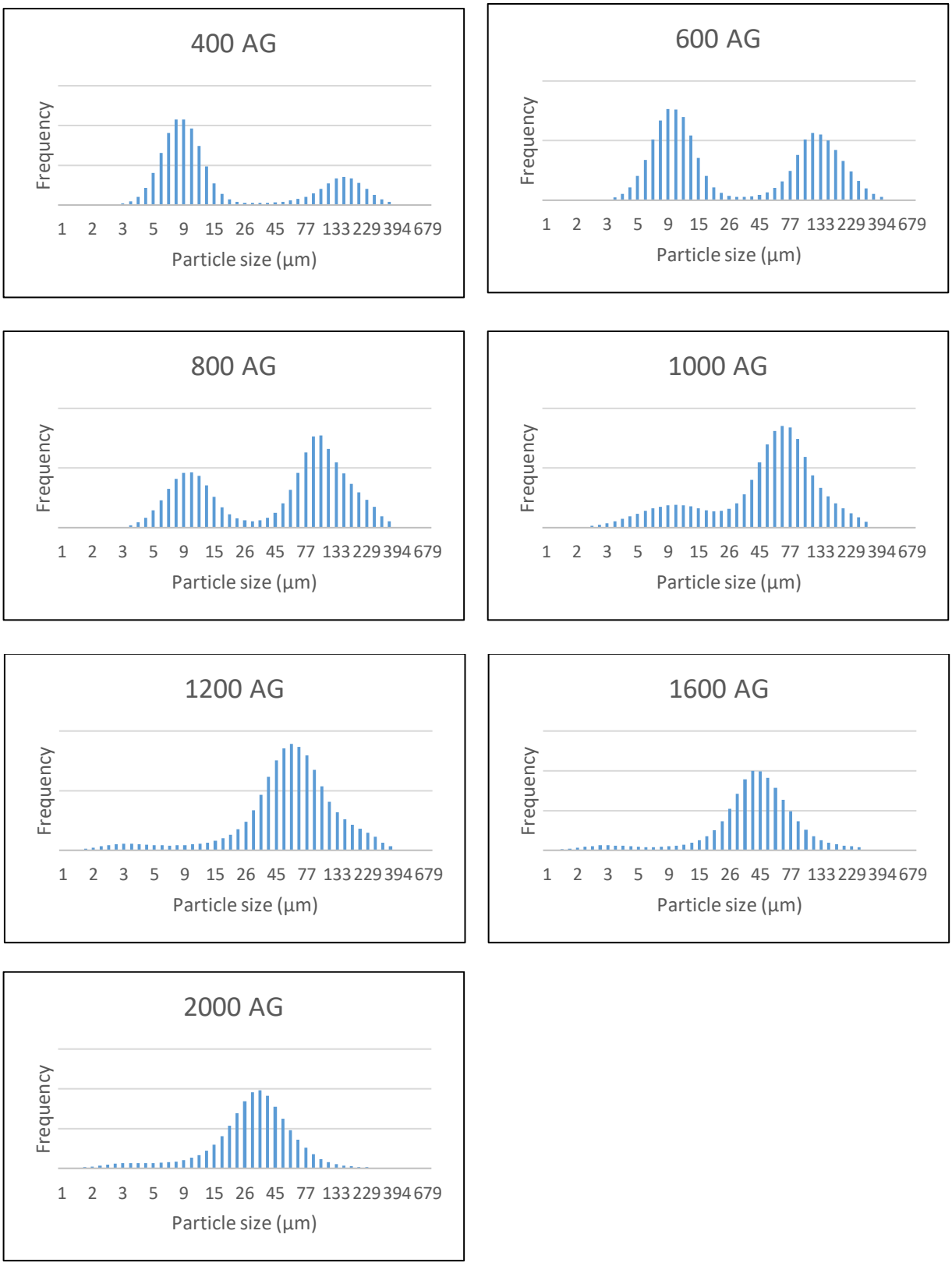

Source: prepared by the author himself.

3.3.3 Encapsulation efficiency

For the two combinations of wall materials used for the production of microcapsules, it was possible to observe that the applied production parameters had no interference in the encapsulation efficiency, but the microcapsules obtained with the pair gelatin/ arabic gum had slightly better results. The microcapsules produced with gelatin and gum Arabic had higher %EE values, around 85%, results similar to those found by Ferreira et al. (2020), who produced microcapsules of ginger oil by complex coacervation using an atomization device. For the gelatin and sodium alginate combination, the values found were lower, around 80%, which can be explained by the smaller homogeneity of the microcapsules, which may have resulted in lower oil retention in individual microcapsules. However, the values were close to those found by Matos et al. (2018) that produced complex coacervated microcapsules of citronella essential oil.

3.3.4 Color analyses

The values of the color parameters are presented in Table 3.3 and it is possible to conclude that the samples were not influenced by the processing conditions, but by the wall material used for their production. All samples showed h values close to 80, which indicates the yellowish color that is derived from the yellow-orange color of buriti oil, values similar to those found by Moser et al. (2019). The values of C* ranged between 50 and 70, which demonstrates that all samples reached a good saturation in their color. The difference between the samples was found in the lightness values (L*): the microcapsules produced using gelatin/sodium alginate had lower values, which can be explained by the higher amount of wall material in their formation, which caused the samples to become darker.

Table 3.3 Particle size, strain rate, encapsulation efficiency (%EE), brightness (L*), chroma (C*), and hue angle (h) of buriti oil microcapsules.

Treatment	$\dot{\gamma}$	Particle size (μm)	Span	%EE	L*	C*	h
GG400	200.06	112.22 ± 4.02^{a}	0.91 ± 0.03^{a}	84.64 ± 1.20^{b}	82.00 ± 0.21^{a}	53.17 ± 0.44^{c}	81.02 ± 0.12^{a}
GG600	300.09	75.12 ± 2.18^{b}	0.94 ± 0.04^{a}	84.79 ± 0.56^{b}	81.17 ± 0.11^{a}	55.69 ± 0.22^{bc}	81.21 ± 0.03^{a}
GG800	400.12	61.83 ± 0.52^{c}	0.93 ± 0.13^{a}	85.88 ± 0.67^{b}	80.35 ± 0.12^{a}	56.55 ± 0.12^{bc}	80.85 ± 0.02^{a}
GG1000	500.15	57.69 ± 0.60^{cd}	1.05 ± 0.01^{a}	83.42 ± 0.84^{b}	81.51 ± 0.06^{a}	56.42 ± 0.14^{bc}	82.08 ± 0.00^{a}
GG1200	600.18	54.61 ± 0.19^{d}	1.07 ± 0.04^{ab}	83.59 ± 1.31^{b}	81.74 ± 0.10^{a}	57.49 ± 0.14^{b}	81.66 ± 0.11^{a}
GG1600	800.24	44.58 ± 0.24^{e}	1.15 ± 0.04^{ab}	85.16 ± 2.16^{b}	82.88 ± 0.22^{a}	57.33 ± 0.02^{b}	80.80 ± 0.06^{a}
GG2000	1000.3	37.19 ± 0.27^{f}	1.18 ± 0.03^{ab}	84.25 ± 0.11^{b}	81.21 ± 0.15^{a}	55.69 ± 0.08^{bc}	81.12 ± 0.12^{a}
GA400	200.06	9.49 ± 0.25^{i}	16.48 ± 0.74^{d}	-	79.64 ± 0.73^{a}	55.88 ± 0.85^{bc}	81.88 ± 0.85^{a}
GA600	300.09	15.33 ± 0.93^{h}	10.78 ± 0.62^{c}	-	78.36 ± 0.82^{b}	53.88 ± 0.53^{c}	82.88 ± 0.53^{a}
GA800	400.12	69.37 ± 2.21^{b}	2.31 ± 0.03^{d}	-	76.25 ± 1.53^{b}	54.85 ± 0.28^{c}	81.85 ± 0.28^{a}
GA1000	500.15	55.28 ± 0.38^{cd}	2.12 ± 0.02^{d}	81.07 ± 1.21^{a}	75.26 ± 0.25^{b}	62.79 ± 0.78^{a}	81.79 ± 0.78^{a}
GA1200	600.18	56.03 ± 0.75^{cd}	2.11 ± 0.02^{d}	80.87 ± 1.57^{a}	74.61 ± 0.48^{b}	62.48 ± 0.33^{a}	80.48 ± 0.33^{a}
GA1600	800.24	39.58 ± 0.07^{f}	1.75 ± 0.01^{c}	80.25 ± 1.81^{a}	72.74 ± 0.93^{c}	54.98 ± 0.86^{bc}	81.98 ± 0.86^{a}
GA2000	1000.3	29.64 ± 0.08^{g}	1.78 ± 0.02^{c}	81.07 ± 1.21^{a}	74.46 ± 0.72^{b}	53.89 ± 0.53^{c}	82.89 ± 0.53^{a}

Source: prepared by the author himself.

3.3.5 Fourier-transform infrared spectroscopy (FTIR)

The infrared spectra of alginate, gelatin, gum Arabic, buriti oil, and microcapsules produced with gelatin/gum Arabic at 800 rpm, as well as microcapsules produced with gelatin/sodium alginate at 1600 rpm, are shown in Figure 3.8. The spectra of the other microcapsules produced were not presented because they have similar characteristics, with slight variations in intensity.

Figure 3.8 FTIR spectra of alginate (GEL), gum Arabic (ARB), gelatin (GEL), buriti oil (OIL), gelatin/gum Arabic microcapsules produced at 800 rpm (ARBGEL), and gelatin/sodium alginate microcapsules produced at 1600 rpm (ALGGEL).

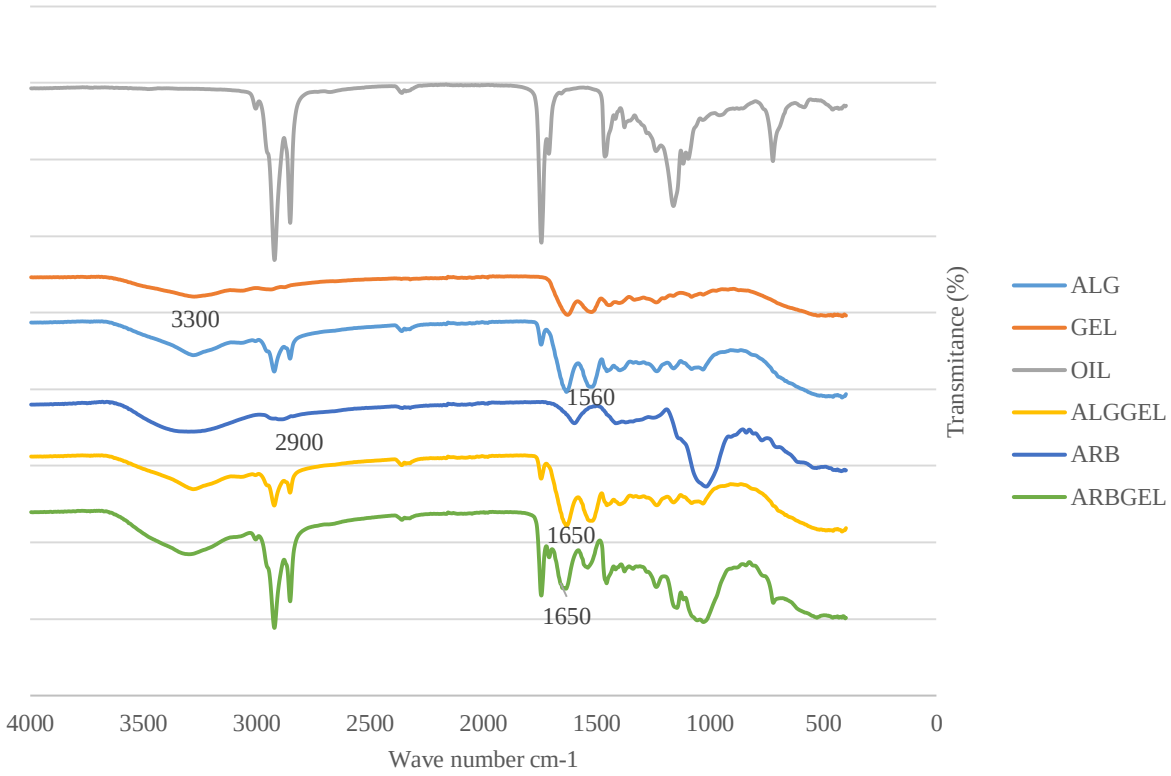

Source: prepared by the author himself.

In the spectrum of gum Arabic, a band at 2900 was observed, close to the values found by Hu et al. (2016), and in the spectrum of sodium alginate it is possible to point out the 1560 band, values close to those found by Bastos et al. (2020), which represent the carboxyl group (C=O). The gelatin spectrum presents the 3300 band that represents the amine group, values similar to those found by Hubner et al. (2020).

In the spectra of the microcapsules, two factors are observed: the bands present in the spectrum of the buriti oil are apparent, demonstrating the presence of oil, and the 1650 band, which represents the amide group, which results from the interaction between the carboxyl and amide, present in gelatin and in the polysaccharides used in the formation of microcapsules, thus indicating that the complex coacervation was performed.

3.4 Conclusions

The results showed that the two wall material combinations used for the production of buriti oil microcapsules by complex coacervation were efficient, with high values of encapsulation efficiency and particles with yellow coloration. However, the rheological behavior of the wall material emulsion that will be the basis for the coacervation is of paramount importance in their production, since shear-thinning emulsions have better responses with high agitation speeds, whereas for shear-thickenning emulsions, the opposite is observed. Therefore, for the production of microcapsules by complex coacervation using shear-thinning emulsions, stirring frequencies above 1000 rpm are desirable and for production with shear-thickenning emulsions, stirring frequencies below 1000 rpm are desirable

REFERENCES

ARANHA, C. P. M. **Microencapsulação por gelificação iônica e interação eletrostática do corante de buriti (*Mauritia flexuosa* L. f.).**, 2015. 117 p. Tese (Doutorado em Engenharia e Ciência de Alimentos), Universidade Estadual Paulista, São José do Rio Preto, 2015.

BASTOS, L. P. H.; VICENTE, V.; SANTOS, C. H. C.; CARVALHO, M. G.; GARCIA-ROJAS, E. E. Encapsulation of black pepper (*Piper nigrum L.*) essential oil with gelatin and sodium alginate by complex coacervation. **Food Hydrocolloids**, v. 102, p. 105605, 2020.

CASTEJÓN, N.; LUNA, P.; SEÑORÁNS, F. J. Microencapsulation by spray drying of omega-3 lipids extracted from oilseeds and microalgae: Effect on polyunsaturated fatty acid composition. **LWT**, v. 148, p. 111789, 2021.

CRUZ, M. B.; OLIVEIRA, W. S.; ARAÚJO, R. L.; FRANÇA, A. C. H.; PERTUZATTI, P. B. Buriti (*Mauritia Flexuosa L.*) pulp oil as an immunomodulator against enteropathogenic *Escherichia coli*. **Industrial Crops and Products**, v. 149, p. 112330, 2020.

FERREIRA, S.; VANIA REGINANICOLETTI, V. R. Complex coacervation assisted by a two-fluid nozzle for microencapsulation of ginger oil: Effect of atomization parameters. **Food Research International**, v. 138, Part B, p. 109828, 2020.

FREITAS, M. L. F.; CHISTÉ, R. C.; POLACHINI, T. C.; SARDELLA, L. A. C. Z.; ARANHA, C. P. M.; RIBEIRO, A. P. B.; NICOLETTI, V. R. Quality characteristics and thermal behavior of buriti (*Mauritia flexuosa* L.) oil. **Grasas y Aceites**, v. 68, n. 4, p. e220, 2017.

HU, Q.; GERHARD, G.; UPADHYAYA, I.; VENKITANARAYANAN, K.; LUO, Y. Antimicrobial eugenol nanoemulsion prepared by gum arabic and lecithin and evaluation of drying Technologies, **International Journal of Biological Macromolecules**, v. 87, p. 130-140, 2016.

HUBNER, P.; DONATI, N.; QUINES, L. K. M.; TESSARO, I. C.; MARCILIO, N. R. Gelatin-based films containing clinoptilolite-Ag for application as wound dressing, **Materials Science and Engineering: C**, v. 107, p. 110215, 2020.

LEMOS, Y. P.; MARFIL, P. H. M.; NICOLETTI, V. R. Particle size characteristics of buriti oil microcapsules produced by gelatin-sodium alginate complex coacervation: Effect of stirring speed**. International journal of food properties**, v. 20, n. S2, p. S1438–S1447, 2017.

LI, F.; WANG, H.; MEI, X. Preparation and characterization of phytosterol-loaded microcapsules based on the complex coacervation. **Journal of Food Engineering**, v. 311, p. 110728, 2021.

LIU, Y.; WINTER, H. H.; PERRY, S. L. Linear viscoelasticity of complex coacervates. **Advances in Colloid and Interface Science**, v. 239, p. 46-60, 2017.

LUO, W.; HUANG, H.; ZHANG, Y.; WANG, F.; YU, J.; LIU, Y.; LI, X. Complex coacervation behavior and the mechanism between rice glutelin and gum arabic at pH 3.0 studied by turbidity, light scattering, fluorescence spectra and molecular docking. **LWT**, v. 150, p. 112084, 2021.

JEGÁT, C.; TAVERDET, L. J. Stirring speed influence study on the microencapsulation process and on the drug release from microcapsules. **Polymer Bulletin**, v. 44, p. 345-351, 2000.

KOUAMÉ, K. J. E. P.; BORA, A. F. M.; LI, X.; SUN, Y.; LIU, L. Novel trends and opportunities for microencapsulation of flaxseed oil in foods: A review. **Journal of Functional Foods**, v. 87, p. 104812, 2021.

MOSER, P.; NICOLETTI, V. R.; DRUSCH, S.; BRÜCKNER-GÜHMANN, M. Functional properties of chickpea protein-pectin interfacial complex in buriti oil emulsions and spray dried microcapsules. **Food Hydrocolloids**, v. 107, p. 105929, 2020.

MOSER, P.; FERREIRA, S.; NICOLETTI, V. R. Buriti oil microencapsulation in chickpea protein-pectin matrix as affected by spray drying parameters, **Food and Bioproducts Processing**, v. 117, p. 183-193, 2019.

MATOS, E. F.; SCOPEL, B. S.; DETTMER, A. Citronella essential oil microencapsulation by complex coacervation with leather waste gelatin and sodium alginate. **Journal of Environmental Chemical Engineering**, v. 6, p. 1989-1994, 2018.

MANSUR, M. C. P. P. R.; CAMPOS, C.; VERMELHO, A. B.; NOBREGA, J.; BOLDRINI, L. C.; BALOTTIN, L.; LAGE, C.; ROSADO, A. S.; RICCI-JÚNIOR, E.; SANTOS, E. P. Photoprotective nanoemulsions containing microbial carotenoids and buriti oil: Efficacy and safety study. **Arabian Journal of Chemistry**, v. 13, p. 6741-6752, 2020.

MUHOZA, B.; QI, B.; HARINDINTWALI, J. D.; KOKO, M. Y. F.; ZHANG, S.; LI, Y. Combined plant protein modification and complex coacervation as a sustainable strategy to produce coacervates encapsulating bioactives. **Food Hydrocolloids**, v. 124, Part B, p. 107239, 2022.

PATHAK, J.; PRIYADARSHINI, E.; RAWAT, K.; BOHIDAR, H. B. Complex coacervation in charge complementary biopolymers: Electrostatic versus surface patch binding. **Advances in Colloid and Interface Science**, v. 250, p. 40-53, 2017.

SHADDEL, R.; HESARI, J.; AZADMARD-DAMIRCHI, S.; HAMISHEHKAR, H.; FATHI-ACHACHLOUEI, B.; HUANG, Q. Use of gelatin and gum Arabic for encapsulation of black raspberry anthocyanins by complex coacervation. **International Journal of Biological Macromolecules**, v. 107, Part B, p. 1800–1810, 2018.

SARAVANAN, M.; RAO, K. P. Pectin–gelatin and alginate–gelatin complex coacervation for controlled drug delivery: Influence of anionic polysaccharides and drugs being encapsulated on physicochemical properties of microcapsules. **Carbohydrate Polymers**, v. 80, p. 808-816, 2010.

STEFFE, J. F. **Rheological methods in food process engineering**. Freeman Press, East Lansing, USA, 1996.

ZHANG, H.; CHEN, K.; YANG, J. Development of a versatile microencapsulation technique for aqueous phases using inverse emulsion. **Colloids and Surfaces A: Physicochemical and Engineering Aspects**, v. 634, p. 127865, 2022.

CAPÍTULO 4

FOAM-MAT AND THIN-FILM DRYING AS ALTERNATIVES TO FREEZE DRYING OF COMPLEX COACERVATED MICROCAPSULES CONTAINING BURITI OIL (*Mauritia Flexuosa* L.)

4. FOAM-MAT AND THIN-FILM DRYING AS ALTERNATIVES TO FREEZE DRYING OF COMPLEX COACERVATED MICROCAPSULES CONTAINING BURITI OIL (*Mauritia flexuosa* L.)

ABSTRACT

In order to protect compounds of interest, such as beta-carotene, microencapsulation emerged as a technique that aims to reduce the interference of the environment in the compounds of interest. Complex coacervation is considered as a suitable technique for the encapsulation of vegetable oils, however, the microcapsules produced by complex coacervation are often dried by lyophilization, which makes the technique more expensive. This work aimed to investigate alternative drying techniques for microcapsules, using foam-mat and thin-film drying. The different drying techniques leaded to good results in terms of encapsulation efficiency, with results close to 85%, demonstrating that the highest temperatures used during drying did not interfere in the microcapsule quality. The characterization of the obtained powders also showed good results, with the main difference found between the samples being in the coloration; the samples dried by thin-film had a small loss of yellow coloration.

4.1 Introduction

The oil extracted from the fruits of buriti (*Mauritia flexuosa* L.), a palm tree that grows in the Brazilian cerrado, is traditionally used in cooking and with medicinal purposes. Buriti oil is rich in beta-carotene and tocopherols, which are bioactive compounds that lower the risk of coronary heart diseases and eye diseases. Buriti oil is widely studied for its nutritional, medicinal, and antimicrobial characteristics, having great potential for application in pharmaceutical, cosmetic and food industries (CRUZ, at al., 2020; MANSUR, et al., 2020; LEÃO, et al., 2019).

The major bioactive compounds found in buriti oil are the carotenoids, which have antioxidant properties and provitamin-A activity. The high carotenoid amount present in this oil makes it a very interesting ingredient to food nutritional enrichment, in addition to confer enhanced product stability by hindering oxidation. On the other hand, the poor

water solubility and the potential fast degradation of these compounds when in contact with oxygen, acids, or when exposed to light or high temperatures, are drawbacks to their use in food formulation (RODRIGUEZ-AMAYA; KIMURA, 2004; SANTOS et al., 2021).

Protection to bioactive compounds can be achieved by microencapsulation techniques, which have been intensively investigated for application in food products (HUANG; YUAN; BAOJUN, 2021; CORRÊA-FILHO; MOLDÃO-MARTINS; ALVES, 2019). One of these techniques is complex coacervation, an appropriate approach to encapsulate hydrophobic substances that are sensitive to high temperatures and that provides high encapsulation efficiency (ALVIM; GROSSO, 2010; LEMOS; MARFIL; NICOLETTI, 2017). Complex coacervation is caused by electrostatic interactions between two or more polymeric molecules (wall materials), usually a protein and a polysaccharide, at pH values in which they present opposite charges. Depending on the wall material formulation, complex coacervation has some advantages, such as thermal stability, controlled release and high loading capacity (LI, et al., 2021; LUO, et al., 2021; MUHOZA, et al., 2021; MUNERATTO; GALLO; NICOLETTI, 2021).

In spite of being a valuable method for microencapsulation, there are some difficulties associated to the scale-up of complex coacervation processes, mainly related to the need of preservation and storage techniques that could easily be adopted at the industrial level (XIAO et al. 2013). Complex coacervation occurs in relatively diluted medium, and after formation of the microcapsules they need to be dried in order to reach sufficiently high concentrations of active ingredients, as well as to provide further protection from hydrothermal degradation, extending their shelf life, and allowing their incorporation to dehydrated products (GLOMM et al., 2021).

Freeze-drying is the most used drying method for complex coacervated microcapsules in studies at bench-scale, but despite generating high-quality dehydrated products, this is an intensively time and energy consuming process (RATTI, 2001). Spray drying has also been applied, with the advantage of being able to produce individual particles, but the shear forces involved in atomization can cause the disintegration of the capsule wall due to its low physical strength, thus requiring crosslinking of the capsules. Unfortunately, in food applications there is a limited choice of crosslinking agents regarded as safe, mainly represented by the enzyme transglutaminase (ALVIM; GROSSO, 2010; GLOMM et al., 2021).

There are alternative drying techniques that allow production of individual particles, use low temperatures, may be more cost-effective than freeze drying, and less harmful to microcapsule integrity than spray-drying. Foam-mat drying offers some advantages, such as high drying rates at low temperatures, maintaining the original characteristics and generating powders with good volatile retention and easy to be reconstituted. Foam-mat drying consists of adding a foaming agent to the material to be dried and using a stirring propeller for incorporating air, thus producing a foam prior to drying, which largely increases the surface area available for mass transfer (QUADRI; SRIVASTAVA; YOUSUF, 2020; HARDY; JIDEANI, 2017). Thin-film drying is a technique highly applied for the production of biodegradable packaging, and basically consists of drying a thin film of the material of interest at temperatures close to ambient. The drying results are very influenced by the materials that make up the film, the film thickness and the temperature used in drying, where high temperatures generate more compact and consequently more brittle films (FALADEA; ADENIYI, 2021; OSAMA, et al., 2021; LI, et a., 2019).

To the best of our knowledge, there are no reported works that have investigated the use of foam-mat or thin-film drying applied to complex coacervated microcapsules as an alternative to freeze-drying. This work investigated the application of these two alternative drying methods to buriti oil microcapsules produced by complex coacervation between gelatin and gum Arabic, aiming to investigate their effects on the particle size, morphology, color, and carotenoid retention.

4.2 Methods and material

4.2.1. Materials

Buriti oil was purchased from Amazon Oil, Brazil. Gelatin extracted from bovine skin, type B, with gel strength of 240 bloom (Gelita, Brazil) and Arabic gum (Dinâmica, Brazil), were used as wall materials for complex coacervation. Albumin 95% (PR Neto, Brazil) was used for the production of foams for drying.

4.2.2. Methods

4.2.2.1. Complex coacervation

The microcapsules were produced following the methodology described by Lemos et al. (2017). Gelatin and gum Arabic solutions (1% w/w) were heated to 50 °C. Buriti oil (1% w/w) was added to the gelatin solution and stirred at 15.000 rpm using an ultraturrax equipment (IKA, model T25, Germany) for 5 min for complete homogenization. The two solutions were added into a stirred vessel (1 L), and the pH was adjusted to 3.5 using acetic acid to trigger the complex coacervation, while the solutions were stirred at 1000 rpm for microcapsule formation. After coacervation, the temperature was reduced to 10 °C, and the suspension was stored in refrigerator to cure the microcapsules. The suspension was left at rest and, 24 hours later, the microcapsules were filtered and stored.

4.2.2.2. Drying methods

4.2.2.2.1. Foam-mat drying

The production and drying of foams were based on the methodology described by Chaux-Guitierrez et al. (2017), with modifications. Albumin (0.1%, w/w) was added to the microcapsule slurry obtained after filtration. The mixture was stirred in a domestic mixer for 7 min, the foam obtained was placed added in 17.5 cm x 26.5 cm trays (Figure 4.1), and dried in an oven with forced air circulation (MA 035, Marconi Equipamentos Para Laboratórios Ltda.) at 25 °C for 24 hours.

Figure 4.1 Aspect of the foam formed by beating the complex coacervated microcapsule slurry added with albumin

Source: prepared by the author himself.

4.2.2.2.2 Thin-film drying

Thin-film drying was based on the methodology described by Amado et al. (2020). After filtering, the microcapsule slurry were added in polyethylene trays with dimensions of 17.5 x 26.5 (Figure 4.2), and dried in an oven with forced air circulation (MA 035, Marconi Equipamentos Para Laboratórios Ltdarconi) at 25 °C. A mass of 100 g of the microcapsule slurry was added to each tray to ensure formation of a 0.3 cm-thick film.

Figure 4.2 Aspect of the thin-film formed by the complex coacervated microcapsule slurry

Source: prepared by the author himself.

4.2.2.2.3 Freeze drying

The microcapsule slurry obtained after filtration was placed in aluminum trays of 8.5 x 14.5 cm (Figure 4.3), and frozen in an ultra-freezer (Liobrás, model FV 500, Brazil) at -40 °C for 24 hours, followed by freeze drying (Liobrás, model L101, Brazil) for approximately 72 h. A mass of 100 g of the microcapsule slurry was added to each tray to ensure formation of a 0.35 cm-thick film.

Figure 4.3 Aspect of the layer of complex coacervated microcapsule slurry for freeze drying

Source: prepared by the author himself.

4.2.2.3 Drying yield

The yield of each drying method was determined in triplicate as the mass ratio of the powder collected after drying and the solids used for the production of microcapsules.

4.2.2.4 Encapsulation efficiency

The encapsulation efficiency was calculated by quantifying the initial carotenoid content in the buriti oil, the carotenoids present on the surface of the microcapsules, and total carotenoids present in the microcapsules, in triplicate, as described by Aranha (2015) with some modifications. The quantification of carotenoids expressed in β-carotene were determined by Equation 4.1. The encapsulation efficiency was calculated by Equation 4.2.

$$C = \frac{Abs \times V \times 10^4}{2396 \times g} \quad (4.1)$$

$$\%EE = \frac{EC}{TC} \times 100 \quad (4.2)$$

4.2.2.5 Moisture content and water activity of microcapsules

The moisture content of the powders was determined by gravimetric method. Aliquots of about 1.5 g of each sample were weighed in triplicate and dried at 100 °C for 8 h. Water activity (aw) was determined at 25 °C in an electric hygrometer (Aw Sprint, Novasina, Axair Ltd., Switzerland).

4.2.2.6 Hygroscopicity

The hygroscopicity of the samples was determined according to the methodology proposed by Pereira et al. (2019). 1 g of the powders were added to desiccators containing a NaCl solution, with humidity at 75.3 %, kept at 25°C. The hygroscopicity values were calculated by the relationship between the initial weight of the powders and the weight gained after one week.

4.2.2.7 Powder dissolution time

Aliquots of 1 g of the samples were added to 100 mL of distilled water and stirred in a magnetic stirrer until complete dissolution, registering the time.

4.2.2.8 Wetting time

Aliquots of the powders (1 g) were dispersed in 500 mL of distilled water at 25°C and the time required for all particles to submerge was recorded.

4.2.2.9 Contact angle

Determination of powder contact angle was made in a tensiometer (Biolin Scientific, Attension Sigma 700/701) using the Washburn's capillary ascending method, in which the liquid rise through the powder bed inside the capillary (PEREIRA; CATTELAN; NICOLETTI, 2019).

4.2.2.10 Bulk density

Aliquots of 1.5 g were added and gently accommodated in a graduated cylinder. The bulk density (ρ_{bulk}) was calculated as the ratio between the mass and the volume occupied by the samples.

4.2.2.11 Tapped density

Aliquots of 2.5 g of the powders were added in a graduated cylinder and compacted with the movement of the cylinder until no change in volume was observed. The tapped density (ρ_{tapped}) was calculated by the ratio of the mass and the tapped volume of the samples.

4.2.2.12 Particle density

Particle density was calculated by the volume displacement method using ethyl alcohol (PA). Aliquots of 2.5 g of the powders and 10 mL of ethyl alcohol were added in a graduated cylinder. The density of the particle ($\rho_{particle}$) was obtained from the relationship between the mass and the variation in volume of the solvent.

4.2.2.13 Bulk porosity

The bulk porosity (ε) was determined from Equation (4.3) (KROKIDA; MAROULIS, 1997).

$$\varepsilon = \left(1 - \frac{\rho_{tapped}}{\rho_{particle}}\right) \times 100 \quad (4.3)$$

4.2.2.14 Powder flowability and cohesiveness

Powder flowability and cohesiveness were calculated from the values of compacted density (ρ_{tapped}) and bulk density (ρ_{bulk}), by Equations 4.4 and 4.5. The Carr index (*CI*) indicates the ability of a powder to flow easily and the Hausner ratio (*HR*) is used to assess the cohesiveness of the powders (ADSARE; ANNAPURE, 2021).

$$CI = \frac{(\rho_{tapped} - \rho_{bulk})}{\rho_{tapped}} \times 100 \quad (4.4)$$

$$HR = \frac{\rho_{tapped}}{\rho_{bulk}} \quad (4.5)$$

4.2.2.15 Angle of repose

Aliquots of 5.0 g of the powders were added in a funnel with the outlet pipe sealed. The funnel was placed on a rod at a height of 10 cm from a flat surface; after opening the outlet pipe, the samples formed a cone on the surface. The angle of repose (θ) was determined from the height (h) and radius (r) of the formed powder cone, according to Equation (4.6).

$$tan\theta = \left(\frac{h}{r}\right) \quad (4.6)$$

4.2.2.16 Particle rehydration

Aliquots of 0.5 g of particles were added to 50 mL of distilled water and stirred in a magnetic stirrer for 10 minutes, followed by observation at optical microscope.

4.2.2.17 Particle morphology

The morphology of the capsules was evaluated in two steps of the production process: After drying and after rehydration. The samples were placed on slides and

analyzed using an optical microscopy (Olympus, CX31) coupled to an 8.1-megapixel digital camera (Sony Cyber-Shot, DSC-W150).

4.2.2.18 Scanning Electron Microscopy

Microcapsule morphology was analyzed by scanning electron microscopy (SEM) using equipment JEOL model JSM7500F with magnifications of 250×. Small aliquots of the powders were fixed on double sided adhesive tape mounted on SEM stubs and coated with gold under vacuum.

4.2.2.19 X-ray diffraction

The crystallinity of the materials forming the microcapsules, and the powders obtained after drying were analyzed using the RINT 2000 (Wide Angle Goniometer). The diffraction angle varied in the range of 5.0° a 90.0°, with a sweep speed of 2θ.

The crystallinity index (C) was determined through the relationship between the total amorphous area (A_a) and the area of the peaks (A_p), Equation 4.7, as proposed by Hayakawa et. al (1997).

$$C = \frac{A_p}{A_a + A_p} \times 100 \quad (4.7)$$

4.2.2.20 Fourier transform infrared spectroscopy (FT-IR)

The FTIR spectra of the materials forming the microcapsules and microcapsules themselves were read in (Bruker Vertex 70). The wavelength used in the analyzes were from 400 to 4000 cm^{-1}.

4.2.2.21 Color attributes

Color analysis was performed using a Konica Minolta colorimeter (CR-S, Konica Minolta, Japan). The color coordinates L*, a*, b*, were measured with D65 illuminant at 10º observation angle.

4.2.2.22 Statistical analysis

All the analyses were carried out in triplicate and the t-test for difference between two means was performed for treatments at a significance level of 95%.

4.3 Results and discussion

In general, the methods used for drying the buriti oil microcapsules had influence on the physical-chemical properties that have great importance in shelf life an in the type of packaging necessary for their storage. All results are shown in Table 4.1.

The drying yield for all the treatments was high, around 90%, which demonstrates that the techniques used are effective for drying this type of microcapsules, the losses that were found are due to adhesion of part of the solids in the vessel used for the production of microcapsules and in the trays used during drying.

Table 4.1 Physicochemical properties of complex coacervation microcapsules of buriti oil after drying by foam-mat, thin-film and freeze drying

Physicochemical properties	Foam-mat	Thin-film	Freeze drying
Drying yield (%)	90.05±0.21^{a}	89.79±0.89^{a}	91.00±1.21^{a}
Encapsulation efficiency (%)	85.23±0.81^{a}	84.48±0.91^{a}	84.38±0.88^{a}
Moisture (%, wet basis)	7.26±0.09^{a}	6.41±0.55^{a}	3.05±0.35^{b}
Water activity	0.342±0.002^{a}	0.304±0.001^{b}	0.231±0.002^{c}
Hygroscopicity (%)	10.83±0.17^{a}	6.88±0.18^{c}	9.21±0.14^{b}
Dissolution time (min)	-	-	-
Wetting time (min)	47.67±3.05^{b}	37.33±4.04^{b}	78.33±9.50^{a}
Contact angle (°)	89.38±0.11^{a}	87.00±2.20^{a}	88.04±1.89^{a}
L*	73.90±0.01^{b}	63.40±0.06^{c}	82.63±0.01^{a}
a*	14.29±0.03^{b}	19.30±0.14^{a}	8.84±0.02^{c}
b*	54.18±0.05^{b}	67.80±0.22^{a}	54.14±0.11^{b}
Bulk density (g/mL)	0.372±0.005^{a}	0.404±0.017^{a}	0.160±0.0125^{b}
Tapped density (g/mL)	0.471±0.027^{a}	0.419±0.018^{a}	0.220±0.023^{b}
Particle density (g/mL)	0.497±0.023^{b}	0.907±0.190^{a}	0.391±0.036^{b}
Bulk porosity (%)	22.25±2.69^{b}	55.24±8.02^{a}	58.59±6.79^{a}

Hausner ratio	1.23±0.06[a]	1.06±0.02[b]	1.37±0.04[a]
Cohesiveness	Intermediate	Low	Intermediate
Carr Index (%)	20.74±3.78[a]	5.37±1.61[b]	29.89±2.26[a]
Flowability	Good	Very good	Fair
Angle of repose (º)	34.38±3.88[a]	26.74±2.16[b]	34.28±0.59[a]
	(good)	(excellent flow)	(good)
Crystallinity (%)	0.400±0.006[a]	0.392±0.0212[a]	0.405±0.014[a]

Source: prepared by the author himself.

The encapsulation efficiency was close ($p > 0.5$) for all samples, demonstrating that drying at low temperatures does not degrade the carotenoids present in buriti oil. The microcapsules presented encapsulation efficiency values above 80%, which are values close to those found by Bordón (2019), who produced chia seed oil microcapsules dried by spray drying, and Hernández-Nava (2020), who produced oregano essential oil microcapsules dried by spray drying.

4.3.1 Shelf-life properties

Drying by lyophilization was the only one that proved to be effective to attain a moisture content close to 3%, which would be sufficiently low to ensure the chemical qualities of the samples during storage; according to Ramakrishnan, et al. (2018) to ensure these qualities, foods must have a moisture content below 5 %. The samples dried by foam-mat and thin-film had moisture levels slightly above 5%, but possibly a few more hours of drying would guarantee the necessary security for good storage. It would be recommended to carry out a complete study of drying kinetics of the microcapsules by foam-mat and thin-film in order to determine the most adequate parameters to be used in these drying methods.

In addition to moisture, other parameters important to determine the safety of dry or powdered foods are the water activity, as well as the hygroscopicity, which indicates how much water is absorbed when the food is stored in an environment with different relative humidity. According to Oliveira et al. (2015), the adsorption of water can modify the characteristics of dry foods, causing the beginning of agglomeration, which difficult its use. The hygroscopicity values were higher for the foam-mat dried sample, and the

lowest value was observed for the thin-film dried sample, which can be explained by the addition of albumin, which would be another compound for the absorption of water during storage, according to Fennema (2010), water molecules can bind to several groups present in proteins, which can vary their hygrocopicity

According to the data presented in Table 4.2, all samples had water activity values below 0.35, demonstrating that they are stable regarding microbial development. According to Hoffmann (2001) and Brazilian legislation (Brasil, 2019), foods with water activity below 0.6 hinder the microbial activity.

4.3.2 Flow properties e microcapsules reconstitution

The reconstitution of powders has great relevance in industrial applications, being a unity operation that involves four physical stages: wetting sinking, dispersion, and – in the case of soluble powders – dissolution. Wettability refers to the time it takes for particles to wet and submerge, which is related to the excess of surface tension between the particles and the liquid medium (GAUDEL, et al. 2022; FOURNAISE et al., 2021). None of the samples were soluble in water, thus it was not possible to measure dissolution time and water solubility values. This is due to the preparation of the microcapsules themselves, since complex coacervation is based on a molecular interaction carried out in aqueous solution, so when the dried capsules are dispersed in water they only goes through rehydration and not disintegrate, as shown in the Figure 4.5 that show the microcapsules after rehydration. It is possible to observe that all the samples were reconstituted to their original morphology.

The values found for the contact angle did not differ from each other, but all had values slightly smaller than 90°. According to Huminic (2021), particles that have contact angles values between $0° \leq \theta \leq 90°$ have hydrophilic characteristics and are able to wet their surface. As the samples had values close to 90°, this indicates that all of them have low hydrophilicity, which corroborates the a_w and hygroscopicity values found.

Powder flow properties are extremely important in some industrial aspects, such as storage, transport and compaction, and can be described by density, porosity, angle of repose, as well as other indicators such as Carr Index (CI) and Hausner Ratio (HR) (BAESSO et al., 2021). The Carr Index allows powder flowability to be classified as 'very good' (CI < 15%), 'good' (15 < CI < 20%), 'fair' (20 < CI < 35%), 'bad' (35 < CI < 45%), and 'very poor' (CI > 45%). Cohesiveness may be classified according to Hausner Ratio

in 'low' (HR < 1.2), 'intermediate' (1.2 < HR < 1.4) and 'high' (HR > 1.4). The angle of repose (θ) indicates 'excellent flow' ($\theta < 30°$), ‘good’ ($31 < \theta < 35°$), ‘fair' ($36 < \theta < 40°$), ‘passable which may hang up' ($41 < \theta < 45°$), ‘poor which must be agitated or vibrated' ($46 < \theta < 55°$) and ‘very poor flow' ($\theta > 56°$) (SHAH et. Al. 2008). According to Adsare; Annapure (2021), the flow properties of powders are essential for the choice of materials used in the packaging for storage, and the values found showed a significant difference between the treatments. The powder dried by the thin-film method stood out, presenting the best flow properties and the lowest cohesiveness, with values close to those found by Zaidul (2020) and Adsare; Annapure (2021).

The bulk powder density was higher for the particles dried by foam-mat and thin-film, methods that applied airflow, with values around 0.4 g/mL. The lyophilized sample presented smaller density values, which can be explained by the drying technique, in which water withdrawal occurs by sublimation, thus leaving the sample with a porous microstructure that leads to low particle density (NAKAGAWA et. al, 2022). The particle and tapped densities showed a significant difference between the samples dried by thin-film in relation to those dried by foam-mat and freeze drying. The particle density results of the thin-film dried samples presented values of 0.907 g/mL and the samples dried by foam-mat and lyophilization had values below 0.50 g/mL, values close to those found by Pereira et al. (2019) for microcapsules of pink pepper essential oil, and Elik (2021) for fish oil microcapsules, respectively.

The porosity of the samples was lower for the foam-mat dried samples, to which albumin was added to aid in drying. The porosity is linked to the presence of pores in the sample, such pores help in the rehydration of dry powders, affecting its stability during storage. Possibly the lowest porosity values found for the sample containing albumin is due to the filling of these pores by the albumin itself, which can be seen in Figure 4.6a, in which the surface of the sample presents a smoother and more compact characteristic. The porosity values of the samples are lower than those found by Zaidul (2020), that encapsulated fish oil with HPMC.

4.3.3 Color analyses

The color parameters L, a* and b* of the samples are shown in Table 1. The parameter L indicates the luminosity, and there was a significant difference between all

samples, with the freeze-dried sample presenting the highest index. Possibly the higher temperatures applied during drying caused a greater darkening of the samples. Parameters a* and b* indicate the color range in which the samples are reddish-yellow, with emphasis on thin-film drying, which indicates that all samples managed to maintain the original color of the oil and the maintenance of its compounds, corroborating with the encapsulation efficiency analyses. The color parameters observed are similar to those found by Moser et. al (2019), for spray dried buriti oil microcapsules.

4.3.4 Morphological properties

Figure 4.4 shows the buriti oil microcapsules produced by complex coacervation. It is possible to observe that the microcapsules had mostly a spherical shape with multinucleated interior, characteristics similar to those found by Ferreira; Nicoletti (2021) in their studies for the production of microcapsules by complex coacervation of ginger oil

Figure 4.4 Optical microscopy of microcapsules obtained after complex coacervation.

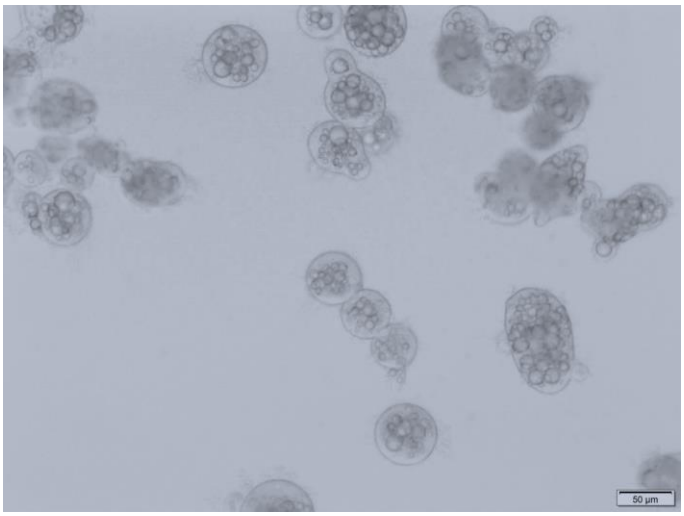

Source: prepared by the author himself.

Analyzing Figure 4.5, which shows the rehydrated microcapsules after the different drying methods, it is possible to observe that in all tests the rehydration resulted in the reconstitution of the microcapsules, in spite of some differences: the foam-mat dried microcapsules returned to their initial shape but with some agglomeration, the samples dried by thin-film, there was a partial reconstitution of some particles that

returned to their original shape with the presence of some agglomerates that continued to retain the buriti oil, while the microcapsules dried by lyophilization showed the best result, with reconstitution of a large part of the microcapsules, presenting some agglomeration and some particles without a specific shape, but without oil release, results similar to those found by Lemos et al. (2017).

Figure 4.5 Optical microscopy of rehydrated complex coacervation microcapsules after dryinf by foam (a), film (b) and lyophilization (c).

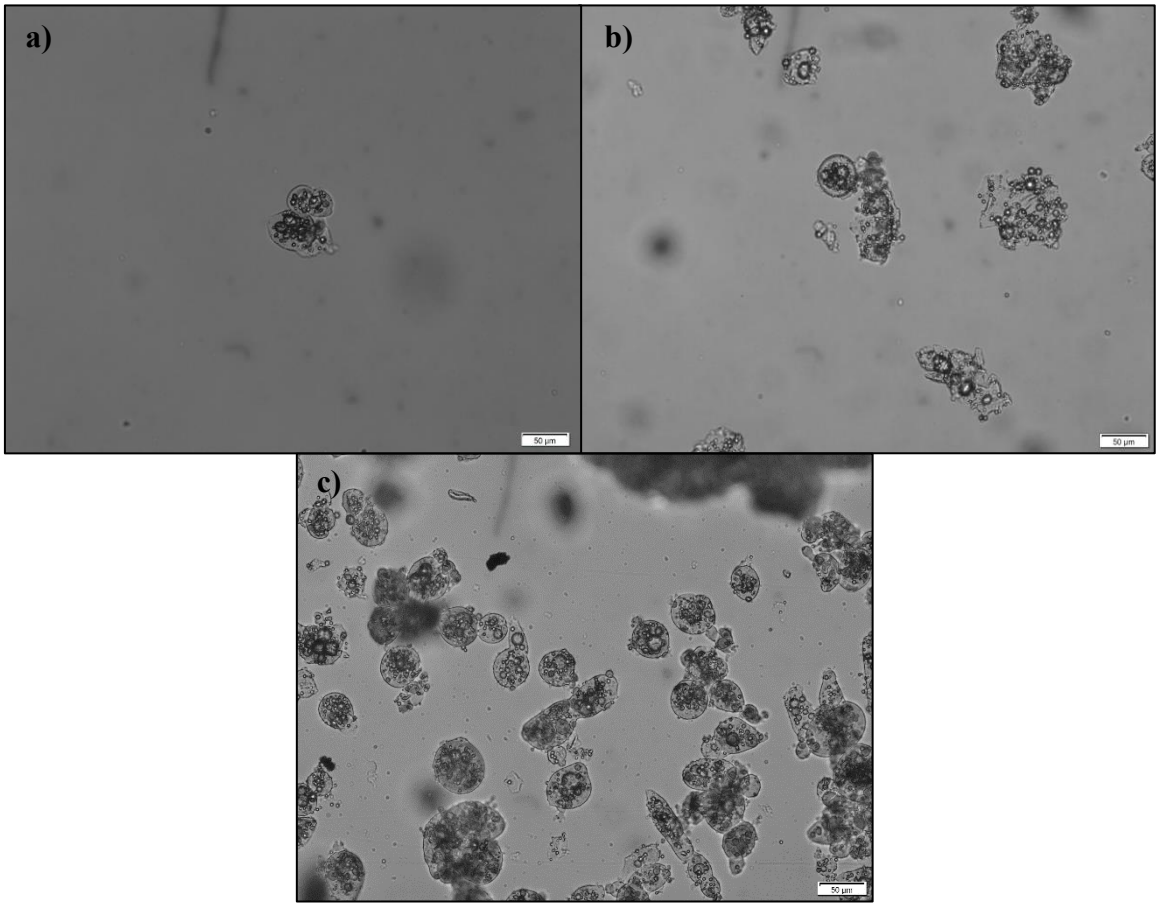

Source: prepared by the author himself.

Figure 4.6 shows the scanning electron microscopy images of the powders obtained after drying. The powders obtained by foam-mat drying had the most smooth surface, whereas the thin-film dried samples had a rougher surface with some voids, and the freeze-dried samples presented a smooth surface but with several voids and empty spaces; in the last two cases this characteristic may have contributed to the higher porosity values, demonstrating similar to the studies by Samakradhamrongthai (2019). The smoother surface of the foam-mat dried samples is probably related to the presence of the

albumin added to produce the foam, and that may have behaved as a second wall material on the particles' surface.

Figure 4.6 Scanning electron microscopy of the powders obtained after drying by foam-mat (a), thin-film (b) and freeze drying (c).

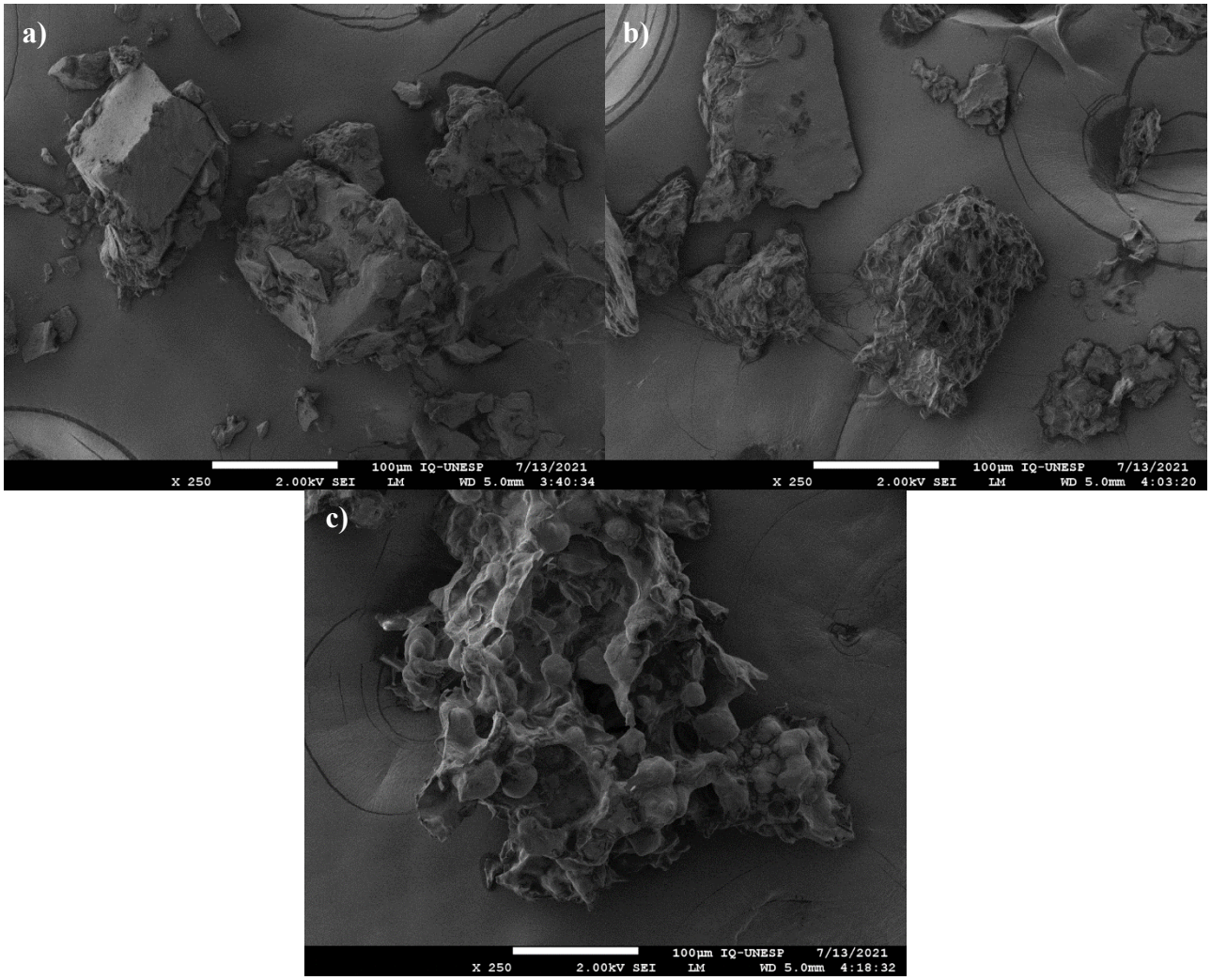

Source: prepared by the author himself.

4.3.5 XDR and FITR

In order to observe whether the drying method would have an influence on the crystallinity of the powders obtained, the X-ray spectrum was recorded (Figure 4.7 shows dried microcapsules after complex coacervation), and all the three samples had values around 40% of crystallinity. The structure of the materials used for the production of microcapsules is very important for their stability, which can interfere with permeability, fluidity, and the greater the crystallinity, the closer the molecules are, limiting interactions

with the environment (SHADDEL et al., 2018). In general, the samples being semi-crystalline and having low hygroscopicity and moisture values demonstrate that the microcapsules and drying methods used can guarantee the integrity of the encapsulated compound.

Figura 4.7. XDR of dried microcapsules after complex coacervation.

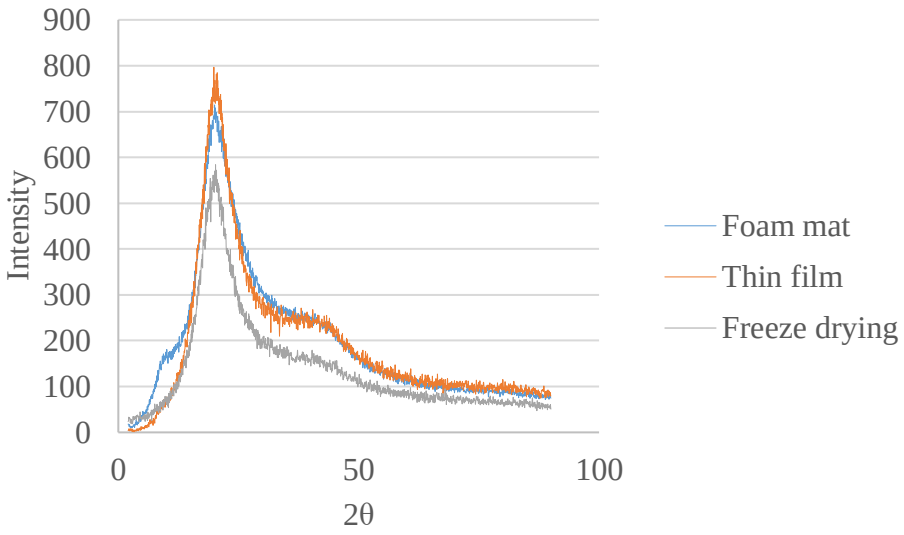

Source: prepared by the author himself.

The FTIR spectrum and also the comparison between the wavelengths of wall materials, buriti oil and dried microcapsules after coacervation are shown in Figure 4.8. The gelatin spectrum showed amine group peaks (N - H) at the wavelength in around 3300 cm^{-1} as observed by Hubner et al. (2020), while the gum Arabic spectrum showed peaks of carboxyl groups with wavelengths around 2900 cm^{-1} (C - O) as observed by Hu et al. (2016). Complex coacervation is based on electrostatic interaction, and in the results found this was observed with the formation of amide groups observed in all spectra of dry microcapsules, which were found at wavelengths close to 1500 cm^{-1} as observed by Shaddel et al. (2018). The presence of the peak corresponding to amine groups in the microcapsules can be observed, which demonstrates that not all ionizable groups were used in coacervation, as also observed by Shaddel et al. (2018). The characteristic peaks at 2928 and 2858 cm−1 of buriti oil were identified in all microcapsules, indicating their presence in the particles.

Figure 4.8 FTIR spectrum of samples and microcapsule forming materials.

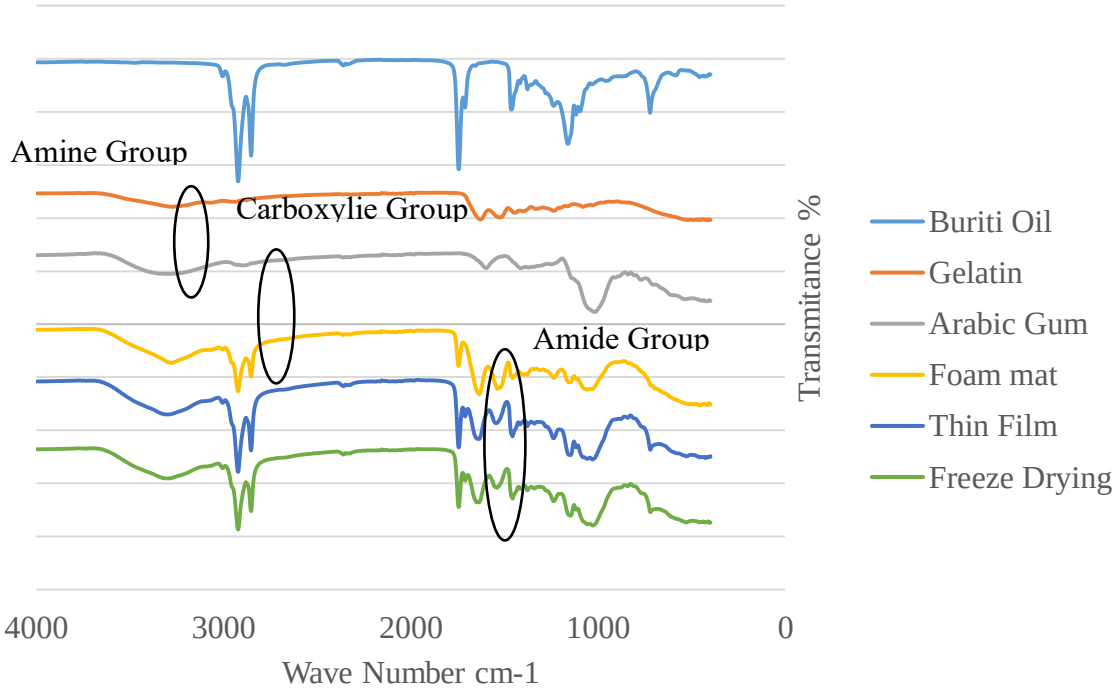

Source: prepared by the author himself.

4.4 Conclusion

The results indicated that the alternative drying methods, by foam-mat and thin-film can be alternatives to drying by lyophilization, which is the most used in drying of microcapsules produced by complex coacervation, since the values of encapsulation efficiency were similar, with no significant differences. The differences found were in some storage characteristics such as porosity and hygroscopicity, however the values found are close to those desirable for storage. In the case of color, drying had a certain influence, with drying at higher temperatures resulted in slight darkening of the microcapsules. On the other hand, when considering energy consumption, the two types of drying used show promise for replacing lyophilization for drying microcapsules produced by complex coacervation.

REFERENCES

ADSARE, S. R.; ANNAPURE, U. S. Microencapsulation of curcumin using coconut milk whey and Gum Arabic, **Journal of Food Engineering**, v. 298, p. 110502, 2021.

ALVIM, I. D.; GROSSO, C. R. F. Microparticles obtained by complex coacervation: Influence of the type of reticulation and the drying process on the release of the core material. **Ciência e Tecnologia de Alimentos**, v. 30, p. 1069-1076, 2010.

AMADO, L. R.; SILVA, K. S.; MAURO, M. A. Effects of interactions between soy protein isolate and pectin on properties of soy protein-based films. **Journal of Applied Polymer Science**, v. 137, p. 48732- 48732, 2020.

ARANHA, C. P. M. **Microencapsulação por gelificação iônica e interação eletrostática do corante de buriti (*Mauritia flexuosa* L. f.).**, 2015. 117 p. Tese (Doutorado em Engenharia e Ciência de Alimentos), Universidade Estadual Paulista, São José do Rio Preto, 2015.

BRASIL, INSTRUÇÃO NORMATIVA N° 60, DE 23 DE DEZEMBRO DE 2019.

BAESSO, I.; KARL, D.; SPITZER, A.; GURLO, A.; GÜNSTER, J.; ZOCCA, A. Characterization of powder flow behavior for additive manufacturing. **Additive Manufacturing**, v. 47, p. 102250, 2021.

BORDÓN, M. G.; PAREDES, A. J.; CAMACHO, N. M.; PENCI, M. C.; GONZÁLEZ, A.; PALMA, S. D.; RIBOTTA, P. B.; MARTINEZ, M. L. Formulation, spray-drying and physicochemical characterization of functional powders loaded with chia seed oil and prepared by complex coacervation. **Powder Technology**, v. 391, p. 479-493, 2021.

CHAUX-GUTIÉRREZ, A. M.; SANTOS, A. B.; GRANDA-RESTREPO, D. M.; MAURO, M. A. Foam mat drying of mango: Effect of processing parameters on the drying kinetics and product quality. **Drying Technology**, v. 35, n. 5, p. 631-641, 2017.

CORRÊA-FILHO, L. C.; MOLDÃO-MARTINS, M.; ALVES, V. D. Advances in the application of microcapsules as carriers of functional compounds for food products. **Applied Sciences**, v. 9, p. 571, 2019.

CRUZ, M. B.; OLIVEIRA, W. S.; ARAÚJO, R. L.; FRANÇA, A. C. H.; PERTUZATTI, P. B. Buriti (*Mauritia Flexuosa L.*) pulp oil as an immunomodulator against enteropathogenic *Escherichia coli*. **Industrial Crops and Products**, v. 149, p. 112330, 2020.

ELIK, A.; YANIK, D. K.; GÖĞÜŞ, F. A comparative study of encapsulation of carotenoid enriched-flaxseed oil and flaxseed oil by spray freeze-drying and spray drying techniques. **LTW**, v. 143, p. 111153, 2021.

FALADEA, O. K.; ADENIYI, O. G. Instant soups from cowpea varieties using foam-mat drying, **LTW**, p. 112191, 2021.

FENNEMA, O. R.; DAMODARAN, S.; PARKIN, K. L. **Química de Alimentos de Fennema**. 4ª ed., Ed. Artmed, 2010. 900 p.

FERREIRA, S.; NICOLETTI, V. R. Microencapsulation of ginger oil by complex coacervation using atomization: Effects of polymer ratio and wall material concentration, **Journal of Food Engineering**, v. 291, p. 110214, 2021

FOURNAISE, T.; PETIT, J.; GAIANIA, C. Main powder physicochemical characteristics influencing their reconstitution behavior. **Powder Technology**, v. 383, p. 65-73, 2021.

GAUDEL, N.; GAIANI, C.; HARSHEB, Y. M.; KAMMERHOFER, J.; POUZOT, M.; DESOBRY, S.; BURGAIN, J. Reconstitution of fruit powders: A process – structure – function approach, **Journal of Food Engineering**, v. 315, p. 110800, 2022.

GLOMM, W. R.; MOLESWORTH, P. P.; SANDRU, E. M.; TRUONG, L. T.; BRUNSVIK, A.; JOHNSEN, H. Microencapsulation of peppermint oil by complex coacervation and subsequent spray drying using bovine serum albumin/gum acacia and an oxidized starch crosslinker. **Applied Sciences**, v. 11, p. 3956, 2021.

HARDY, Z.; JIDEANI, V. A. Foam-mat drying technology: A review. **Critical Reviews in Food Science and Nutrition**, v. 57, n. 12, p. 2560, 2017.

HAYAKAWA, K.; TANAKA, K.; NAKAMURA, T.; ENDO, S., HOSHINO, T. Quality Characteristics of Waxy Hexaploid Wheat (*Triticum aestivum L.*): Properties of Starch Gelatinization and Retrogradation. **Cereal Chemistry**, v. 74, p. 576-580, 1997.

HERNÁNDEZ-NAVA, R.; LÓPEZ-MALO, A.; PALOU, E.; RAMÍREZ-CORONA, N.; JIMÉNEZ-MUNGUÍA, .M T. Encapsulation of oregano essential oil (*Origanum vulgare*) by complex coacervation between gelatin and chia mucilage and its properties after spray drying. **Food Hydrocolloids**, v. 109, p. 106077, 2020.

HOFFMANN. F. L.; Fatores limitantes à proliferação de microorganismos em alimentos. **Brasil Alimentos**, n. 9, 2001.

HU, Q.; GERHARD, G.; UPADHYAYA, I.; VENKITANARAYANAN, K.; LUO, Y. Antimicrobial eugenol nanoemulsion prepared by gum Arabic and lecithin and evaluation of drying Technologies, **International Journal of Biological Macromolecules**, v. 87, p. 130–140, 2016.

HUANG, K.; YUAN, Y.; BAOJUN, X. A critical review on the microencapsulation of bioactive compounds and their application. **Food Reviews International**, p. 1-41, 2021.

HUBNER, P.; DONATI, N.; QUINES, L. K. M.; TESSARO, I. C.; MARCILIO, N. R. Gelatin-based films containing clinoptilolite-Ag for application as wound dressing, **Materials Science and Engineering: C**, v. 107, p. 110215, 2020.

HUMINIC, A.; AHUMINIC, G.; FLEACA, C.; DUMITRACHE, F.; MORJAN, I. Influence of solid surface, temperature and concentration on contact angle of water-FeC nanofluid. **International Communications in Heat and Mass Transfer**, v. 128, p. 105650, 2021.

KREUTZ, T.; CARNEIRO, S. B.; SOARES, K. D.; LIMBERGER, R. P.; APEL, M. A.; VEIGA-JUNIOR, V. F.; KOESTER, L. S. *Aniba canelilla* (Kunth) Mez essential oil-

loaded nanoemulsion: Improved stability of the main constituents and in vitro antichemotactic activity, **Industrial Crops and Products**, v. 171, p. 113949, 2021.

KROKIDA, M. K.; MAROULIS, Z. B. Effect of drying method on shrinkage and porosity. **Drying Technology**, v. 15, p. 2441–2458, 1997.

LEÃO, K. M. M.; REIS, L. V. C.; SPERANZA, P.; RODRIGUES, A. P.; RIBEIRO, A. P. B.; MACEDO, J. A.; MACEDO, G. A. Physicochemical characterization and antimicrobial activity in novel systems containing buriti oil and structured lipids nanoemulsions, **Biotechnology Reports**, v. 24, p. e00365, 2019.

LEMOS, Y. P.; MARFIL, P. H. M.; NICOLETTI, V. R. Particle size characteristics of buriti oil microcapsules produced by gelatin-sodium alginate complex coacervation: Effect of stirring speed. **International journal of food properties**, v. 20, n. 2, p. 1438–1447, 2017.

LI, F.; WANG, H.; MEI, X. Preparation and characterization of phytosterol-loaded microcapsules based on the complex coacervation, **Journal of Food Engineering**, v. 311, p. 110728, 2021.

LI, C.; WUA, K.; SU, Y.; RIFFAT, S. B.; NI, X.; JIANG, F. Effect of drying temperature on structural and thermomechanical properties of konjac glucomannan-zein blend films, **International Journal of Biological Macromolecules**, v. 138, p. 135–143, 2019.

LIU, Z.; LI, H.; ZHU, Z.; HUANG, D.; QI, Y.; MA, C.; ZOU, Z.; NI, H. *Cinnamomum camphora* fruit peel as a source of essential oil extracted using the solvent-free microwave-assisted method compared with conventional hydrodistillation. **LWT – Food Science and Technology**, v. 153, p. 112549, 2022.

LUO, W.; HUANG, H.; ZHANG, Y.; WANG, F.; YU, J.; LIU, Y.; LI, X. Complex coacervation behavior and the mechanism between rice glutelin and gum Arabic at pH 3.0 studied by turbidity, light scattering, fluorescence spectra and molecular docking, **LWT – Food Science and Technology**, v. 150, p. 112084, 2021.

MANSUR, M. C. P. P. R.; CAMPOS, C.; VERMELHO, A. B.; NOBREGA, J.; BOLDRINI, L. C.; BALOTTIN, L.; LAGE, C.; ROSADO, A. S.; RICCI-JÚNIOR, E.; SANTOS, E. P. Photoprotective nanoemulsions containing microbial carotenoids and buriti oil: Efficacy and safety study. **Arabian Journal of Chemistry**, v. 13, p. 6741-6752, 2020.

MOSER, P.; FERREIRA, S.; NICOLETTI, V. R. Buriti oil microencapsulation in chickpea protein-pectin matrix as affected by spray drying parameters, **Food and Bioproducts Processing**, v. 117, p. 183-193, 2019.

MUHOZA, B.; QI, B.; HARINDINTWALI, J. D.; YAGOU, M.; KOKO, F.; ZHANGA, S.; LI, Y. Combined plant protein modification and complex coacervation as a sustainable strategy to produce coacervates encapsulating bioactives, **Food Hydrocolloids**, v. 124, p. 107239, 2021.

MUNERATTO, V. M.; GALLO, T. C. B.; NICOLETTI, V. R. Oregano essential oil encapsulation following the complex coacervation method: Influence of temperature, ionic strength, and pH on the release kinetics in aqueous medium. **Ciência e Agrotecnologia**, v. 45, p. e003221, 2021.

NAKAGAWA, K.; KAMISAKI, H.; SUZUKI, T.; SANO, N. Model-based prediction of the moisture sorption kinetics and humidity-induced collapse for freeze–dried cakes. **Chemical Engineering Science**, v. 248, Part A, p. 117129, 2022

OLIVEIRA, P.R.; JESUS, R.S.; BATISTA, G.M.; LESSI, E. Avaliação sensorial, físico-química e microbiológica do pirarucu (*Arapaima gigas, Schinz* 1822) durante estocagem em gelo. **Brazilian Journal of Food Technology**, v. 17, p. 67-74, 2014.

OSAMA, K.; YOUNIS, K.; QADRI, O. S.; PARVEEN, S.; SIDDIQUI, M. H. Development of under-utilized kadam (*Neolamarkia cadamba*) powder using foam mat drying, **LWT**, v. 154, p. 112782, 2021.

PEREIRA, A. R. L.; CATTELAN, M. G. C.; NICOLETTI, V. R. Microencapsulation of pink pepper essential oil: Properties of spray-dried pectin/SPI double-layer versus SPI single-layer stabilized emulsions. **Colloids and Surfaces A**, v. 581, p. 123806, 2019.

QADRI, O. S.; SRIVASTAVA, A. K.; YOUSUF, B. Trends in foam mat drying of foods: Special emphasis on hybrid foam mat drying technology. **Critical Reviews in Food Science and Nutrition**, v. 60, n.10, p. 1667-1676, 2020.

RAMAKRISHNAN, Y.; ADZAHAN, N. M.; YUSOF, Y. A.; MUHAMMAD, K. Effect of wall materials on the spray drying efficiency, powder properties and stability of bioactive compounds in tamarillo juice microencapsulation, **Powder Technology**, v. 328, p. 406-414, 2018.

RATTI, C. Hot air and freeze-drying of high-value foods: a review. **Journal of Food Engineering**, v. 49, n. 4, p. 311-319, 2001.

RODRIGUEZ-AMAYA, D. B.; KIMURA, M. **Harvestplus Handbook for Carotenoid Analysis**. HarvestPlus Technical Monograph 2. Washington, DC and Cali: Int. Food Policy Research Institute; Int. Center for Tropical Agriculture, 57 p. 2004. https://assets.publishing.service.gov.uk/media/57a08cbae5274a31e00013d4/tech02.pdf

SAMAKRADHAMRONGTHAI, R. S.; ANGELI, P. T.; KOPERMSUB, P.; UTAMA-ANG, N. Optimization of gelatin and gum arabic capsule infused with pandan flavor for multi-core flavor powder encapsulation, **Carbohydrate Polymers** v. 226, p. , 115262, 2019.

SANTOS, P. D. F.; RUBIO, F. T. V.; SILVA, M. P.; PINHO, L. S.; FAVARO-TRINDADE, C. S. Microencapsulation of carotenoid-rich materials: A review. **Food Research International**, v. 147, p. 110571, 2021.

SHADDEL, R.; HESARI, J.; AZADMARD-DAMIRCHI, S.; HAMISHEHKAR, H.; FATHI-ACHACHLOUEI, B.; HUANG, Q. Double emulsion followed by complex coacervation as a promising method for protection of black raspberry anthocyanins, **Food Hydrocolloids**, v. 77, p. 803-816, 2018

SHAH, R. B.; TAWAKKUL, M. A.; KHAN, M. A. Comparative evaluation of flow for pharmaceutical powders and granules, **AAPS PharmSciTech,** v. 9, p. 250–258, 2008.

XIAO, Z.; LIU, W.; ZHU, G.; ZHOU, R.; NIU, Y. A review of the preparation and application of flavor and essential oils microcapsules based on complex coacervation technology. **Journal of the Science of Food and Agriculture**, v. 94, p. 1482-1494, 2014.

ZAIDUL, I. S. M.; FAHIM, T. K.; SAHENA, F.; AZAD, A. K.; RASHID, M. A.; HOSSAIN, M. S. Dataset on applying HPMC polymer to improve encapsulation efficiency and stability of the fish oil: In vitro evaluation, **Data in Brief**, v. 32, p. 106111, 2020.

CAPÍTULO 5

NUTRITIONAL ENRICHMENT OF CORN EXTRUDATES WITH CAROTENOID MICROCAPSULES: PHYSICOCHEMICAL PROPERTIES AND CAROTENE RETENTION

5. NUTRITIONAL ENRICHMENT OF CORN EXTRUDATES WITH CAROTENOID MICROCAPSULES: PHYSICOCHEMICAL PROPERTIES AND CAROTENE RETENTION

Abstract

The addition of microencapsulated buriti oil to traditional starchy extruded snacks can improve their nutritional properties by adding β-carotene in their composition, whereas microencapsulation may represent a tool to allow protection to this bioactive compound as well as to facilitate the incorporation of the oil in the extruded dough; however, the physicochemical properties of the extruded products need to be considered. In this study, four different routes for incorporating buriti oil in the formulations (microencapsulated versus non-encapsulated oil, and before versus after extrusion cooking) were compared, with extrusion being performed at different temperatures (100, 120 or 140 °C). The physicochemical properties of the extruded snacks were evaluated (expansion, density, hardness, color parameters), as well as their carotenoid content. The results showed that the encapsulated buriti oil added prior to extrusion had higher retention values when compared to the oil added freely, obtaining values of carotene retention close to 1.0 µg of carotenoids/g of snack, whereas increasing the processing temperature decreased the physicochemical characteristics of the snacks.

5.1 Introduction

Deficiency in vitamin A consumption is observed in developing and underdeveloped countries, which can affect about 33% of children in pre-school age and also 15% of pregnant women. Lack of vitamin A intake can cause eye problems, including night blindness, low resistance to infections, and even death (NKHATA, 2020; LIMA, 2018). An alternative to overcome this problem is to improve the availability of nutrient-enriched foods. The vitamin A precursor β-carotene is the most abundant carotene in foods and the most economically interesting, as it has greater vitamin activity, being found especially in orange-yellow vegetables and fruits and in dark green leafy vegetables (RODRIGUEZ-AMAYA, 1999).

The buriti palm tree (*Mauritia flexuosa*), which belongs to the Aracaceae family, is a valuable vegetable resource available in the Amazon region. The oil extracted from the pulp of buriti fruits contains a large amount of β-carotene, reaching concentrations of

750 ppm (GUNSTONE; PADLEY, 1997; RODRIGUEZ-AMAYA, 2001). This is higher than the β-carotene concentration found in other foods that are widely consumed by Brazilians, such as guava, pitanga, papaya, passion fruit, and carrots, as well as in other fruits from the Amazon region, such as palm nuts, peach palm and tucumã (RODRIGUEZ-AMAYA, 1996; DE ROSSO; MERCADANTE, 2007). In spite of this important nutritional property, buriti palm tree is not yet commercially cultivated and processed; buriti oil consumption is relatively low, being used mostly as a regional food ingredient and in the cosmetic industry.

Corn extruded products are widely consumed as part of diets around the world, as they are highly available and convenient to consume. Nevertheless, as being made almost exclusively from corn, they are very rich in energy but not very nutritious, opening up a range of possibilities for finding enrichment alternatives with highly nutritionally loaded compounds, such as vitamins and other supplements. Extrusion cooking presents technological feasibility for the fortification or nutritional enrichment of carbohydrate-based snacks with functional ingredients (ORTAK et al., 2017), although the impact of the extrusion process on bioactive compounds is very complex and has not been comprehensively studied (HIRTH et al., 2014). Whereas critical process variables such as temperature, screw speed, and moisture content may induce desirable modifications - such as improving palatability and technological properties of extruded products - these conditions may affect the bioactive compounds of the extrudates. In general, studies have shown that extrusion processing significantly reduces bioactive compounds in food products (BRENNAN et al., 2011).

When used as additives and subjected to food processing, carotenoids are relatively unstable because they are sensible to light, oxygen, temperature and self-oxidation (non-enzymatic cleavage), which causes their rapid degradation (RODRIGUEZ-AMAYA; KIMURA, 2004). The addition of different carotenoid-rich ingredients to extruded products has been reported, including winter squash flour (DELGADO-NIEBLAS et al., 2015), dried Hokkaido pumpkin (OBRADOVIĆ et al., 2015), peach palm flours (BASTO et al., 2016), tomato pulp (TONYALI; SENSOY; KERAKAYA 2016), carrot pomace (KAISANGSRI et al., 2016), and carrot pulp (ORTAK et al., 2017), all of these additives being in the form of dried particulate materials. Besides the susceptibility to degradation, incorporating carotenoid-rich oils to extrusion cooked formulations can bring some additional drawbacks: high lipid content in the feeding material could determine reduction of starch dispersion with consequent

decrease of product expansion, which imparts a compact structure; furthermore, high content of fats may cause oil loss from dough during extrusion process, and subsequently percolation from the extruder (PILLI et al., 2008). Microencapsulation of carotenoid-rich compounds such as palm oil (MARFIL et al., 2018) and buriti oil (LEMOS et al., 2017) by complex coacervation may protect these bioactive compounds as well as enabling the use of the microcapsules to nutritional enrichment of dry food formulations, at the same time as functioning as a natural pigment given the intense reddish-orange to yellow-orange color of the oils.

Based on the above considerations, the aim of this study was to investigate the feasibility and potentiality of enriching extruded snacks produced from corn grits with the addition of microencapsulated buriti oil as a source of β-carotene. Four different routes for incorporating buriti oil in the formulations (microencapsulated versus non-encapsulated oil, and before versus after extrusion cooking) were compared, with extrusion being performed at different temperatures (100, 120 or 140 °C), and the physicochemical properties of expansion, as well as the β-carotene content of the snacks were determined.

5.2 Material and methods

5.2.1 Material

The extruded snacks were produced from corngrits purchased at the local market. Buriti oil (Amazon Oil, Brazil) was microencapsulated by complex coacervation using gelatin extracted from bovine skin, type B, with gel strength of 240 bloom (Gelita, Brazil) and gum Arabic (Dinâmica, Brazil). The pH adjustment during coacervation was performed with 99.7% acetic acid (Dinâmica, Brazil). The solutions were prepared using distilled water. Additional chemicals used were analytical grade.

5.2.2 Methods

5.2.2.1 Microencapsulation of buriti oil

The preparation of the microcapsules was based on the methodology described by Lemos et al. (2017) and Marfil et al. (2016). Individual solutions of gum Arabic (1% w /

w) and gelatin (1% w/w) were stirred and heated up to 50 ± 3 °C until the complete dispersion of the polymers was accomplished. Buriti oil was incorporated (1% w/w) into the gelatin solution and homogenized by using an ultraturrax equipment (IKA, model T25, Germany) at 15,000 rpm for 5 min. The two solutions were mixed in a stirred vessel and the coacervation was induced by lowering the pH to 3.5 ± 0.01 using acetic acid. The agitation system consisted of a jacketed vessel (1 L) with one stirring radial impeller and coupled baffles. During the coacervation process, the solution temperature was maintained at 50 ± 3 °C by circulating water heated in a thermostatic bath through the vessel jacket. After coacervation, the vessel content was cooled up to 10 ± 2 °C by changing the temperature of the water circulating through the jacket, with the aid of a second thermostatic bath. The dispersion was then covered with aluminum foil to protect against light and stored for 24 hours in a refrigerator (Consul, model 280, Brazil) at 5 °C for complete sedimentation and hardening of the particles. The sedimented material was recovered by filtration, placed in aluminum trays, and frozen in an ultra-freezer (Liobras, model FV 500, Brazil) at -40 °C for 24 hours for subsequent freeze drying (Liobras, model L101, Brazil) for 72 h. Finally, the freeze-dried coacervates were macerated in a mortar, protected from illumination and stored in a desiccator to further analyzes and application.

5.2.2.2 Extrusion cooking

The selected experimental design was adopted to allow comparison of four different routes for incorporating buriti oil in the formulations (microencapsulated versus non-encapsulated oil, before versus after extrusion cooking), with extrusion being performed at three different combinations of moisture and temperature (Table 5.1).

Corn grits were extruded in an RXPQ Labor 24 single screw extruder (INBRAMAQ, Ribeirão Preto, Brazil) with five independent heating zones. The extrusion conditions were: helicoidally grooved barrel; screw with a large step, one exit, with a compression ratio of 2.3:1 and length-to-diameter ratio of 15.5:1; pre-die extruder with holes of 3.01 mm; extruder die with a diameter of 2.93 mm (round hole); feed rate of 265 g/min; screw speed at 237 rpm; temperatures in zones 1 to 3: off (approximately 40 ºC), 70 ºC and 90 ºC, respectively. Three combinations of moisture and temperature were used, as follows.

i) intermediate condition: 15% moisture (dry basis) and 120 °C;

ii) most severe condition (lower moisture and higher temperature): 10% moisture (dry basis) and 140 °C;

iii) less severe condition (higher moisture and lower temperature): 20% moisture (dry basis) and 100 °C.

The temperature at zone 4 was always 15 °C lower than at zone 5, and the sequence of the assays was established from the lowest to the highest temperature, in order to facilitate temperature changes. Within each temperature, the extrusion order was: pure corn grits, corn grits added with microcapsules, and corn grits added with non-encapsulated oil. The amount of added carotenoid was determined based on Brazilian legislation (INSTRUÇÃO NORMATIVA - IN Nº 28, DE 26 DE JULHO DE 2018), to ensure a minimum daily intake of vitamin A of 135 µm/day (for adults).

Table 5.1 Extrusion tests performed and their codification

Sample	Code	Moisture (% dry basis)	Temperature (°C)	Route for buriti oil addition
1	OA10			Post-extrusion oil addition*
2	CA10			Post-extrusion microcapsule addition*
3	EO10	10	140	Pre-extrusion oil addition
4	EC10			Pre-extrusion microcapsule addition
5	NO10			No oil addition (control treatment)
6	OA15			Post-extrusion oil addition*
7	CA15			Post-extrusion microcapsule addition*
8	EO15	15	120	Pre-extrusion oil addition
9	EC15			Pre-extrusion microcapsule addition
10	NO15			No oil addition (control treatment)
11	OA20			Post-extrusion oil addition*
12	CA20			Post-extrusion microcapsule addition*
13	EO20	20	100	Pre-extrusion oil addition
14	EC20			Pre-extrusion microcapsule addition
15	NO20			No oil addition (control treatment)

*The oil or the microcapsules were added along with the condiments.

Source: prepared by the author himself.

5.2.2.3 β-carotene content

The quantification of carotenoids in the microcapsules was performed by adding 1 g of microcapsules to a closed erlenmeyer containing 10 mL of acetone, which was kept under stirring for 24 hours protected from light; after that, an aliquot was removed and analyzed in a spectrophotometer (Model UV – M31, BEL Photonics), at a wavelength of 450 nm.

For quantifying the carotenoids present in the snacks, 20 g of the extruded sample was ground in a mixer and added to a closed erlenmeyer containing 100 mL of acetone, protected from light, and stirred for 24 hours; an aliquot was removed and analyzed in a spectrophotometer as described above.

The carotenoid content was calculated by Equation 5.1 and expressed as β-carotene (mg/g).

$$C = \frac{Abs \times V \times 10^4}{2396 \times g} \quad (5.1)$$

5.2.2.4 Expansion ratio and density of the extruded products

The expansion ratio was determined by the ratio between the diameter of the snack, measured using an IP54 digital caliper (Digimess, São Paulo, Brazil), and the diameter of the extruder die (2.93 mm), after 10 random measurements. Density was determined from 10 random measurements of the diameter (D, cm) and length (L, cm) of the snacks, which were also weighed (W, g) in analytical balance (Model AUW220D, Shimadzu). Density (ρ, g/cm^3) was calculated by Equation 5.2.

$$\rho = \frac{4W}{\pi D^2 L} \quad (5.2)$$

5.2.2.5 Hardness

The force required to completely break the snacks was determined using the TA.XT/Plus/50 texture analyzer (Stable Micro Systems, Godalming, UK) and software Texture Exponent 32 (Stable Micro Systems, Godalming, UK), using a Blade Set with

guillotine probe. Ten samples of approximately 5 cm in length were cut perpendicularly using a pre-test speed of 5 mm/s and test speed of 1 mm/s, to obtain force × time curves. The maximum force (N) was considered the cutting force of the snack (PAULA; CONTI-SILVA, 2014).

5.2.2.6 Optical microscopy

The morphology of the capsules and the extruded snacks were evaluated. The snacks were manually broken in small pieces. The samples were placed on slides and analyzed using an optical microscopy (Olympus, CX31) coupled to an 8.1-megapixel digital camera (Sony Cyber-Shot, DSC-W150).

The morphology and particle size distribution of the microcapsules was also determined by optical microscopy. The scanned images were analyzed by CellSens 1.11 image analysis software (Olympus, Japan). The reported diameter is the mean calculated after measurement of 300 microcapsules (FERREIRA; NICOLETTI, 2021).

5.2.2.7 Color attributes

Color analysis was performed using a Konica Minolta colorimeter (CR-S, Konica Minolta, Japan). The color coordinates L^*, a^* and b*, were measured with D65 illuminant and 10º observation angle. The extrudates were transformed into powders, using a mixer, and the powders were homogeneously packed in the probe for color analysis in triplicate.

5.2.2.8 Statistical analysis

The assays were repeated three times in sequence and the analyses were performed in at least in triplicate, if a higher number of repetitions has not been specified. The values of the analytical determinations were subjected to analysis of variance (ANOVA) and mean comparisons by Tukey's test ($p < 0.05$) using the software Minitab 16.1.1.

5.3 Results and discussion

5.3.1 Microcapsule size and morphology

Figure 5.1 shows the microcapsules after complex coacervation, in which it is possible to observe their morphological characteristics. The microcapsules have a circular and multinucleated shape, with the average mean diameter size of 57.69 µm and span of 1.05, values similar to those found by Shadel et al., (2018).

Figure 5.1 Morphological aspect of the microcapsules after complex coacervation

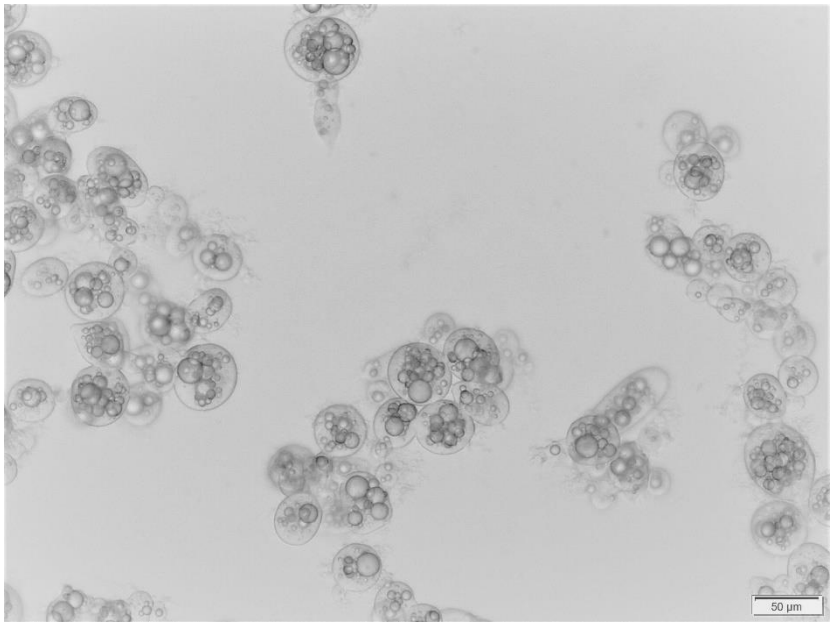

Source: prepared by the author himself.

5.3.2 Extruded snacks

5.3.2.1 Physical characteristics

Expansion ratio: expansion is an important feature to be analyzed, as it has a great influence on consumer acceptability. The expansion ratio of the produced snacks ranged between 222% and 298% as shown in Table 5.2.

In the samples produced at higher temperature the expansion was greater in cases where the oil was added before extrusion when compared to the control treatment, reaching values 30% higher. In general, the increase in temperature caused an increase in

the expansion of the snacks, which corroborates to what Moraru and Kokini (2003) observed in their studies. These authors concluded that temperature is directly related to the expansion of the snacks until an optimal temperature, which after being surpassed, causes the expansion to decline. Possibly, in the studies performed, this optimum temperature was not reached, and this expansion decline was not observed. The increase in the expansion ratio caused by the higher temperature can be explained by the increase in the pressure differential at the outlet of the extruder, which is caused by the increase in temperature that generates a decrease in the viscosity of the dough inside the extruder, and an increase in the temperature of the super-heated water contained in the dough, favoring the formation of bubbles and increased expansion (SAELEAW et al., 2012; CAMPANELLA et al., 2002).

Product density: Density is a parameter that can be used to assess the degree of expansion of extruded products because, whereas the expansion ratio considers only the cross section, density considers the expansion in all directions, and in the case of extruded products, a low density is desirable.

The density study is used to compare the vacuoles created in the extrudates during extrusion. Density values ranged from 0.183 to 0.079 g/cm^3, as shown in Table 5.2. Higher temperatures resulted in lower density values, which is in agreement to what was found for the expansion factor, i.e., more expanded extrudates presented lower density. Such features were also found by Magali et al. (2010), which produced manioc flour snacks enriched with orange fiber.

Hardness: The hardness is obtained through the maximum force necessary to fracture the extrudates, and the obtained values varied from 15.0 to 69.9 kg, as show in Table 5.2. This property of the extrudates was also affected by the extrusion temperature. With the increase in extrusion temperature, a decrease in the fractureability of the extruded material was observed, corroborating the density values, since, with smaller bubbles, the extruded material becomes denser and more difficult to fracture.

Color analysis: The values of the color attributes are shown in Table 5.3. In general, the values of a* and b* showed that the samples were close to yellow coloring with a reddish tendency.

The increase in temperature caused a decrease in b* values, losing a little yellow color due to greater cooking of the samples. However, the samples that contained the oil and capsules added to the dough before extrusion had higher b* values when compared to the standard, since buriti oil has large b* values.

Analyzing the lightness (L*), the temperature also had a direct influence: higher temperatures generated darker extrudates, but the presence of oil in the extrusion improved this characteristic.

Table 5.2 Density, expansion ratio and hardness of the extrudate products

Treatment	Density (g/cm^3)	Expansion	Hardness
OA20	0.183 ± 0.026^{a}	2.24 ± 0.21^{defg}	52.73 ± 17.89^{b}
CA20	0.181 ± 0.025^{a}	2.30 ± 0.16^{efg}	54.15 ± 19.06^{ab}
EO20	0.106 ± 0.022^{bcd}	2.98 ± 0.31^{a}	24.98 ± 9.90^{c}
EC20	0.179 ± 0.021^{bcd}	2.22 ± 0.11^{g}	52.57 ± 12.47^{b}
NO20	0.183 ± 0.031^{a}	2.28 ± 0.16^{fg}	69.89 ± 18.73^{a}
OA15	0.107 ± 0.011^{bcd}	2.46 ± 0.10^{cdefg}	25.96 ± 4.75^{c}
CA15	0.113 ± 0.018^{bc}	2.42 ± 0.17^{defg}	30.75 ± 8.55^{c}
EO15	0.120 ± 0.014^{bcd}	2.68 ± 0.10^{bcd}	25.30 ± 4.21^{c}
EC15	0.107 ± 0.020^{bcd}	2.50 ± 0.23^{cdefg}	16.93 ± 5.85^{cd}
NO15	0.108 ± 0.018^{bcd}	2.46 ± 0.13^{cdefg}	26.93 ± 6.43^{c}
OA10	0.084 ± 0.020^{cd}	2.90 ± 0.16^{ab}	15.00 ± 6.10^{cd}
CA10	0.079 ± 0.019^{d}	2.54 ± 0.18^{cdef}	18.58 ± 2.66^{cd}
EO10	0.114 ± 0.014^{bc}	2.56 ± 0.12^{cdef}	20.78 ± 7.48^{cd}
EC10	0.102 ± 0.018^{bcd}	2.58 ± 0.28^{cde}	18.51 ± 6.18^{cd}
NO10	0.090 ± 0.006^{bcd}	2.72 ± 0.16^{abc}	18.40 ± 5.28^{cd}

Source: prepared by the author himself.

5.3.3 Optical microscopy analysis

Figures 5.2 shows the optical micrographs of the snacks produced with microencapsulated buriti oil added before the extrusion at different conditions, i.e., treatments EC10, EC15 and EC20. The marked region in Figure 5.2a appears to be a portion of free oil present inside the starchy matrix, indicating that the capsules did not

withstand the high temperature (140 °C) attained in this extrusion condition, in spite of the oil remaining entrapped in the extrudate material. On the other hand, in Figure 5.2b it is possible to identify a pair of microcapsules present in the extrudate, indicating that at a lower temperature (120 °C) at least a part of the microcapsules resisted the extrusion process. This is confirmed by Figure 5.2c, which shows a large number of microcapsules that remained integer during the mildest extrusion conditions.

Figure 5.2 Optical microscopy of extruded products containing microencapsulated buriti oil added before extrusion at different conditions: (a) 10% moisture/140 °C (EC10); (b) 15% moisture/120 °C (EC15); (c) 20% moisture/100 °C (EC20) (images collected with 10x objective lens).

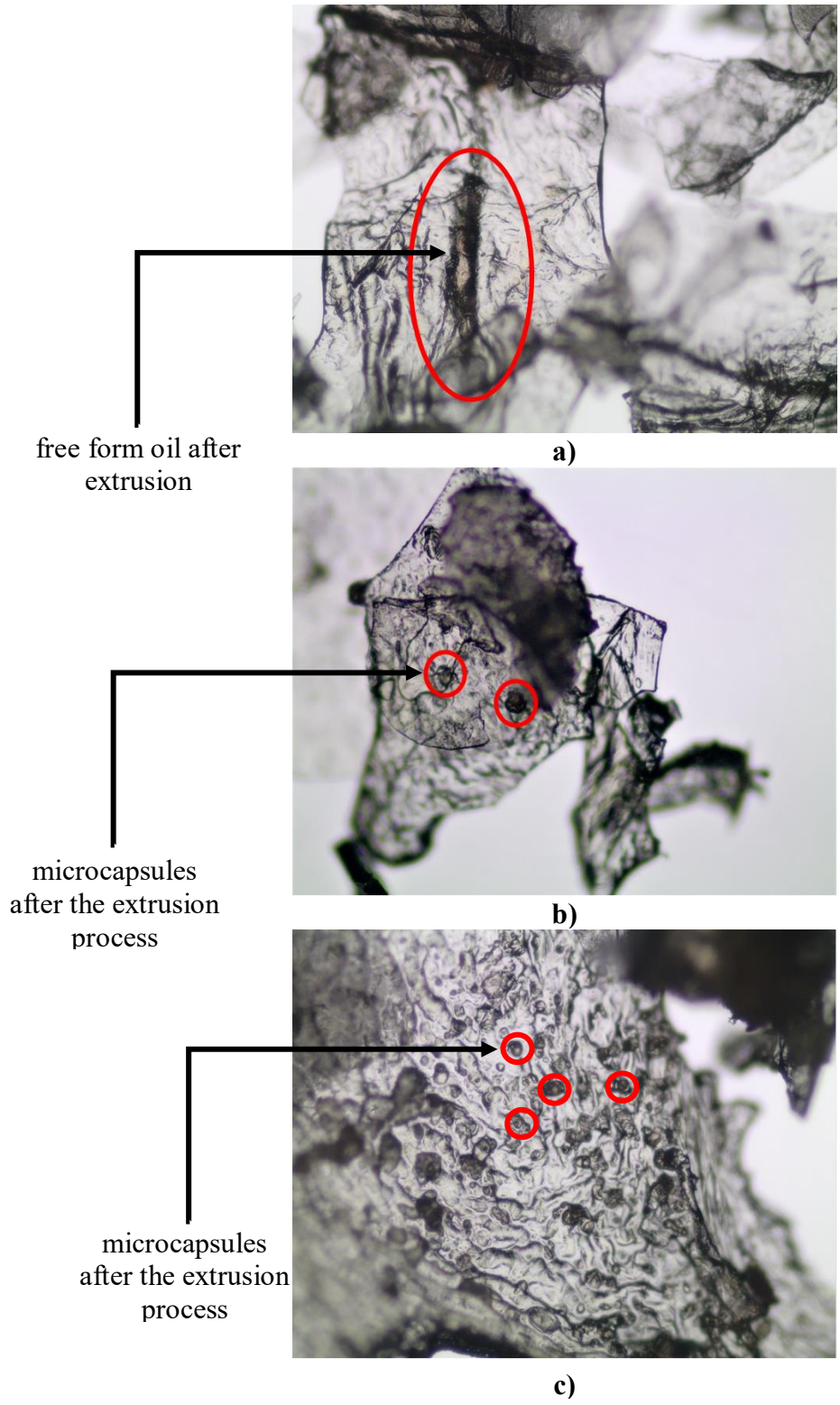

Source: prepared by the author himself.

5.3.4 β-carotene content

The β-carotene contents measured in the extruded material are shown in Table 5.3, and as shown by the data obtained, in all cases there was a loss of carotenoids, which is much greater in the extruded samples. For all the treatments in which the oil was added after extrusion, the values of retained carotenoids were the highest, as expected, followed by extrudates with microcapsules added before extrusion.

The extruded samples formulated with free buriti oil had the lowest retention values of carotenoids, since these compounds suffer from high temperatures and had a large part degraded during the process, as in the results found by Singh et al, who reported that extrusion temperatures between 94°C and 140°C have an impact on the stability of carotenoids, reaching 40% degradation (DELGADO-NIEBLAS et al., 2012). On the other hand, the extrudates that contained buriti oil microcapsules showed good carotenoid retention values, except for the sample extruded at the highest temperature (140 °C), in which the microcapsules were broken as shown in Figure 5.2a, thus losing their protective effect and allowing higher the degradation of the oil present.

Table 5.3 Content of β-carotene and color attributes of the extrudate products

Treatment	**β-carotene content (mg/g)**	**L***	**a***	**b***
Microcapsules	74.67 ± 1.53	82.63 ± 0.01	54.86 ± 0.11	80.73 ± 0.01
Buriti oil	265 ± 2.56	25.70 ± 0.15	20.57±0.18	22.75 ± 0.01
OA10	4.90 ± 0.58^{a}	65.00 ± 0.06^{b}	32.74 ± 0.07^{k}	3.56 ± 0.013^{j}
CA10	1.37 ± 0.35^{b}	63.10 ± 0.02^{b}	31.09 ± 0.02^{l}	3.08 ± 0.01^{k}
EO10	nt	72.85 ± 0.06^{g}	40.06 ± 0.17^{i}	5.89 ± 0.09^{f}
EC10	nt	70.75 ± 0.05^{i}	37.83 ± 0.09^{j}	4.59 ± 0.02^{i}
NO10	nt	66.52 ± 0.03^{k}	32.83 ± 0.03^{k}	3.65 ± 0.01^{j}
OA15	4.68 ± 1.25^{a}	78.15 ± 0.15^{b}	43.72 ± 0.34^{g}	6.70 ± 0.14^{c}
CA15	1.38 ± 0.47^{b}	78.70 ± 0.05^{a}	42.68 ± 0.06^{bc}	7.16 ± 0.05^{g}
EO15	0.60 ± 0.09^{c}	72.72 ± 0.04^{h}	46.27 ± 0.11^{e}	5.36 ± 0.03^{h}
EC15	1.02 ± 0.01^{c}	70.39 ± 0.05^{j}	41.53 ± 0.04^{h}	4.98 ± 0.03^{cd}
NO15	nt	78.58 ± 0.05^{a}	41.71 ± 0.09^{h}	7.38 ± 0.04^{a}
OA20	4.62 ± 1.98^{a}	75.83 ± 0.04^{e}	49.44 ± 0.10^{c}	6.49 ± 0.06^{d}

CA20	1.32 ± 0.83^{b}	74.50 ± 0.12^{f}	50.82 ± 0.27^{b}	6.10 ± 0.08^{e}
EO20	0.45 ± 0.13^{c}	70.69 ± 0.14^{i}	47.48 ± 0.20^{d}	6.59 ± 0.06^{c}
EC20	1.43 ± 0.71^{b}	76.57 ± 0.07^{d}	51.15 ± 0.10^{a}	6.68 ± 0.05^{c}
NO20	nt	76.82 ± 0.09^{c}	50.65 ± 0.28^{f}	$^{5.90}$ 0.06^{f}

nt: untraceable
Source: prepared by the author himself.

5.4 Conclusion

Enrichment of extruded snacks with buriti oil enhances their nutritional attributes by adding β-carotene. This work demonstrated that the addition of carotenoids in extruded materials is feasible as long as it is protected in some way, indicating that the use of the microencapsulation technique makes the process viable. It was also possible to conclude that higher temperatures produce extrudates with better expansion ratio and lower density, but with poorer color and greater carotene degradation.

REFERENCES

BASTO, G. J.; CARVALHO, C. W. P.; SOARES, A. G.; COSTA, H. T. G. B.; CHÁVEZ, D. W. H.; GODOY, R. L. O.; PACHECO S. Physicochemical properties and carotenoid content of extruded and non-extruded corn and peach palm (Bactris gasipaes, Kunth), **LWT - Food Science and Technology**, v. 69, p. 312-318, 2016.

BRENNAN, C.; BRENNAN, M.; DERBYSHIRE, E.; TIWARI, B. K. Effects of extrusion on the polyphenols, vitamins and antioxidant activity of foods, **Trends in Food Science & Technology**, v. 22, p. 570-575, 2011.

CAMPANELLA, O. H.; LI, P. X.; ROSS, K. A.; OKOS, M. R.The role of rheology in extrusion. In:WELTI-CHANES, J.;BARBOSA-CÁNOVAS,G. V.; AGUILERA,J. M. (Eds.), **Engineering And Food For The 21st Century**. Boca Raton: CRC Press, 2002. p. 393-413.

DELGADO-NIEBLAS, C. I.; ZAZUETA-MORALES, J. J.; GALLEGOS-INFANTE,J. A.; AGUILAR-PALAZUELOS, E.; CAMACHO-HERNÁNDEZ, I. L.; ORDORICA-FALOMIR, C. A.;PIRES DE MELO, M.; CARRILLO-LÓPEZ, A. Elaboration of functional snack foods using raw materials rich in carotenoids and dietary fiber: effects of extrusion processing**. CyTA - Journal of Food**, v. 13, p. 69-79, 2015.

DELGADO-NIEBLAS, C; AGUILAR-PALAZUELOS, E; GALLEGOS-INFANTE, A; ROCHA-GUZMÁN, N; ZAZUETA-MORALES, J; CARO-CORRALES, J. Characterization and optimization of extrusion cooking for the manufacture of third-generation snacks with winter squash (*Cucurbita moschata D.*) flour. **Cereal Chemistry**, v, 89, p. 65–72, 2012.

DE PILLI, T., CARBONE, B. F., DEROSSI, A., FIORE, A. G., SEVERINI, C. Effects of operating conditions on oil loss and structure of almond snacks**. International Journal of Food Science and Technology**, v. 43, p. 430-439, 2008.

DE ROSSO, V. V.; MERCADANTE, A. Z. Identification and quantification of carotenoids, by HPLC-PDA-MS/MS, from Amazonian fruits. **Journal of Agricultural and Food Chemistry**, v. 55, p. 5062–5072, 2007.

FERREIRA, S.; NICOLETTI, V. R. Microencapsulation of ginger oil by complex coacervation us ing atomization: Effects of polymer ratio and wall material concentration, **Journal of Food Engineering**, v. 291, p. 110214, 2021

HIRTH, M.; LEITER, A.; BECK, S. M.; SCHUCHMANN, H. P. Effect of extrusion cooking process parameters on the retention of bilberry anthocyanins in starch based food. **Journal of Food Engineering**, v. 125, p. 139-146, 2014.

KAISANGSRI, N.; KOWALSKI, R.; WIJESEKARA, I.; KERDCHOECHUEN, O.; LAOHAKUNJIT, N.; GANJYAL, G. Carrot pomace enhances the expansion and nutritional quality of corn starch extrudates, **LWT - Food Science and Technology**, v. 68, p. 391-399, 2016.

LEMOS, Y. P.; MARFIL, P. H. M.; NICOLETTI, V. R. Particle size characteristics of buriti oil microcapsules produced by gelatin-sodium alginate complex coacervation: Effect of stirring speed**. International journal of food properties**, v. 20, n. S2, p. S1438–S1447, 2017.

LIMA, D. B.; DAMIANI, L. P.; FUJIMORI, E. Vitamin A deficiency in brazilian children and associated variables. **Revista Paulista de Pediatria**, v. 36, n. 2, p. 176-185, 2018.

MAGALI, L.; SOUZA, L. B.; MISCHAN, M. M. Production of extruded snacks from cassava starch and orange fiber. **Ciência Rural**, v. 40, p. 1411-1417, 2010.

MARFIL, P. H. M.; VASCONCELOS, F. H. T.; PONTIERI, M. H.; TELIS, V. R. N. Development and validation of analytical method for palm oil determination in microcapsules produced by complex coacervation. **Química Nova,** v. 39, n. 1, p. 94-99, 2016.

MORARU, C. L., & KOKINI, J. L. Nucleation and expansion during extrusion and microwave heating of cereal foods**. Comprehensive Reviews in Food Science and Food Safety**, v. 2, 147–165, 2003

NKHATA, S. G.; CHILUNGO, S.; MEMBA, A.; MPONELA, P. Biofortification of maize and sweet potatoes with provitamin A carotenoids and implication on eradicating vitamin A deficiency in developing countries. **Journal of Agriculture and Food Research**, v. 2, p. 100068, 2020.

OBRADOVIĆ, V.; BABIĆ, J.; ŠUBARIĆ, D.; JOZINOVIĆ, A.; AČKAR, D.; KLARIĆ, I. Influence of dried Hokkaido pumpkin and ascorbic acid addition on chemical properties and colour of corn extrudates. **Food Chemistry**, v. 183, p. 136-143, 2015.

ORTAK, M.; CALTINOGLU, C.; SENSOY, I.; KARAKAYA, S.; MERT, B. Changes in functional properties and in vitro bioaccessibilities of β-carotene and lutein after extrusion processing. **Journal of Food Science and Technology**, v. 54, p. 3543–3551, 2017.

PAULA, A. M, CONTI-SILVA, A. C. Texture profile and correlation between sensory and instrumental analyses on extruded snacks. **Journal of Food Engineering**, v. 121, p. 9-14, 2014.

RODRIGUEZ-AMAYA, D. B.; KIMURA, M. **Harvestplus Handbook for Carotenoid Analysis**. HarvestPlus Technical Monograph 2. Washington, DC and Cali: International Food Policy Research Institute (IFPRI) and International Center for Tropical Agriculture (CIAT), 57p. 2004.

RODRIGUEZ-AMAYA, D. B. **A guide to carotenoid analysis in foods**, Washington, International Life Sciences Institute, 1999.

RODRIGUEZ-AMAYA D. B. Assessment of the provitamin A contents of foods - The Brazilian experience. **Journal Food Composition and Analysis**, v. 9, p. 196-230, 1996.

SHADDEL, R.; HESARI, J.; AZADMARD-DAMIRCHI, S.; HAMISHEHKAR, H.; FATHI-ACHACHLOUEI, B.; HUANG, Q. Use of gelatin and gum Arabic for encapsulation of black raspberry anthocyanins by complex coacervation. **International Journal of Biological Macromolecules**, v. 107, Part B, p. 1800–1810, 2018.

SAELEAW, M.; DÜRRSCHMID, K.; SCHLEINING, G. The effect of extrusion conditions on mechanical-sound and sensory evaluation of rye expanded snack. **Journal of Food Engineering, Essex**, v. 110, n. 4, p. 532-540, 2012.

TONYALI, B., SENSOY, I., AND KARAKAYA, S. The effect of extrusion on the functional components and in vitro lycopene bioaccessibility of tomato pulp added corn extrudates. **Food & Function Journal**, v. 7, p. 855-860, 2016.

CONCLUSÕES GERAIS E SUGESTÕES PARA TRABALHOS FUTUROS

CONCLUSÕES GERAIS

Foi possível determinar a melhor condição de processo para a produção das microcápsulas de óleo de butiri por coacervação complexa, utilizando o par gelatina/ goma arábica, sendo as melhores condições encontradas: frequência de agitação de 1000 rpm e a utilização de defletores no vaso de agitação, o que proporcionou as melhores microcápsulas quando observado seus valores médios e de span. Também foi possível concluir que os parâmetros reológicos das emulsões formadoras das microcápsulas são de suma importância para a sua produção; nesse trabalho foi possível observar que emulsões dilatantes necessitam de menores valores de agitação para a produção das microcápsulas e emulsões pseudoplásticas necessitam de maiores valores de agitação para apresentarem melhores resultados.

Os dois pares testados apresentaram bons resultados para a produção das microcápsulas apresentando bons valores de eficiência de microencapsulação, com valores acima de 80% e nas melhores condições valores médios abaixo de 50 µm. A secagem dos dois pares por espuma e por filme se mostrou boa alternativa à liofilização, sendo uma condição para mitigação dos custos de produção de microcápsulas.

A aplicação de microcápsulas para enriquecer snacks de milho com carotenoides se mostrou eficiente, apresentando bons teores de carotenoides por grama de snack até mesmo para as amostras em que as microcápsulas foram extrusadas. No entanto, os melhores valores encontrados foram para as amostras aonde o óleo e as microcápsulas foram adicionados junto com os condimentos.

De maneira geral, o trabalho obteve boas conclusões de quais são os parâmetros que influenciam diretamente nas condições finais das microcápsulas, produzindo boas microcápsulas que foram aplicadas em um produto alimentício como uma possível fonte de carotenoides.

SUGESTÕES PARA TRABALHOS FUTUROS

- Avaliar a estabilidade oxidativa do óleo de buriti microencapsulado.
- Realizar um estudo de digestibilidade das microcápsulas.
- Avaliar a taxa de liberação das microcápsulas em diferentes pHs
- Avaliar o efeito das concentrações dos materiais formadores das microcápsulas
- Realizar o aumento de escala para o vaso agitador obtido no estudo
- Avaliar a possibilidade de secagem das microcápsulas por *spray drying* como alternativa à liofilização.